ANL-7764

# Argonne National Laboratory

## NOTES ON ELECTRON PARAMAGNETIC RESONANCE SPECTROSCOPY

by

Juan A. McMillan

Printed in the United States of America
Available from
National Technical Information Service
U.S. Department of Commerce
5285 Port Royal Road
Springfield, Virginia 22151
Price: Printed Copy $3.00; Microfiche $0.95

ANL-7764
Physics

ARGONNE NATIONAL LABORATORY
9700 South Cass Avenue
Argonne, Illinois 60439

# NOTES ON
# ELECTRON PARAMAGNETIC RESONANCE SPECTROSCOPY

by

Juan A. McMillan

Solid State Science Division

December 1970

# PREFACE

These notes were prepared for a 30-hr course I taught at Hunter College, City University of New York, as visiting professor of Chemistry in the Graduate Division, in the Fall of 1970. The course was aimed at faculty and graduate students and was supplemented with experimental sessions in the afternoon. Although I assumed a basic knowledge of quantum mechanics and familiarity with group-theoretical arguments, a detailed revision of electron wavefunctions and the elementary theory of angular-momentum operators proved useful, as well as a brief incursion into basic aspects of electromagnetic theory and tensor algebra. The chapters on the theory of the g tensor and on hyperfine interactions were developed in detail, for these are aspects of utmost importance in spectroscopic applications. On the other hand, due to lack of time, the theory of crystal-field terms in $S^2$ and higher orders was only outlined.

If the course was successful, it was certainly due to the enthusiasm of the audience that encouraged me to discuss some of the topics beyond the limits of the written material, helping me to improve the presentation.

I would like to express my appreciation to Prof. Horst W. Hoyer, Executive Officer in Chemistry, for having arranged my visit, and to the faculty and graduate students of the School of Chemistry for having made my stay most pleasant.

Juan A. McMillan

TABLE OF CONTENTS

TABLE OF CONTENTS

# TABLE OF CONTENTS

## LIST OF FIGURES

LIST OF FIGURES

# LIST OF TABLES

# NOTES ON ELECTRON PARAMAGNETIC RESONANCE SPECTROSCOPY

by

Juan A. McMillan

## ABSTRACT

This report presents the fundamental aspects of electron paramagnetic resonance spectroscopy, with emphasis on the theoretical principles underlying the interpretation of results. A basic knowledge of quantum mechanics and familiarity with group-theoretical arguments are assumed. Some aspects of electromagnetic theory, electron wavefunctions, the theory of angular-momentum operators, and tensor algebra are briefly reviewed. The theory of the g tensor and of hyperfine interactions in transition metal ions are treated in detail. Tables of expectation values of hyperfine separations based on recent Hartree-Fock calculations are given in the appendixes.

## 1. MAGNETIC FIELD

### 1.1 Definitions

The properties of the magnetic field are adequately described by a vector $\vec{B}$ (called induction by some authors) such that

(a) The torque $\vec{T}$ that acts upon a linear magnetic dipole of moment $\vec{\mu}$ in a uniform magnetic field $\vec{B}$ is given by

$$\vec{T} = \vec{\mu} \times \vec{B}. \tag{1.1}$$

(b) The electromotive force along a closed path induced by its time variation is

$$\oint \vec{E} \cdot d\vec{\ell} = -\frac{1}{c}\frac{d}{dt}\int_{\Sigma} \vec{B} \cdot d\vec{\sigma}, \tag{1.2}$$

where $\vec{E}$ is the electric field vector and c is the velocity of light. Unless otherwise noticed, the cgs system of units is used throughout. Equation 1.2 holds for any surface $\Sigma$ enclosed by the loop and is valid in sign, provided that the sense of integration on the left-hand term and the direction of the

normal to the surface element $d\vec{\sigma}$ are related by the right-hand convention, in other words, if the integration proceeds counterclockwise when observed from the positive end of $d\vec{\sigma}$.

To define $\vec{B}$ by either equation, however, it is necessary to define either $\vec{\mu}$ or $\vec{E}$. The electric vector $\vec{E}$ is defined as the force acting on the positive, unit point charge and, in general,

$$d\vec{F} = \vec{E}\, dq. \tag{1.3}$$

The magnetic moment $\vec{\mu}$ may be defined by

$$\vec{\mu} = \frac{1}{c}\int_{\Sigma} i\, d\vec{\sigma} \tag{1.4}$$

in a loop carrying an electric current i.

If $\vec{B}$ is defined by means of Eq. 1.2, which requires the definition of Eq. 1.3, Eq. 1.1 may then be used to define $\vec{\mu}$, which is then found to be related to the electric current through Eq. 1.4. If the loop of Eq. 1.4 is a ring of radius a, then the magnetic field in the center is, in turn,

$$B_c = \frac{2\pi}{ca} i, \tag{1.5}$$

and its direction is determined by the right-hand convention, illustrated in Fig. 1. Since q and i are related by

$$i = \frac{dq}{dt}, \tag{1.6}$$

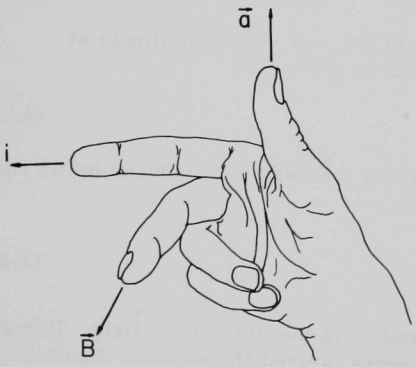


Fig. 1. Right-hand Convention

and Coulomb's law of interaction between electric charges imposes a natural unit for q, the whole system is consistent and may be defined on the sole basis of the units of mass, length, and time in the cgs system. The mks system, on the other hand, requires the additional definition of the Coulomb or the ampere to adopt the practical units of the electric system. The only ambiguity left is provided by $4\pi$, which may or may not appear in other definitions, according to whether the magnetization is defined already containing or not the factor $4\pi$. Elimination of $4\pi$ in

the definition of polarizations, as proposed in the so-called rationalized mksq system, however, is made at the expense of the appearance of $4\pi$ in other equations and does not seem to have, in my opinion, any obvious advantage.

## 1.2 Properties of the Magnetic-field Vector $\vec{B}$

As the counterpart for the electrostatic scalar potential V related to $\vec{E}$ by

$$\vec{E} = -\nabla V, \tag{1.7}$$

where $\nabla$ is the operator

$$\nabla = \vec{k}_1 \frac{\partial}{\partial x} + \vec{k}_2 \frac{\partial}{\partial y} + \vec{k}_3 \frac{\partial}{\partial z}, \tag{1.8}$$

with $\vec{k}_i$ symbolizing the unit vectors in the three orthogonal directions of space, the magnetic field has

$$\vec{B} = \nabla \times \vec{A}, \tag{1.9}$$

where $\vec{A}$ is called the magnetic vector potential. The cross indicates vector product. The operations by $\nabla$ are also called:

(1) Gradient when $\nabla$ is applied to a scalar, i.e.,

$$\vec{E} = -\nabla V = -\left(k_1 \frac{\partial V}{\partial x} + k_2 \frac{\partial V}{\partial y} + k_3 \frac{\partial V}{\partial z}\right) = -\text{grad } V. \tag{1.10}$$

(2) Curl when it involves vector product by a vector, i.e.,

$$\vec{B} = \nabla \times \vec{A} = \begin{vmatrix} \vec{k}_1 & \vec{k}_2 & \vec{k}_3 \\ \frac{\partial}{\partial x} & \frac{\partial}{\partial y} & \frac{\partial}{\partial z} \\ A_x & A_y & A_z \end{vmatrix} = \text{curl } \vec{A} \text{ or rot } \vec{A}. \tag{1.11}$$

(3) Divergence when it involves scalar product by a vector, i.e.,

$$\nabla \cdot \vec{B} = \frac{\partial B_x}{\partial x} + \frac{\partial B_y}{\partial y} + \frac{\partial B_z}{\partial z} = \text{div } \vec{B} = 0. \tag{1.12}$$

Equation 1.12 introduces us to an important property of $\vec{B}$, a property that is believed to hold everywhere and should be compared with

$$\text{div } \vec{D} = 4\pi\rho, \tag{1.13}$$

where $\vec{D}$ is the electric induction vector, defined in Eq. 1.15, and $\rho$ is the volume density of electric charges. Equation 1.12 is interpreted as an indication that there are no separable north-seeking and south-seeking magnetic charges, called monopoles. It is not ruled out, however, that separate monopoles may appear in some high-energy processes. The search for an isolated magnetic charge, the monopole, is one of the goals of high-energy physicists. If a monopole is found, we will have to state that Eq. 1.12 is true everywhere, except for a small region of space, unreachable under normal conditions, and will not affect the low- and medium-energy magnetic phenomena that occupy us.

That div $\vec{B}$ must be zero follows from considering Fig. 2a, illustrating the magnetic lines of force associated with a ring current. The lines of force are closed: There is neither source nor sink, and the number of lines entering and leaving any close surface is the same. That div $\vec{B}$ may not necessarily be zero everywhere follows from Fig. 2b, illustrating the magnetic lines of force associated with a black box of unknown content, such as the magnetic dipole of a subatomic or subnuclear particle. Outside the box, no distinction can be made between the two sources. If the black box cannot be opened at low and medium energies, we may not rule out the possibility that it contains two monopoles of opposite charge, separable at very high energies such as those involved in subnuclear phenomena, in which case div $\vec{B}$ would no longer be zero inside the box.

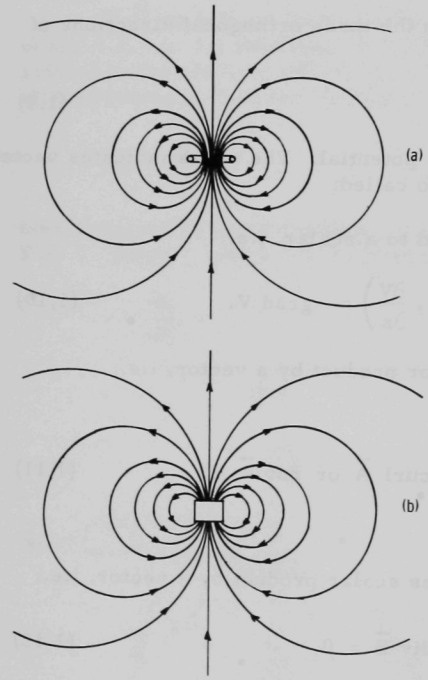


Fig. 2. Magnetic Fields of a Ring Current (a) and a Magnetic Dipole (b) in a Black Box

An important equation of electromagnetism is

$$\text{curl } \vec{B} = 4\pi\vec{J} + \frac{\hat{\epsilon}}{c}\frac{d}{dt}\vec{E}, \qquad (1.14)$$

where $\vec{J}$ is the current density and $\hat{\epsilon}$ the dielectric tensor. Equation 1.14 is also written in terms of the electric induction vector $\vec{D}$ related to $\vec{E}$ by

$$\vec{D} = \hat{\epsilon} \cdot \vec{E}. \qquad (1.15)$$

In isotropic dielectrics, $\hat{\epsilon}$ reduces to the scalar $\epsilon$, called the dielectric constant, and $\vec{D}$ and $\vec{E}$ have the same direction in all orientations. The term in $\vec{D}$ is called displacement current and is needed to close the circuit between

the plates of any capacitor present in it. It is zero when $\vec{D}$ is time-independent and appears only in circuits that are the seat of an alternate current. Therefore, for steady (direct) currents, Eq. 1.14 simplifies to

$$\text{curl } \vec{B} = 4\pi\vec{J}. \tag{1.16}$$

However, if matter is present, it is possible to distinguish between two types of currents--bound and free--and Eq. 1.16 then takes the form

$$\text{curl } \vec{B} = 4\pi\vec{J}_{\text{total}} = 4\pi\vec{J}_{\text{bound}} + 4\pi\vec{J}_{\text{free}}. \tag{1.17}$$

Free currents are those that may be turned on and off by switches; bound currents are those associated with microscopic angular momenta, such as orbital and spin, and are responsible for the magnetization $\vec{M}$, which is defined by

$$\text{curl } \vec{M} = \vec{J}_{\text{bound}}. \tag{1.18}$$

In turn, it is advantageous to introduce a magnetic field vector $\vec{H}$, sometimes called intensity, to account specifically for the free currents, i.e.,

$$\text{curl } \vec{H} = 4\pi\vec{J}_{\text{free}}. \tag{1.19}$$

The vectors $\vec{B}$, $\vec{M}$, and $\vec{H}$ are clearly related by

$$\vec{B} = \vec{H} + 4\pi\vec{M}, \tag{1.20}$$

but this expression is useful mainly inside the yoke of an electromagnet. Curiously enough, in the cgs system, $\vec{B}$ and $\vec{H}$ are measured in different units (gauss and oersted, respectively). The mksq system removes this ambiguity by introducing a conversion factor that makes $\vec{B}$ and $\vec{H}$ very different in order of magnitude.

Since $\vec{B}$ and $\vec{H}$ cannot be distinguished in the absence of magnetization, most books use $\vec{H}$ and not $\vec{B}$ in Eq. 1.1. As a matter of fact, tradition has somewhat imposed the use of $\vec{H}$ instead of $\vec{B}$. To redeem for the sin, the magnetic field, which is symbolized $\vec{H}$, is, however, expressed in gauss. We will not bow to the tradition of using $\vec{H}$, but use $\vec{B}$ instead.

When matter is placed in a magnetic field whose value in a vacuum is $\vec{B}_0$, the magnetic field inside the sample is

$$\vec{B} = \vec{B}_0 + 4\pi\vec{M} = \vec{B}_0(1 + 4\pi\kappa), \tag{1.21}$$

where

$$\kappa = \frac{M}{B_0} \tag{1.22}$$

is called the magnetic susceptibility per unit volume and

$$\vec{M} = \kappa \vec{B}_0 \tag{1.23}$$

is then the net magnetization, a concept that sets the basis for classification of matter into three categories, namely:

diamagnetic, when $\kappa < 0$;

paramagnetic, when $\kappa > 0$ and is independent of the magnetic field; and

ferro- and antiferromagnetic, when $\kappa > 0$ and depends on $\vec{B}$.

For anisotropic substances, such as noncubic crystals, the susceptibility is a second-rank, symmetric tensor.

## 1.3 Magnetic Moment and Angular Momentum of an Electric Charge

When a point body of mass m is moving in a central field of force, its angular momentum due to the motion

$$\vec{G} = m\vec{v} \times \vec{r}, \tag{1.24}$$

where $\vec{v}$ is its linear velocity and $\vec{r}$ the radius vector, is constant in the absence of external torque. If the body is electrically charged, the angular motion will create a magnetic moment

$$\vec{\mu} = \frac{1}{c} \int_{\Sigma} i \, d\vec{\sigma}, \tag{1.4}$$

where $d\sigma$ is an element of the area enclosed by the orbit and i is the equivalent current. The integral of Eq. 1.4 clearly includes orbits of any shape. One can substitute $d\vec{\sigma}$ by

$$d\vec{\sigma} = \tfrac{1}{2} \vec{r} \times d\vec{\ell} \tag{1.25}$$

as illustrated in Fig. 3 for a circular orbit, where $d\vec{\ell}$ is an element of the

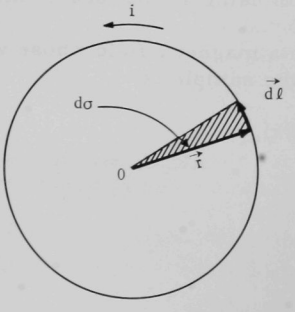


Fig. 3
Element of Area in a Circular Orbit

orbit. Since

$$i\,\vec{d\ell} = \frac{dq}{dt}\vec{v}\,dt = \vec{v}\,dq, \tag{1.26}$$

Eq. 1.4 becomes, after elimination of i and $\vec{d\ell}$,

$$\mu = \frac{1}{2c}\int(\vec{v}\times\vec{r})\,dq = \frac{1}{2c}\,q(\vec{v}\times\vec{r}). \tag{1.27}$$

Comparison of Eqs. 1.24 and 1.27 leads to

$$\vec{\mu} = \gamma\vec{G}, \tag{1.28}$$

where

$$\gamma = \frac{q\ (esu)}{2mc} = \frac{q\ (emu)}{2m} \tag{1.29}$$

is known as the magnetogyric ratio.

## 1.4 Precession Theorem

When an atom with a permanent magnetic moment $\vec{\mu}$ is placed in a uniform magnetic field $\vec{B}$, a torque

$$\vec{T} = \vec{\mu}\times\vec{B} \tag{1.1}$$

acts upon it. The angular momentum $\vec{G}$ then changes at a rate equal to this torque; i.e.,

$$\frac{d}{dt}\vec{G} = \vec{\mu}\times\vec{B}. \tag{1.30}$$

Since $\vec{G}$ is parallel to $\vec{\mu}$, the vector product $\vec{\mu}\times\vec{B}$ is perpendicular to $\vec{G}$. The meaning of $(d/dt)\vec{G}$ is then clear: The vector $\vec{G}$ rotates, but remains unchanged in length; namely it precesses about $\vec{B}$.

Introduction of Eq. 1.28 into Eq. 1.30 leads to

$$\frac{d}{dt}\vec{G} = \gamma\vec{G}\times\vec{B}. \tag{1.31}$$

To solve this vector equation, one writes the components in an orthogonal reference frame chosen in order to have $B_x = B_y = 0$, in which case,

$$\frac{d}{dt} G_x = \gamma B G_y, \tag{1.32}$$

$$\frac{d}{dt} G_y = -\gamma B G_x, \tag{1.33}$$

and

$$\frac{d}{dt} G_z = 0. \tag{1.34}$$

Interpretation of Eq. 1.34 is trivial: The component of $\vec{G}$ along the direction of $\vec{B}$ is constant. Since the absolute value of $\vec{G}$ is unaffected, its direction and the direction of $\vec{B}$ must subtend a time-independent angle $\alpha$. The solution of the other two equations is easily obtained. If Eq. 1.32 is again differentiated with respect to time and $(d/dt)G_y$ is replaced by its expression as given in Eq. 1.33, one arrives at

$$\frac{d^2}{dt^2} G_x = -(\gamma B)^2 G_x. \tag{1.35}$$

Analogous handling of Eq. 1.33 leads to

$$\frac{d^2}{dt^2} G_y = -(\gamma B)^2 G_y. \tag{1.36}$$

Equations 1.35 and 1.36 have the well-known form $(d^2/dt^2)x = -\omega^2 x$ of the harmonic oscillatory motion. The solutions of Eqs. 1.32-1.34 are then

$$G_x = G \sin \alpha \cos (\omega_L t + \phi_0), \tag{1.37}$$

$$G_y = G \sin \alpha \sin (\omega_L t + \phi_0), \tag{1.38}$$

and

$$G_z = G \cos \alpha, \tag{1.39}$$

where $G \sin \alpha$ is the amplitude of the oscillatory motion and

$$\omega_L = -\gamma B \tag{1.40}$$

is the angular velocity. The phase constant $\phi_0$ depends on the arbitrary choice of the origin of time. We will later see that the angle $\alpha$, which in the classical case depends on the initial conditions prevailing when the magnetic field was turned on, is fixed for atomic systems by the rules of quantization.

## 1.5 Field of a Dipole

Interaction between dipoles plays an important role in EPR, for the anisotropic contribution to the hyperfine splitting arises from the interaction between nuclear and electronic magnetic dipoles (spins). Since the energy of interaction may be expressed as the magnetic energy of either dipole in the field of the other, probably the best way to study the problem is to derive the expression for the magnetic field due to a dipole, which, not very close to the source, is the same in the electric and the magnetic cases.

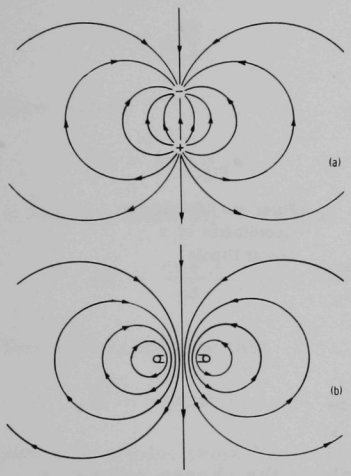


Fig. 4. Fields of an Electric Dipole (a) and a Ring Current (b)

Figure 4 illustrates the field of force of an electric dipole of two point charges of opposite sign (a) and that of a ring current (b). The field inside the ring is entirely different from the field between the electric charges. This intrinsic difference is contained in the already-known operator equations

$$\text{div } \vec{D} = 4\pi\rho; \qquad (1.13)$$

$$\text{div } \vec{B} = 0. \qquad (1.12)$$

As one moves farther away from the source, any difference disappears, and the magnetic field of a ring current may be formally treated as if it were associated with two magnetic charges of opposite kind, which is precisely what we suspect might exist inside the black box of Fig. 2b. It is therefore justified to solve the electric case and apply the equations to the magnetic case outside the black box. It is not that the same expression cannot be rigorously derived for the ring current; it is, if one starts from another equation we already know, i.e.,

$$\vec{B} = \text{curl } \vec{A}. \qquad (1.9)$$

But the physical meaning of the interaction is more evident when one treats the electric dipole or when one imagines the existence of a coupled pair of magnetic charges, in which case one may formally treat the magnetic field as derived from a scalar potential. To solve the problem, we are going to imagine a point dipole of moment

$$\vec{d\mu} = q\, \vec{d\ell} \qquad (1.41)$$

The vector $\vec{d\ell}$ is chosen as pointing toward the negative charge, so that $\vec{d\mu}$ has the direction of the field between the charges. Under this convention, $\vec{d\mu}$ lines up parallel to an electric field in the orientation of minimum potential energy.

We choose an arbitrary point 0 (Fig. 5) and after setting the z axis parallel to $\vec{d\mu}$, proceed to calculate the electric field at that point.

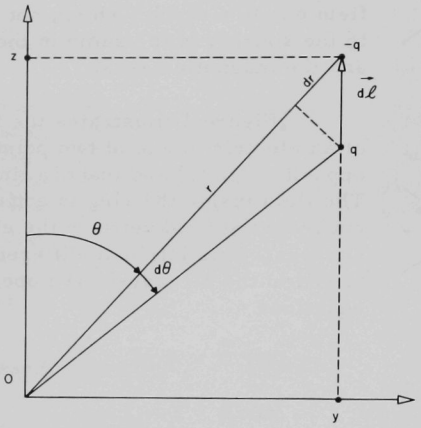


Fig. 5

Polar and Rectangular Coordinates of a Linear Dipole

Let $\vec{r}$ be the radius vector of the dipole in the chosen reference frame. The scalar potential at 0 due to the positive charge is

$$V_+ = \frac{q}{r}; \tag{1.42}$$

that due to the negative charge is

$$V_- = -\frac{q}{r + dr}, \tag{1.43}$$

where q is, in both cases, the absolute value of the charge of one sign. The total potential results in

$$dV = V_+ + V_- = -q\left(\frac{1}{r + dr} - \frac{1}{r}\right). \tag{1.44}$$

After making

$$r + dr = r\left(1 + \frac{dr}{r}\right), \tag{1.45}$$

one can write, to first order,

$$\frac{1}{1+\frac{dr}{r}} = 1 - \frac{dr}{r}, \tag{1.46}$$

after which Eq. 1.44 becomes

$$dV = q\frac{dr}{r^2}. \tag{1.47}$$

Now, since

$$dr = \cos\theta \, d\ell, \tag{1.48}$$

it follows from Eq. 1.47 that

$$dV = \frac{\cos\theta}{r^2} q \, d\ell = \frac{\cos\theta}{r^2} d\mu. \tag{1.49}$$

Remembering now that

$$\vec{E} = -\text{grad } V, \tag{1.7}$$

one may write, from Eq. 1.10,

$$dE_z = -\frac{\partial}{\partial z} dV. \tag{1.50}$$

From Fig. 5, one obtains

$$r^2 = y^2 + z^2 \tag{1.51}$$

and

$$\cos\theta = \frac{z}{r} \tag{1.52}$$

and finally arrives at

$$dE_z = -\frac{\partial}{\partial z}\left[\frac{z \, d\mu}{(y^2+z^2)^{3/2}}\right] = -d\mu\left[\frac{1}{(y^2+z^2)^{3/2}} - \frac{3z^2}{(y^2+z^2)^{5/2}}\right] = \frac{d\mu}{r^3}(3\cos^2\theta - 1). \tag{1.53}$$

Analogous expressions may be derived for $dE_x$ and $dE_y$. In the magnetic case, $\vec{B}$ takes the place of $\vec{E}$. The components $B_x$ and $B_y$ usually do not count in the strong-field case, for any magnetic moment is assumed to be

quantized along z, and therefore its energy in the field of a dipole, which is in turn quantized in the same direction, is determined by $B_z$ alone. For an extended dipole, the $B_z$ component is given by

$$B_z = \int \frac{3\cos^2\theta - 1}{r^3}\, d\mu. \tag{1.54}$$

In Section 7.4, we will see how Eq. 1.54 is adapted to atomic phenomena.

## 1.6 Symmetry of Electric and Magnetic Fields

Because EPR is essentially a magnetic experiment performed on an electric system, the symmetry properties of both fields present interest. To gain knowledge on these fields, let us look at the operations of symmetry that can be performed in each case, after assuming infinitely extended, uniform fields. In practice, the symmetry operations will affect, to first order, only the immediate environment, so that the conclusions reached for infinitely extended fields will still be valid for finite fields.

A rotation through any angle about any axis that is parallel to the field direction is a symmetry operation. Let its symbol be $C_\infty^\alpha$, where $\alpha$ is any angle about such axis. The electric field, in addition, is sent into itself by reflection through an infinite number of planes containing the rotation axis, planes that are symbolized $\sigma_v$. Its symmetry point group is therefore $C_{\infty v}$ ($\infty$m), in Schoenflies and international notation, respectively. Inversion, in reversing the electric field, is not a symmetry operation. This is due to the polar (irrotational) character of $\vec{E}$, which is given by

$$\vec{E} = -\nabla V. \tag{1.7}$$

The $\nabla$ operator changes sign under inversion, since

$$\vec{k}_1 \frac{\partial}{\partial(-x)} + \vec{k}_2 \frac{\partial}{\partial(-y)} + \vec{k}_3 \frac{\partial}{\partial(-z)} = -\left(\vec{k}_1 \frac{\partial}{\partial x} + \vec{k}_2 \frac{\partial}{\partial y} + \vec{k}_3 \frac{\partial}{\partial z}\right) \tag{1.55}$$

while V, being a true scalar, does not change sign; i.e.,

$$i \cdot V(x, y, z) = V(-x, -y, -z) = V(x, y, z). \tag{1.56}$$

In turn, $\vec{B}$ does not change sign under inversion, because

$$\vec{B} = \nabla \times \vec{A} \tag{1.9}$$

and both $\nabla$ and $\vec{A}$ do change sign. The vector potential $\vec{A}$ is polar. Therefore, a $\sigma_h$ plane--perpendicular to the direction of the field--will send $\vec{B}$ into itself, since

$$\sigma_h = i \cdot C_\infty^\pi = i \cdot C_2 \qquad (1.57)$$

and both i and $C_\infty^\pi$ are symmetry operations of the magnetic-field group. But the $\sigma_v$ planes that are present in the electric case would reverse $\vec{B}$, for since i is a symmetry operation in the magnetic case, if the $\sigma_v$ planes were also symmetry elements, there would exist twofold axes perpendicular to $C_\infty$ that would reverse $\vec{B}$. The reflection properties of $\vec{B}$ can be seen in Fig. 6, where, for simplicity, only one magnetic line associated to a ring current is shown reflected in an ordinary mirror. The symmetry point group of the magnetic field is then $C_{\infty h}$ - $\infty/m$. For further information, see Appendix A.

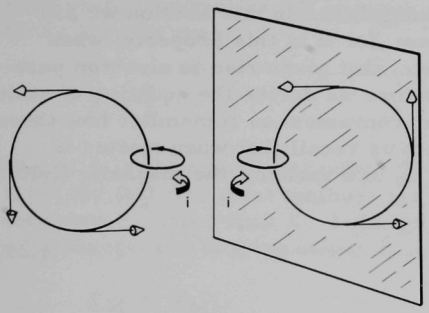

Fig. 6. Reflection Properties of Magnetic Lines

A somewhat peculiar consequence of this argument arises from the application of such an analysis to the black box of Fig. 2; a little thinking will convince us that north poles have to become south poles after reflection (and conversely) as long as the reflection is performed through the physicist's mirror (P mirror for brevity) that we have used so far. The P mirror does not change the electric charges. Consequently, when some nuclear phenomena are considered, one arrives at the conclusion that the laws of nature could be different after reflection. This ambiguity is removed if the mirror reverses time (T mirror) and changes electric charges (C mirror). Nature is then symmetric under reflection through the PCT mirror. At least, no experiment has so far been performed that proves otherwise.

# 2. MAGNETIC SUSCEPTIBILITY AND PARAMAGNETIC RESONANCE

## 2.1 The Magnetic Properties of Matter

In the previous section we referred to the classification of matter into dia-, para-, ferro-, and antiferromagnetic. In this section we are going to consider mainly paramagnetism, for it is this property, when measured under conditions of resonance, that gives rise to electron paramagnetic resonance (EPR or ESR). Before we derive the equation of state for paramagnetic substances, it will be convenient to remember how these properties are defined and studied. Let us recall that when matter is placed in a magnetic field of strength $\vec{B}_0$ in a vacuum, the magnetic field $\vec{B}$ inside the sample is given by

$$\vec{B} = \vec{B}_0 + 4\pi\vec{M} = B_0(1 + 4\pi\kappa), \tag{1.21}$$

where

$$\kappa = \frac{M}{B_0} \tag{1.22}$$

is called the volume susceptibility and represents the magnetization induced by the unit magnetic field. As we anticipated before, $\kappa$ is negative in diamagnetic substances, and positive otherwise. When $\kappa$ is positive, one encounters two situations: Either $\kappa$ is independent of the applied magnetic field, or it is not. In the former case, the substance is said to be paramagnetic and an equation of state relating the magnetization, the applied field, and the temperature may be found. Otherwise, $\kappa$ exhibits a strong dependence upon the applied magnetic field, there is hysteresis, and as a consequence it is not possible, in general, to establish an equation of state because the sample is not in thermodynamic equilibrium. Paramagnetism, on the other hand, implies thermodynamic equilibrium, and an equation of state may then be formulated. While diamagnetism is a universal property of matter that may eventually be disguised by the superposition of para-, ferro-, or antiferromagnetism, these latter occur only when the substance contains electrons whose spins are not compensated. When these latter do not significantly interact among one another, they are independently and reversibly polarized by an external magnetic field, and the substance exhibits paramagnetism. When, on the contrary, interaction among spins is strong, they couple together, lining up at a particular orientation within certain boundaries known as magnetic domains, thus giving rise to ferro- and antiferromagnetism and other spin alignments as yet unclassified.

The bearing of magnetic properties in chemistry was early recognized, and a whole new branch, magnetochemistry, soon developed. But it was not until the advent of EPR that interpretations could be freed of

sometimes false working assumptions. Before we proceed with a more detailed study of paramagnetism, it will be convenient to introduce two useful definitions.

The volume susceptibility $\kappa$, although of theoretical interest, is not very useful in practice. It is more convenient to work with the susceptibility per unit mass

$$\chi = \frac{\kappa}{\delta}, \tag{2.1}$$

where $\delta$ is the specific gravity. The advantage of using $\chi$ over $\kappa$ arises from the fact that most methods for determining magnetic susceptibilities measure $\chi$ rather than $\kappa$. Although $\chi$ has a practical value, it does not have theoretical bearing unless it is referred to one mole, i.e.,

$$\chi_M = W_M \chi, \tag{2.2}$$

where $W_M$ is the molecular weight and $\chi_M$ is known as the molar susceptibility.

## 2.2 Paramagnetic Susceptibility

To derive an equation of state for paramagnetic substances, we are going to simplify the problem by assuming a paramagnetic gas of molecules containing one unpaired electron with no orbital angular momentum, in which case the magnetic properties arise exclusively from the spin of the electron. Later we will see the reason for this simplification. In the absence of a magnetic field, all the molecules may be described as having the same energy $E_0$. It is true that there is an energy distribution, but if we wait long enough, both the time and the space average will approach $E_0$. Upon application of a magnetic field of strength B, some spins will line up parallel ($m_S = -\frac{1}{2}$) and have minimum potential energy, while others will line up antiparallel ($m_S = \frac{1}{2}$) and have maximum potential energy, as illustrated in Fig. 7. The energy levels are the Zeeman levels of energies

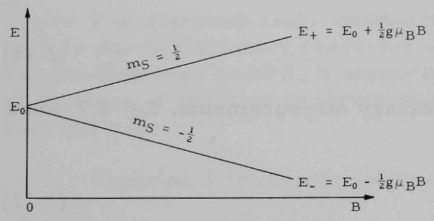


Fig. 7. Zeeman Splitting of Electronic Levels

$$E_+ = E_0 + m_S g \mu_B B \quad \text{for } m_S = \tfrac{1}{2} \tag{2.3}$$

and

$$E_- = E_0 + m_S g \mu_B B \quad \text{for } m_S = -\tfrac{1}{2}, \tag{2.4}$$

and the energy difference between both states is

$$\Delta E = g\mu_B B, \tag{2.5}$$

where g is the free-electron spectroscopic splitting factor (Landé factor), equal to 2.0023, and $\mu_B = 0.9273 \times 10^{-20}$ erg/G is the Bohr magneton.

In thermal equilibrium, the populations of the levels are related by

$$\frac{N_+}{N_-} = \exp(-g\mu_B B/kT) \tag{2.6}$$

and the net magnetization is

$$M = \tfrac{1}{2} g\mu_B (N_- - N_+). \tag{2.7}$$

The difference $N_- - N_+$ is obtained from Eq. 2.6 as

$$N_- - N_+ = 2N_- - N = N\left(2\frac{e^x}{1+e^x} - 1\right), \tag{2.8}$$

where

$$N = N_+ + N_- \tag{2.9}$$

is the total number of molecules and

$$x = \frac{g\mu_B B}{kT}. \tag{2.10}$$

For

$$g\mu_B B \ll kT, \tag{2.11}$$

which is the prevailing condition in ordinary measurements, Eq. 2.7, after substitution of Eq. 2.8, reduces to

$$M = \frac{Ng^2\mu_B^2}{4kT} B. \tag{2.12}$$

If N is the Avogadro number, M represents the molar magnetization, and the equation of state may be written as

$$\chi_M = \frac{C}{T} \tag{2.13}$$

or

$$M = \frac{C}{T} B, \tag{2.14}$$

known as Curie's law of paramagnetism, where

$$C = \frac{Ng^2\mu_B^2}{4k} = 0.3752 \text{ cgs deg} \tag{2.15}$$

is called the Curie constant.

The value of $\chi$ at room temperature ($T \approx 300°K$) turns out to be small; for this reason, tradition has imposed the use of $10^{-6}$ cgs as the unit of susceptibility. Typical values for spin-only paramagnetism at room temperature are of the order of 1200 ($10^{-6}$ cgs) per mole. Departures from this value indicate existence of orbital angular momentum, these departures having been of utmost importance in magnetochemistry.

## 2.3 The Susceptibility Tensor

Although the preceding derivation of Curie's law carries an important physical meaning, the real situation in most cases is by far more complicated. It is precisely having this view in mind that we chose a very special kind of paramagnetic substance. When measurements are performed in single crystals of lesser than cubic symmetry, the magnetization vector is no longer parallel to the applied magnetic field at all orientations. In general, Eq. 1.23 must be substituted for by

$$\vec{M} = \hat{\kappa} \cdot \vec{B}, \tag{2.16}$$

where $\hat{\kappa}$ is a second-rank, symmetric tensor. Since the tensor character of $\hat{\kappa}$ is due to the tensor character of the various terms of the spin Hamiltonian used in EPR, it seems appropriate to develop the basic algebra of this type of operator in view that it will be needed time and again in further analyses.

Equation 2.16 may be written in matrix notation as

$$\begin{pmatrix} M_x \\ M_y \\ M_z \end{pmatrix} = \begin{pmatrix} \kappa_{xx} & \kappa_{xy} & \kappa_{xz} \\ \kappa_{yx} & \kappa_{yy} & \kappa_{yz} \\ \kappa_{zx} & \kappa_{zy} & \kappa_{zz} \end{pmatrix} \cdot \begin{pmatrix} B_x \\ B_y \\ B_z \end{pmatrix}, \tag{2.17}$$

where the vertical arrays are column vectors and the square array is a 3 x 3 matrix. Equation 2.17 is a short notation for the three equations

$$\left.\begin{aligned} M_x &= \kappa_{xx}B_x + \kappa_{xy}B_y + \kappa_{xz}B_z; \\ M_y &= \kappa_{yx}B_x + \kappa_{yy}B_y + \kappa_{yz}B_z; \\ M_z &= \kappa_{zx}B_x + \kappa_{zy}B_y + \kappa_{zz}B_z. \end{aligned}\right\} \tag{2.18}$$

The 3 x 3 matrix of Eq. 2.17 is referred to as a second-rank tensor; it transforms an independent vector variable into a dependent vector quantity. Since vectors are tensors of first rank, we may say, in general, that the rank of the property tensor (in this case, the magnetic susceptibility) is equal to the sum of the ranks of the tensors representing the independent variable (in this case, the applied magnetic field) and the dependent quantity (in this case, the magnetization).

The susceptibility tensor $\hat{\kappa}$, together with most second-rank tensor properties, satisfies the condition of being symmetric with respect to the diagonal, i.e.

$$\kappa_{ij} = \kappa_{ji}, \tag{2.19}$$

where the subscripts i and j stand for the coordinates. For convenience, many authors use the numeral subscripts 1, 2, and 3 taking the place of x, y, and z, respectively, a convention that we adopt, and write

$$\hat{\kappa} = \begin{pmatrix} \kappa_{11} & \kappa_{12} & \kappa_{13} \\ \kappa_{12} & \kappa_{22} & \kappa_{23} \\ \kappa_{13} & \kappa_{23} & \kappa_{33} \end{pmatrix}, \tag{2.20}$$

in which allowance has already been made for the symmetric character. This latter may be proved on thermodynamic grounds in the case of polarization in general. When the tensor properties represent steady states and not equilibrium states, such as transport phenomena, the symmetric character appears as a consequence of Onsager's reciprocity theorem of irreversible thermodynamics. It is possible, however, to arrive at the symmetric character by accepting the experimental fact that there is a privileged orthogonal reference frame, called canonical, along whose axes the dependent vector quantity and the independent vector variable are parallel. In this reference frame, the off-diagonal matrix elements vanish and Eq. 2.17 takes the diagonal form

$$\begin{pmatrix} M_x \\ M_y \\ M_z \end{pmatrix} = \begin{pmatrix} \kappa_{11} & 0 & 0 \\ 0 & \kappa_{22} & 0 \\ 0 & 0 & \kappa_{33} \end{pmatrix} \cdot \begin{pmatrix} B_x \\ B_y \\ B_z \end{pmatrix}. \tag{2.21}$$

A change of reference frame represented by the orthogonal matrix

$$\hat{Q} = \begin{pmatrix} \ell_1 & \ell_2 & \ell_3 \\ m_1 & m_2 & m_3 \\ n_1 & n_2 & n_3 \end{pmatrix}, \tag{2.22}$$

where the matrix elements are direction cosines, may be used to transform $\hat{\kappa}$. Since $\hat{\kappa}$ is a 3 x 3 matrix, its expression in the new reference frame is obtained by a similarity transformation by $\hat{Q}$, i.e.,

$$\hat{\kappa}' = \hat{Q}^{-1} \cdot \hat{\kappa} \cdot \hat{Q}, \tag{2.23}$$

where $\hat{Q}^{-1}$ is the inverse of $\hat{Q}$, obtained by exchanging rows and columns. It is then found by direct computation that, for an arbitrary $\hat{Q}$, the matrix elements of $\hat{\kappa}$ satisfy the condition of Eq. 2.19.

When consideration is given to the symmetry of the crystal, symmetry requirements impose restrictions on the matrix elements of tensor properties. These restrictions are immediately obtained by performing the similarity transformation of Eq. 2.23 by the symmetry operations characteristic of the crystal. For example, the cubic system is characterized by four threefold rotation axes along the cube diagonals which, in Miller notation, are referred to as the (111) directions. One such axis is, for example, defined by the direction

$$\vec{k}_{111} = \frac{1}{\sqrt{3}} (\vec{k}_{100} + \vec{k}_{010} + \vec{k}_{001}), \tag{2.24}$$

where the $\vec{k}$'s are unit vectors in the directions indicated by their subscripts. A rotation through $2\pi/3$ about this axis is represented by the orthogonal matrix

$$C_3 = \begin{pmatrix} 0 & 0 & 1 \\ 1 & 0 & 0 \\ 0 & 1 & 0 \end{pmatrix} \tag{2.25}$$

in the crystal reference frame, which, incidentally, diagonalizes the susceptibility tensor. Direct calculation leads to

$$\begin{pmatrix} \kappa_2 & 0 & 0 \\ 0 & \kappa_3 & 0 \\ 0 & 0 & \kappa_1 \end{pmatrix} = \begin{pmatrix} 0 & 1 & 0 \\ 0 & 0 & 1 \\ 1 & 0 & 0 \end{pmatrix} \cdot \begin{pmatrix} \kappa_1 & 0 & 0 \\ 0 & \kappa_2 & 0 \\ 0 & 0 & \kappa_3 \end{pmatrix} \cdot \begin{pmatrix} 0 & 0 & 1 \\ 1 & 0 & 0 \\ 0 & 1 & 0 \end{pmatrix}. \tag{2.26}$$

But since the threefold rotation is an operation of symmetry,

$$\begin{pmatrix} \kappa_2 & 0 & 0 \\ 0 & \kappa_3 & 0 \\ 0 & 0 & \kappa_1 \end{pmatrix} = \begin{pmatrix} \kappa_1 & 0 & 0 \\ 0 & \kappa_2 & 0 \\ 0 & 0 & \kappa_3 \end{pmatrix}, \tag{2.27}$$

which can only be true if

$$\kappa_1 = \kappa_2 = \kappa_3 = \kappa, \tag{2.28}$$

and since

$$\begin{pmatrix} \kappa & 0 & 0 \\ 0 & \kappa & 0 \\ 0 & 0 & \kappa \end{pmatrix} = \kappa \begin{pmatrix} 1 & 0 & 0 \\ 0 & 1 & 0 \\ 0 & 0 & 1 \end{pmatrix} = \kappa \tag{2.29}$$

is a scalar, we conclude that there cannot be second-rank anisotropy in the cubic system.

In crystals of the trigonal, tetragonal, and hexagonal systems, rotations about the principal axis (chosen as z axis) make it impossible to distinguish between x and y; thus,

$$\kappa_1 = \kappa_2 = \kappa_\perp; \quad \kappa_3 = \kappa_\parallel, \tag{2.30}$$

which may be proved by performing the similarity transformation by the rotation matrix

$$C_n = \begin{pmatrix} \cos(2\pi/n) & -\sin(2\pi/n) & 0 \\ \sin(2\pi/n) & \cos(2\pi/n) & 0 \\ 0 & 0 & 1 \end{pmatrix} \tag{2.31}$$

with n = 3, 4, 6.

In orthorhombic crystals, there is no restriction other than that the tensor shall be diagonal in the crystal reference frame. The three values of $\kappa$ are different.

The monoclinic case, having only one axis fixed, which is either a twofold rotation axis or the normal to a plane of symmetry, introduces one independent parameter: the direction of one axis (x or y in the first setting, x or z in the second), in addition to the three principal values of the susceptibility, adding to four independent parameters.

Finally, the triclinic system, having no axis fixed by symmetry, leaves six independent parameters: the three principal values of the susceptibility and, for example, three Euler angles.

The derivation of these restrictions using the theorem of group intersection is shown in Appendix A. These properties have an important bearing in EPR, where they hold for local, rather than bulk, symmetry and will often be recalled.

The macroscopic susceptibility is restricted by the symmetry of the crystal, while the susceptibility of each individual paramagnetic center within the crystal is restricted by the local symmetry of its environment. This fact subtracts, to some extent, interest from bulk measurements, for they simply represent spatial averages and do not carry any obvious information about the local symmetries which have always been the subject of an educated guess in magnetochemistry. This is probably one of the biggest shortcomings of magnetochemistry in general. Such ambiguities are lifted by EPR since it is possible to independently observe centers that due to their anisotropic character resonate at different magnetic fields.

That the local symmetry of a paramagnetic center need not be the symmetry of the crystal, even in the absence of distortions, follows from inspection of Fig. 8 where there are indicated 10 sites in a simple-cube unit cell whose local symmetries are:

| | |
|---|---|
| $\Gamma$: $O_h$ (eightfold coordination); | M: $D_{4h}$ (001); |
| R: $O_h$ (sixfold coordination); | $\Lambda$: $C_{3v}$ (111); |
| S: $C_{2v}$ (101); | $\Sigma$: $C_{2v}$ (110); |
| Z: $C_{2v}$ (100); | $\Delta$: $C_{4v}$ (010); |
| X: $D_{4h}$ (010); | T: $C_{4v}$ (001). |

This information is particularly important in the study of interstitial paramagnetic impurities and trapped radicals produced by irradiation. For paramagnetic metal ions, these latter usually occupy the $\Gamma$ site. However, the onset of Jahn-Teller distortions usually descends the symmetry of the site to that of one of the lattice subgroups.

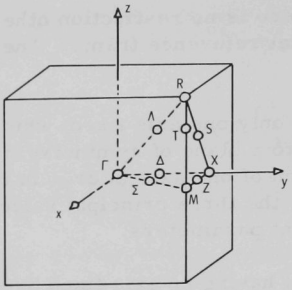


Fig. 8

Sites of Different Symmetry in a Simple-cube Unit Cell

## 2.4 Magnetic Transitions: EPR

A second look at Fig. 7 suggests the possibility of promoting electrons from the lower to the upper level by absorption of photons of energy

$$h\nu = g\mu_B B \tag{2.32}$$

as long as the lower level remains more populated than the upper one. This is the basic principle of EPR. Replacing figures for the parameters, one immediately finds that for a field of 3500 G and g = 2, for example, one may expect to find resonance for frequencies of the order of 10 GHz. Fields of up to 15,000 G may be readily obtained in the laboratory, and gadgetry to produce and handle microwave frequencies of some 8-10 GHz had been fully developed by the end of World War II for use in radar installations. It is only natural that under such circumstances EPR had to start, as a full-fledged technique, in this region of the electromagnetic spectrum, although the first experiments were done at lower frequencies.

We will have opportunity to discuss the advantages and disadvantages of working in different bands. For the time being, it will be convenient to return to Eq. 2.32 and the statement that resonance does occur and electrons are pumped to the upper level. But if resonance does occur and electrons are pumped to the upper level, the difference in population that made resonance possible in the first place will soon disappear and the absorption of photons will stop. Fortunately, nature has provided electrons in the upper level in excess over the thermal-equilibrium value with a radiationless process by which they may return to the lower level, thus securing a steady resonance absorption. This mechanism, called spin-lattice relaxation, allows the excess electrons in the upper level to transfer their excess energy to the lattice. The electromagnetic energy absorbed by the transition is then released to the lattice in the form of heat, by phonon processes. These processes, however, are characterized by relaxation times whose values limit, sometimes severely, the microwave power that may be used in the experiment, lest saturation occur. Although saturation imposes a limit to the power, it is extremely useful

in at least two instances, namely, when one is interested in studying the spin-lattice relaxation mechanisms themselves, and when one is interested in performing double-resonance experiments such as ENDOR (discussed in Section 7.10).

The importance of EPR does not obviously lie in the performance of an experiment such as the one involving the resonance of Eq. 2.32 when g = 2. Its interest lies in that g is often anisotropic, due to orbital contributions, in which case Eq. 2.32 must be replaced for by a Hamiltonian of the type

$$\mathcal{H} = \mu_B \hat{S} \cdot \hat{g} \cdot \vec{B}, \tag{2.33}$$

where $\hat{g}$ is now a second-rank, symmetric tensor, and $\hat{S}$ is the effective-spin vector operator, which is defined after making the multiplicity of the level equal to 2S + 1. The eigenvalues of Eq. 2.33 are the energy levels between which resonance transitions are in principle possible. The Hamiltonian of Eq. 2.33 is obtained by perturbation theory and has to be thoroughly justified, especially because of the definition of the effective-spin vector operator, which operates not only on the spin part of the perturbed electron wavefunction but also on the orbital admixture.

An additional feature of EPR is provided by the presence of nuclei with spin, for in such a case the unpaired electron will experience an effective field due to the superposition of the applied magnetic field and the magnetic field at the electron due to the nuclear magnetic moment. If the spin of the nucleus is, for example, $I = \frac{1}{2}$, each level of Fig. 7 will in turn be split into two, corresponding to the nuclear spin eigenvalues $\pm\frac{1}{2}$. Two resonance transitions are then observed, and their separation, provided the nuclear magnetic moment is known, contains relevant information about the electron wavefunction. Figure 9 illustrates the case of $S = \frac{1}{2}$, $I = \frac{1}{2}$, discussed above. This interaction is also, in general, a tensor quantity and is written

$$\hat{S} \cdot \hat{A} \cdot \hat{I}, \tag{2.34}$$

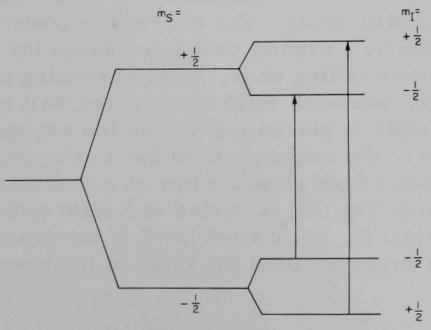


Fig. 9

Splitting of Magnetic Levels in the System $S = I = \frac{1}{2}$

where $\hat{A}$ is known as the hyperfine-interaction tensor. The Hamiltonian then takes the form

$$\mathcal{H} = \mu_B \hat{S} \cdot \hat{g} \cdot \vec{B} + \hat{S} \cdot \hat{A} \cdot \hat{I}, \tag{2.35}$$

which is by no means complete, but anticipates the type of work involved in the interpretation of paramagnetic spectra.

Our knowledge of second-rank tensors indicates that in cubic local symmetries the Hamiltonian of Eq. 2.35 reduces to its simplest form, which is

$$\mathcal{H} = \mu_B g \hat{S} \cdot \vec{B} + A \hat{S} \cdot \hat{I}, \tag{2.36}$$

where g and A are now scalar quantities. In axial symmetries,

$$\mathcal{H} = \mu_B [g_\parallel \hat{S}_z B_z + g_\perp (\hat{S}_x B_x + \hat{S}_y B_y)] + A_\parallel \hat{S}_z \hat{I}_z + A_\perp (\hat{S}_x \hat{I}_x + \hat{S}_y \hat{I}_y), \tag{2.37}$$

and in orthorhombic symmetries,

$$\mathcal{H} = \mu_B (g_z \hat{S}_z B_z + g_x \hat{S}_x B_x + g_y \hat{S}_y B_y) + A_z \hat{S}_z \hat{I}_z + A_x \hat{S}_x \hat{I}_x + A_y \hat{S}_y \hat{I}_y. \tag{2.38}$$

In lower symmetries, $\hat{g}$ and $\hat{A}$ need not be diagonal in the same reference frame, in which case if one is diagonal it is necessary to compute off-diagonal terms in the other. The situation, however, can be handled with a bit of experience and the two diagonalizing frames readily identified after enough spectra at appropriate orientations are obtained.

## 2.5 Experimental Detection of Resonance

When microwave frequencies are used in EPR experiments, the condition of resonance must be searched for by varying the magnetic field, because microwave sources can usually be tuned within a rather narrow band. A simplified scheme of transmission spectrometer is shown in Fig. 10. A source generates microwaves that are transmitted by a waveguide of rectangular cross section and metallic walls. The microwave power transmitted down the line is detected by a crystal rectifier chosen for its linear response to the microwave power falling on it. Some absorbing material, usually graphite-coated plastic, prevents reflections in the wall behind the detector. A paramagnetic sample is placed just inside the waveguide through a hole in the narrow face, where the magnetic field due to the microwave is a maximum. The static magnetic field generated by an electromagnet (one of whose pole pieces is shown in Fig. 10) is varied at a slow rate as the crystal current is plotted against B. A constant level of microwave power falling on the detector is thus recorded until the value of the resonance field

is reached. At this point, absorption by the sample increases, as indicated at the bottom of Fig. 10, thus decreasing the microwave power that reaches the detector. As soon as the condition of resonance is no longer fulfilled, the power falling on the crystal detector increases and the crystal current rises to its former value. Although conceptually simple, this device is not a particularly sensitive one. Other devices, based on a special array of transmission lines, make it possible to detect as little as $10^{11}$ spins for a linewidth of 1 G. The techniques involved in the experimental detection of resonance are critically evaluated in Charles Poole's book, cited in the list of references.

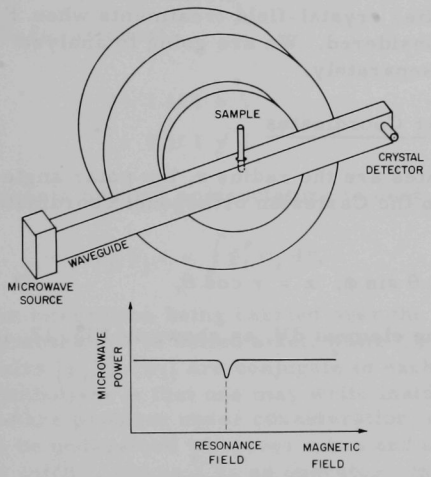


Fig. 10

Simplified Microwave Transmission Spectrometer

# 3. ELECTRON WAVEFUNCTIONS

## 3.1 Choice of Reference Frame

A study of the mechanics involved in handling electron wavefunctions when crystal field and magnetic phenomena are taken into consideration is of utmost importance. Electron wavefunctions are solutions of the Schroedinger equation, which may be expressed in different systems of coordinates. Among them, spherical polar and Cartesian orthogonal coordinates are preferred. While the first frame is more useful in most theoretical considerations, the second one leads to straightforward bases for group representation and simplifies crystal-field treatments when F and higher multiplicity states are considered. We are going to analyze these solutions in the two systems, separately.

## 3.2 Wavefunctions in Spherical Polar Coordinates

The spherical polar coordinates are the radius r, the polar angle $\theta$, and the azimuthal angle $\phi$, related to the Cartesian orthogonal coordinates by

$$x = r \sin\theta \cos\phi; \quad y = r \sin\theta \sin\phi; \quad z = r \cos\theta, \tag{3.1}$$

as illustrated in Fig. 11. The volume element dV, as shown in Fig. 12, is in turn given by

$$dV = r^2 \sin\theta \, dr \, d\theta \, d\phi. \tag{3.2}$$

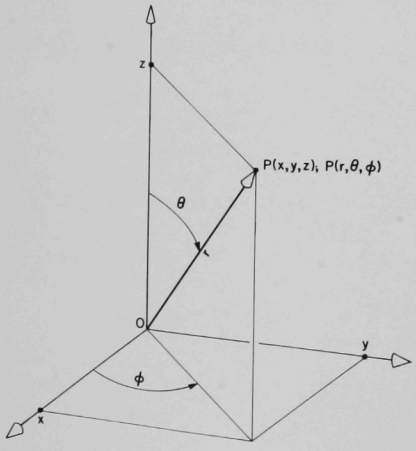


Fig. 11. Spherical Polar and Cartesian Orthogonal Coordinates

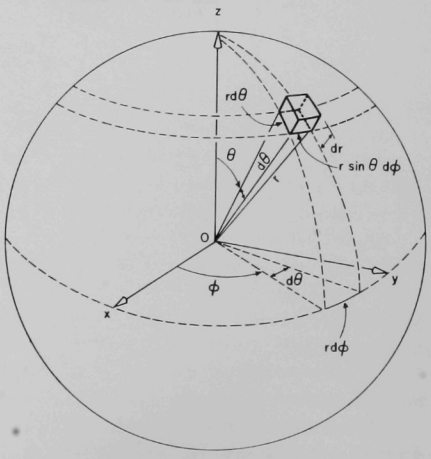


Fig. 12. Volume Element in Spherical Polar Coordinates

In this reference frame, the solutions of the Schroedinger equation for a single electron in a free atom (central force system) take the form

$$\psi = N^{\frac{1}{2}} R_{n,\ell}(r) \cdot P_{\ell,|m|}(\cos\theta) \cdot e^{im\phi}, \tag{3.3}$$

where $N^{\frac{1}{2}}$ is a normalization coefficient, n, $\ell$, and m are the principal, angular, and magnetic quantum numbers, and $P_{\ell,|m|}(\cos\theta)$ is a Legendre polynomial, listed in Table I. The set of wavefunctions is orthonormal; i.e.,

$$\langle \psi_i | \psi_j \rangle = \delta_{ij}, \tag{3.4}$$

where, as usual,

$$\delta_{ij} \begin{cases} = 1 \text{ if } i = j \\ = 0 \text{ if } i \neq j. \end{cases} \tag{3.5}$$

Dirac's bracket nomenclature is used, meaning

$$\langle \psi_i | \psi_j \rangle = \int \psi_i^* \psi_j \, d\tau, \tag{3.6}$$

the integration being carried over the whole configuration space. The symbol $|\psi_j\rangle$ is called a ket, while $\langle \psi_i|$ is referred to as a bra and the pairs $|\psi_i\rangle$, $\langle \psi_i|$ are conjugate to each other. The advantage of the bracket symbolism is that one may write inside whatever symbol may be relevant for the problem under consideration, omitting the integration sign, which is to be understood whenever a bra and a ket are fused together as in $\langle i|j\rangle$ or in $\langle i|\hat{f}|i\rangle$, where $\hat{f}$ is an operator. In this symbolism, the expectation value f

TABLE I. Legendre Polynomials up to $\ell = 4$

| | |
|---|---|
| $P_{0,0}(z) = 1$ | $P_{3,2}(z) = 15z(1 - z^2)$ |
| $P_{1,0}(z) = z$ | $P_{3,3}(z) = 15(1 - z^2)^{\frac{3}{2}}$ |
| $P_{1,1}(z) = (1 - z^2)^{\frac{1}{2}}$ | $P_{4,0}(z) = (1/8)(35z^4 - 30z^2 + 3)$ |
| $P_{2,0}(z) = \frac{1}{2}(3z^2 - 1)$ | $P_{4,1}(z) = (5/2)z(1 - z^2)^{\frac{1}{2}}(7z^2 + 3)$ |
| $P_{2,1}(z) = 3z(1 - z^2)^{\frac{1}{2}}$ | $P_{4,2}(z) = (15/2)(1 - z^2)(7z^2 - 1)$ |
| $P_{2,2}(z) = 3(1 - z^2)$ | $P_{4,3}(z) = 105z(1 - z^2)^{\frac{3}{2}}$ |
| $P_{3,0}(z) = \frac{1}{2}z(5z^2 - 3)$ | $P_{4,4}(z) = 105(1 - z^2)^2$ |
| $P_{3,1}(z) = (3/2)(1 - z^2)^{\frac{1}{2}}(5z^2 - 1)$ | |

Note: $z = \cos\theta$.

of an operator $\hat{f}$ is then given by

$$\langle f \rangle = \langle \psi_i | \hat{f} | \psi_j \rangle. \tag{3.7}$$

Since f is an observable and must therefore span the totally symmetric representation of the configuration symmetry group, symbolized $\Gamma_1$, the following relation must be satisfied, lest f vanish:

$$\Gamma_1 \in \Gamma_i \times \Gamma_f \times \Gamma_j, \tag{3.8}$$

where $\Gamma_i$, $\Gamma_f$, and $\Gamma_j$ are the representations spanned by $\psi_i$, $\hat{f}$, and $\psi_j$, the cross indicates direct product, and the symbol $\in$ should be read "is contained in."

The radial functions $R_{n,\ell}(r)$ are orthonormal; i.e.,

$$\langle n, \ell | n', \ell' \rangle = \delta_{nn'} \delta_{\ell\ell'}. \tag{3.9}$$

They are spherically symmetrical, i.e.,

$$\Gamma_{R(r)} = \Gamma_1, \tag{3.10}$$

and are also symbolized

$$R(r) = \frac{1}{r} P(r) \tag{3.11}$$

in Hartree-Fock theory.

The angular functions are gathered together in what is called a spherical harmonic whose general expression is

$$Y_{\ell,m} = (-1)^{(m+|m|)/2} \left[ \frac{2\ell+1}{4\pi} \cdot \frac{(\ell - |m|)!}{(\ell + |m|)!} \right]^{\frac{1}{2}} \cdot P_{\ell,|m|} (\cos \theta) \cdot e^{im\phi}, \tag{3.12}$$

where

$$(-1)^{(m+|m|)/2}$$

is a phase factor consistent with the application of the angular-momentum ladder operators to the $2\ell + 1$ manifold corresponding to each value of $\ell$. This is due to the fact that $\hat{\ell}_+ = \hat{\ell}_x + i\hat{\ell}_y$ and $\hat{\ell}_- = \hat{\ell}_x - i\hat{\ell}_y$ change the sign of the wavefunctions when either the wavefunction operated on or the operated one have positive, odd m. This phase setting was introduced by Condon and Shortley and, if followed, leads to linear combinations for real solutions that sometimes differ from the expressions commonly used in chemistry books.

In most cases, however, the phases do not play an important role, although they have to be taken into consideration when operating with the angular-momentum ladder operators, to be discussed in some detail in the next chapter.

The spherical harmonics of Eq. 3.12 are orthonormal; i.e.,

$$\langle \ell m | \ell' m' \rangle = \delta_{\ell\ell'}\delta_{mm'}. \tag{3.13}$$

They fulfill the requirements needed to form a $(2\ell+1)$-dimensional vector space, which is called the $2\ell + 1$ manifold of the wavefunctions of a given $\ell$. They span the $D^{(\ell)}$ representation of the full rotation group O(3), indicating $(2\ell+1)$-fold orbital degeneracy in the free atom.

Due to the spherical symmetry of filled shells, the spherical harmonics are still rigorous solutions of the Schroedinger equation for many-electron atoms. The radial functions have to be computed by iteration methods, such as Hartree-Fock theory.

The spherical harmonics of Eq. 3.12 are eigenfunctions of the angular-momentum operator $\hat{\ell}_z$ with the eigenvalue m; i.e.,

$$\hat{\ell}_z Y_{\ell,m} = m Y_{\ell,m}, \tag{3.14}$$

since the z axis is, by definition, the axis of quantization. In turn,

$$\hat{\ell}^2 Y_{\ell,m} = \ell(\ell+1)\, Y_{\ell,m}, \tag{3.15}$$

with the same eigenvalue within the $2\ell + 1$ manifold. The algebra of the angular-momentum operators is discussed in detail in the next chapter.

In the crystal field, when states of +m and -m cannot be distinguished, the following linear combinations are introduced:

$$\psi^c_m = \frac{1}{\sqrt{2}}\left(Y_{\ell,-m} + Y^*_{\ell,-m}\right) \tag{3.16}$$

and

$$\psi^s_m = \frac{i}{\sqrt{2}}\left(Y_{\ell,-m} - Y^*_{\ell,-m}\right), \tag{3.17}$$

where it is easy to verify that

$$Y^*_{\ell,-m} = (-1)^{(m+|m|)/2} Y_{\ell,m}. \tag{3.18}$$

This procedure is used to avoid complications arising from phase considerations, since $Y_{\ell,-m}$ with $m > 0$ is always positive.

The wavefunctions of Eqs. 3.16 and 3.17 are real and carry no angular momentum; i.e.,

$$\langle \psi_m^{c \text{ or } s} | \hat{\ell}_z | \psi_m^{c \text{ or } s} \rangle = 0, \tag{3.19}$$

although, of course,

$$\hat{\ell}^2 \psi_m^{c \text{ or } s} = \ell(\ell+1)\, \psi_m^{c \text{ or } s}. \tag{3.20}$$

Solution of Eq. 3.12 for several values of $\ell$ and m leads to the following cases:

$\ell = 0$, s electrons

$$\psi_s = |0, 0\rangle = \frac{1}{\sqrt{4\pi}}. \tag{3.21}$$

$\ell = 1$, p electrons

$$\psi(0) = |1, 0\rangle = \sqrt{\frac{3}{4\pi}} \cos\theta = \sqrt{\frac{3}{4\pi}}\, z; \tag{3.22}$$

$$\psi(1) = |1, 1\rangle = -\sqrt{\frac{3}{8\pi}} \sin\theta\, (\cos\phi + i \sin\phi) = -\sqrt{\frac{3}{8\pi}}(x + iy); \tag{3.23}$$

$$\psi(-1) = |1, -1\rangle = \sqrt{\frac{3}{8\pi}} \sin\theta\, (\cos\phi - i \sin\phi) = \sqrt{\frac{3}{8\pi}}(x - iy), \tag{3.24}$$

where x, y, and z are referred to unit radius and are therefore dimensionless, taking the place of $x/r$, $y/r$, and $z/r$, respectively, in Eqs. 3.1.

The solution $|1, 0\rangle$ corresponds to m = 0 and is, of course, real. The other solutions correspond to states of m = 1 and m = -1 that represent orbital angular momenta which are counterclockwise and clockwise, respectively, when the system is observed from the positive end of the axis of quantization (z).

$\ell = 2$, d electrons

$$\psi(0) = |2, 0\rangle = \sqrt{\frac{5}{16\pi}}(3z^2 - 1); \tag{3.25}$$

$$\psi(1) = |2, 1\rangle = -\sqrt{\frac{15}{8\pi}}\, z(x + iy); \tag{3.26}$$

$$\psi(-1) = |2, -1\rangle = \sqrt{\frac{15}{8\pi}}\, z(x - iy); \tag{3.27}$$

$$\psi(2) = |2, 2\rangle = \sqrt{\frac{15}{32\pi}}\,(x + iy)^2; \tag{3.28}$$

$$\psi(-2) = |2, -2\rangle = \sqrt{\frac{15}{32\pi}}\,(x - iy)^2. \tag{3.29}$$

Solutions for higher values of $\ell$ are available in the specialized literature.

The real combinations of Eqs. 3.16 and 3.17 are, in turn, the following:

$\ell = 1$

$$p_x = |1, 1+\rangle = \frac{1}{\sqrt{2}}(|1, -1\rangle - |1, 1\rangle) = \sqrt{\frac{3}{4\pi}}\, x; \tag{3.30}$$

$$p_y = |1, 1-\rangle = \frac{i}{\sqrt{2}}(|1, -1\rangle + |1, 1\rangle) = \sqrt{\frac{3}{4\pi}}\, y. \tag{3.31}$$

Notice the appearance of changed signs as a consequence of the phase convention affecting states of positive odd m only. The sign indicated in the kets $|1, 1+\rangle$ and $|1, 1-\rangle$ always corresponds to $\psi^c_m$ and $\psi^s_m$, respectively.

$\ell = 2$

$$d_{x^2-y^2} = |2, 2+\rangle = \frac{1}{\sqrt{2}}(|2, -2\rangle + |2, 2\rangle) = \sqrt{\frac{15}{16\pi}}\,(x^2 - y^2); \tag{3.32}$$

$$d_{xy} = |2, 2-\rangle = \frac{i}{\sqrt{2}}(|2, -2\rangle - |2, 2\rangle) = \sqrt{\frac{15}{4\pi}}\, xy; \tag{3.33}$$

$$d_{xz} = |2, 1+\rangle = \frac{1}{\sqrt{2}}(|2, -1\rangle - |2, 1\rangle) = \sqrt{\frac{15}{4\pi}}\, xz; \tag{3.34}$$

$$d_{yz} = |2, 1-\rangle = \frac{i}{\sqrt{2}}(|2, -1\rangle + |2, 1\rangle) = \sqrt{\frac{15}{4\pi}}\, yz. \tag{3.35}$$

Solutions for higher values are available in the literature.

Just as for the complex wavefunctions discussed earlier, each manifold of a given $\ell$ is $2\ell + 1$ degenerate in the free atom--O(3) symmetry--and in spherical symmetry in general. The degeneracies in typical crystal fields will be discussed in Section 6.1. The set of real

wavefunctions is also orthonormal and defines, together with $|\ell, 0>$, a $(2\ell+1)$-dimensional vector space for each value of $\ell$. These wavefunctions serve as bases for the representation of symmetry point groups, but are broken down to their complex components under a magnetic field, giving rise to various degrees of incompletely quenched orbital angular momentum, depending on the strength of the crystal field.

## 3.3 Wavefunctions in Cartesian Orthogonal Coordinates

The solution of the angular part of the Schroedinger equation in Cartesian orthogonal coordinates leads to the so-called cubic harmonics, which have the general, real form

$$\psi = N^{\frac{1}{2}} x^a y^b z^c, \tag{3.36}$$

where x, y, and z are dimensionless and defined in the interval (1, -1), and

$$a, b, c = 0, +|k| \tag{3.37}$$

with k integer,

$$a + b + c = \ell \tag{3.38}$$

and $N^{\frac{1}{2}}$ is a normalization coefficient. Appropriate linear combinations of particular solutions of Eq. 3.36 are usually taken in order to satisfy the orthogonality condition, as follows:

$\ell = 0$, s electrons $\quad a + b + c = 0, \quad a = b = c = 0$

$$\psi_s = N^{\frac{1}{2}}. \tag{3.39}$$

$\ell = 1$, p electrons $\quad a + b + c = 1$

$$p(a = 1) = N^{\frac{1}{2}} x; \tag{3.40}$$

$$p(b = 1) = N^{\frac{1}{2}} y; \tag{3.41}$$

$$p(c = 1) = N^{\frac{1}{2}} z. \tag{3.42}$$

$\ell = 2$, d electrons $\quad a + b + c = 2$

There are six solutions for Eq. 3.36, namely,

$$x^2, y^2, z^2, xy, xz, yz. \tag{3.43}$$

However, they define a five-dimensional vector space because of the existence of one linear relation,

$$x^2 + y^2 + z^2 = 1, \tag{3.44}$$

that decreases to five the number of linearly independent functions. An orthogonal set is, for example,

$$3z^2 - 1,\ x^2 - y^2,\ xy,\ xz,\ yz \tag{3.45}$$

aside from normalization coefficients. The linear relation of Eq. 3.44, incidentally, identifies with an s state, already counted for a = b = c = 0.

$\ell$ = 3, f electrons  a + b + c = 3

The number of solutions is ten, namely,

$$x^3,\ y^3,\ z^3,\ xy^2,\ xz^2,\ yx^2,\ yz^2,\ zx^2,\ zy^2,\ xyz. \tag{3.46}$$

Among them, one finds three linear relations:

$$\left.\begin{aligned} x^3 + xy^2 + xz^2 &= x; \\ yx^2 + y^3 + yz^2 &= y; \\ zx^2 + zy^2 + z^3 &= z, \end{aligned}\right\} \tag{3.47}$$

which identify with the already-counted p functions and reduces the number of independent functions to seven. They are chosen as

$$xyz,\ x(y^2 - z^2),\ y(z^2 - x^2),\ z(x^2 - y^2),$$

$$x(2x^2 - 3y^2 - 3z^2),\ y(2y^2 - 3z^2 - 3x^2),\ z(2z^2 - 3x^2 - 3y^2) \tag{3.48}$$

to satisfy the orthogonality conditions.

In general, solution of Eq. 3.36 leads to $\frac{1}{2}(\ell+1)(\ell+2)$ expressions, of which only $2\ell + 1$ are linearly independent. The advantage of the cubic over the spherical harmonics lies in that the behavior of cubic harmonics under operations of symmetry is simple and the finding of group representations becomes straightforward.

## 3.4 Spin Functions

In the previous treatment, no consideration has been given to the electron spin. The quantum-mechanical description of the electron spin is formally analogous to the treatment of orbital angular momentum. A spin function which is not a function of the spatial coordinates is introduced in the electron wavefunction. This function is named $|\alpha>$ or $|\beta>$, according to whether the spin is "up" $(+\frac{1}{2})$ or "down" $(-\frac{1}{2})$. Analogously to what is done

for the orbital angular momentum, the following operators are defined: $\hat{S}_z$, $\hat{S}_x$, $\hat{S}_y$, and $\hat{S}^2$. It will be sufficient now to state the fundamental equations

$$\hat{S}_z|\alpha> = \tfrac{1}{2}|\alpha>, \quad \hat{S}_z|\beta> = -\tfrac{1}{2}|\beta>; \tag{3.49}$$

$$\hat{S}^2|\alpha> = \tfrac{1}{2}(\tfrac{1}{2}+1)|\alpha>, \quad \hat{S}^2|\beta> = \tfrac{1}{2}(\tfrac{1}{2}+1)|\beta>. \tag{3.50}$$

We will see later how these operators simplify the theoretical treatment.

# 4. ANGULAR-MOMENTUM OPERATORS

## 4.1 Infinitesimal-rotation Operator

The elements of symmetry of a free atom, which belongs to the group of all proper and improper rotations, are three orthogonal, infinitesimal-rotation operators to be defined later in this section, the spatial inversion operator, and the corresponding products, which are the improper-rotation operators. From the point of view of most physical applications, we restrict our discussion to the subgroup $O^+(3)$ of all proper rotations. Notice that there is a nondenumerably infinite number of rotations generated by each infinitesimal-rotation operator, and that the use of the infinitesimal-rotation operators $\hat{I}_x$, $\hat{I}_y$, and $\hat{I}_z$ is justified by the fact that any infinitesimal rotation in quantum mechanics may be decomposed, to first order in the angle, into three infinitesimal rotations about orthogonal axes. The choice of these axes to define the rotation operators is clearly arbitrary since, due to the high symmetry of the group, all axes are strictly equivalent; in other words, the physical space is isotropic. The laws of nature are invariant under the group of all rotations (isotropy of space) and under the group of all translations (uniformity of space). However, to simplify the treatment of the group of all rotations, it is convenient to adopt, arbitrarily, three axes, x, y, and z, and preserve z as the unique axis of symmetry when the symmetry is descended to that of the axial groups. The first task that we face is the definition of the infinitesimal-rotation operators. This may be accomplished in a conventional way by considering a rotation through an angle $\alpha$ about, say, the z axis.

Let $R(\alpha,z)$ be such a rotation and $R(0,z)$ the identity. We define the infinitesimal-rotation operator, as applied to a vector $\vec{r}$ in the xy plane, as

$$\lim_{\alpha \to 0} \frac{R(\alpha,z) \cdot \vec{r} - R(0,z) \cdot \vec{r}}{\alpha} = \frac{d}{d\alpha} \vec{r}. \tag{4.1}$$

The operation of Eq. 4.1 may be expressed, in terms of partial differentials, as

$$\frac{d\vec{r}}{d\alpha} = \frac{\partial \vec{r}}{\partial x} \frac{\partial x}{\partial \alpha} + \frac{\partial \vec{r}}{\partial y} \frac{\partial y}{\partial \alpha} = \left( \frac{\partial x}{\partial \alpha} \frac{\partial}{\partial x} + \frac{\partial y}{\partial \alpha} \frac{\partial}{\partial y} \right) \vec{r}. \tag{4.2}$$

Since the square of the radius vector

$$r^2 = x^2 + y^2 \tag{4.3}$$

is constant, a differential rotation through $d\alpha$ will result in

$$r^2 = (x + dx)^2 + (y + dy)^2 = x^2 + y^2 + 2(x\,dx + y\,dy), \tag{4.4}$$

and then

$$x\,dx + y\,dy = 0;\quad dy/x = -dx/y. \tag{4.5}$$

Figure 13 shows, in addition, that

$$d\alpha = -dx/y = dy/x, \tag{4.6}$$

which follows immediately when $\vec{r}$ is rotated to coincide with y and x, respectively. From Eq. 4.6 it follows that

$$\frac{\partial x}{\partial \alpha} = -y;\quad \frac{\partial y}{\partial \alpha} = x, \tag{4.7}$$

and Eq. 4.2 becomes

$$\frac{d}{d\alpha} = x\frac{\partial}{\partial y} - y\frac{\partial}{\partial x}, \tag{4.8}$$

which is the differential-rotation operator about z that we were looking for.

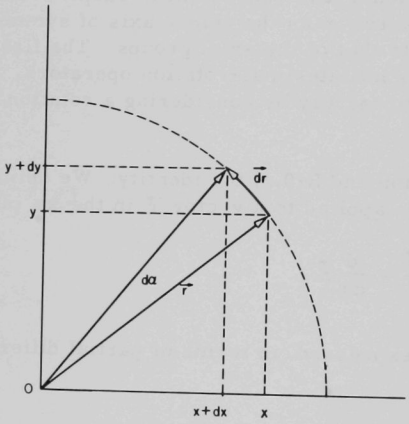


Fig. 13

Infinitesimal Rotation in the xy Plane

Since the quantum-mechanical, differential operator associated with rotation about z is

$$\hat{I}_z = -i\left(x\frac{\partial}{\partial y} - y\frac{\partial}{\partial x}\right), \tag{4.9}$$

we may write

$$\frac{d}{d\alpha} = i\hat{I}_z \tag{4.10}$$

in view of forthcoming applications to be discussed later. Equation 4.1 may now be written

$$\lim_{\alpha \to 0} \frac{R(\alpha,z) - 1}{\alpha} = i\hat{I}_z, \tag{4.11}$$

where we have written 1 for the identity transformation. The rotation $R(\alpha,z)$ is then given by

$$R(\alpha,z) = 1 + i\alpha\hat{I}_z \quad \text{for } \alpha \ll 1. \tag{4.12}$$

Although Eq. 4.12 is clearly restricted to infinitesimal rotations, $R(\alpha,z)$ can always be expressed in terms of the infinitesimal-rotation operator $\hat{I}_z$ for an arbitrary value of $\alpha$. Any rotation through $\alpha$ may be performed by $\underline{n}$ successive $\alpha/n$ rotations, in which case $\alpha/n$ can be made small enough to apply Eq. 4.12. Therefore,

$$R(\alpha,z) = R^n(\alpha/n,z) = \lim_{n\to\infty} [1 + i(\alpha/n)\hat{I}_z]^n = 1 + i\alpha\hat{I}_z$$

$$+ \frac{(i\alpha\hat{I}_z)^2}{2!} + \frac{(i\alpha\hat{I}_z)^3}{3!} + \ldots = e^{i\alpha\hat{I}_z}. \tag{4.13}$$

The exponential expression is, however, formal and should be understood as an abbreviated notation for the series, since in each case the exponential has to be expanded in order to operate on a function due to the differential character of $\hat{I}_z$.

Let us now study the decomposition of a small-angle rotation into elemental orthogonal rotations. For simplicity, we first consider a rotation about an axis $\xi$ lying in the yz plane, as illustrated in Fig. 14. One may write

$$R(\alpha,\xi) = R(\alpha \sin\theta, y) \cdot R(\alpha \cos\theta, z) + O(\alpha^2), \tag{4.14}$$

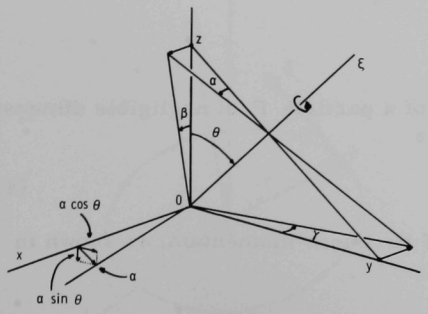


Fig. 14

Decomposition of an Infinitesimal Rotation in the yz Plane into Two Infinitesimal Rotations about y and z

where the term $O(\alpha^2)$ is a correction to second order in $\alpha$ that tends to zero more rapidly than $\alpha$, representing the difference between the length of the arc and that of the tangent segment. In view of Eq. 4.12 we may rewrite Eq. 4.14 as

$$R(\alpha \sin \theta, y) \cdot R(\alpha \cos \theta, z) = (1 + i\alpha \sin \theta \cdot \hat{I}_y) \cdot (1 + i\alpha \cos \theta \cdot I_z), \tag{4.15}$$

neglecting terms in $\alpha^2$. By equating Eqs. 4.12 and 4.15, i.e.,

$$1 + i\alpha \hat{I}_\xi = 1 + i\alpha \sin \theta \cdot \hat{I}_y + i\alpha \cos \theta \cdot \hat{I}_z, \tag{4.16}$$

one finally obtains

$$\hat{I}_\xi = \sin \theta \, \hat{I}_y + \cos \theta \, \hat{I}_z. \tag{4.17}$$

It is left to the reader to generalize the argument to any arbitrary orientation of the $\xi$ axis which leads to the general expression

$$\hat{I}_\xi = \sin \theta \cos \phi \, \hat{I}_x + \sin \theta \sin \phi \, \hat{I}_y + \cos \theta \, \hat{I}_z \tag{4.18}$$

in spherical coordinates or

$$\hat{I}_\xi = \ell \hat{I}_x + m \hat{I}_y + n \hat{I}_z, \tag{4.19}$$

where $\ell$, m, and n are the direction cosines of the $\xi$ axis in an orthogonal reference frame.

In conclusion, we notice that with the help of Eqs. 4.18 or 4.19 and 4.13 we may express any rotation in terms of three infinitesimal-rotation operators $\hat{I}_x$, $\hat{I}_y$, and $\hat{I}_z$, and that in consequence these may be used to generate the full rotation group. Next, we have to derive some interesting properties of these operators arising from the fact that they do not commute with one another, for which we are going to introduce the quantum-mechanical angular-momentum operators in order not to lose contact with the physical problem.

## 4.2 Classical Angular Momentum

The angular momentum $\vec{M}$ of a particle P of negligible dimensions is defined in classical mechanics as

$$\vec{M} = \vec{r} \times \vec{p}, \tag{4.20}$$

where $\vec{r}$ is its radius vector and $\vec{p}$ its linear momentum, as shown in Fig. 15.

In Cartesian orthogonal coordinates, Eq. 4.20 becomes

$$\vec{M} = \begin{vmatrix} \vec{k}_1 & \vec{k}_2 & \vec{k}_3 \\ x & y & z \\ p_x & p_y & p_z \end{vmatrix} = \vec{k}_1(yp_z - zp_y) + \vec{k}_2(zp_x - xp_z) + \vec{k}_3(xp_y - yp_x), \tag{4.21}$$

where $\vec{k}_1$, $\vec{k}_2$, and $\vec{k}_3$ are the three orthogonal unit vectors in the directions of x, y, and z, and

$$\vec{r} = x\vec{k}_1 + y\vec{k}_2 + z\vec{k}_3 \tag{4.22}$$

and

$$\vec{p} = p_x\vec{k}_1 + p_y\vec{k}_2 + p_z\vec{k}_3. \tag{4.23}$$

Since

$$\vec{M} = M_x\vec{k}_1 + M_y\vec{k}_2 + M_z\vec{k}_3, \tag{4.24}$$

a comparison with Eq. 4.21 immediately leads to

$$M_x = yp_z - zp_y, \tag{4.25}$$

$$M_y = zp_x - xp_z, \tag{4.26}$$

and

$$M_z = xp_y - yp_x, \tag{4.27}$$

which are the expressions of the components of the classical angular momentum in Cartesian coordinates.

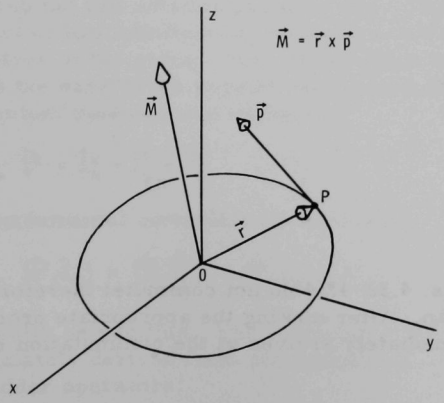


Fig. 15

Angular Momentum of a Particle of Linear Momentum $\vec{p}$

## 4.3 Quantum-mechanical Angular-momentum Operator

In quantum mechanics, the dynamic variables are replaced by operators, which are:

coordinate operator: multiplication by coordinate q, and

linear-momentum operator: left operation by $-i\hbar \frac{\partial}{\partial q}$.

After substitution, the classical components $M_q$ of Eqs. 4.25-4.27 become the quantum mechanical operators $\hat{L}_q$ according to

$$\hat{L}_x = -i\hbar\left(y \frac{\partial}{\partial z} - z \frac{\partial}{\partial y}\right), \tag{4.28}$$

$$\hat{L}_y = -i\hbar\left(z \frac{\partial}{\partial x} - x \frac{\partial}{\partial z}\right), \tag{4.29}$$

and

$$\hat{L}_z = -i\hbar\left(x \frac{\partial}{\partial y} - y \frac{\partial}{\partial x}\right), \tag{4.30}$$

which have dimensions of an angular momentum. However, it is convenient to work with the dimensionless, Hermitian rotation operators $\hat{I}_q$ of Eq. 4.9, related to $\hat{L}_q$ by

$$\hat{I}_q = \frac{1}{\hbar} \hat{L}_q, \tag{4.31}$$

which result, for each coordinate in turn, in

$$\hat{I}_x = -i\left(y \frac{\partial}{\partial z} - z \frac{\partial}{\partial y}\right), \tag{4.32}$$

$$\hat{I}_y = -i\left(z \frac{\partial}{\partial x} - x \frac{\partial}{\partial z}\right), \tag{4.33}$$

and

$$\hat{I}_z = -i\left(x \frac{\partial}{\partial y} - y \frac{\partial}{\partial x}\right). \tag{4.34}$$

The $\hat{I}_q$ operators of Eqs. 4.32-4.34 do not commute; therefore the full rotation group is not Abelian. After making the appropriate products by direct calculations, one immediately arrives at the commutation relations

$$\hat{I}_x\hat{I}_y - \hat{I}_y\hat{I}_x = [\hat{I}_x,\hat{I}_y] = i\hat{I}_z, \tag{4.35}$$

$$\hat{I}_y\hat{I}_z - \hat{I}_z\hat{I}_y = [\hat{I}_y,\hat{I}_z] = i\hat{I}_x, \tag{4.36}$$

and

$$\hat{I}_z\hat{I}_x - \hat{I}_x\hat{I}_z = [\hat{I}_z,\hat{I}_x] = i\hat{I}_y, \tag{4.37}$$

where the expression in brackets is the symbol for commutator; i.e.,

$$[\hat{A},\hat{B}] = \hat{A}\hat{B} - \hat{B}\hat{A} \tag{4.38}$$

Very useful definitions to be explored later are those of the ladder operators:

$$\text{Raising operator: } \hat{I}_+ = \hat{I}_x + i\hat{I}_y \tag{4.39}$$

and

$$\text{Lowering operator: } \hat{I}_- = \hat{I}_x - i\hat{I}_y \tag{4.40}$$

whose commutation relations with $\hat{I}_z$ and with each other are easily found to be

$$[\hat{I}_z,\hat{I}_+] = \hat{I}_+, \tag{4.41}$$

$$[\hat{I}_z,\hat{I}_-] = -\hat{I}_-, \tag{4.42}$$

and

$$[\hat{I}_+,\hat{I}_-] = 2\hat{I}_z. \tag{4.43}$$

To complete the argument, it is necessary to introduce an operator of a type not yet mentioned, which arises naturally in the algebra of Lie groups, of which the full rotation group is one. This operator consists of the scalar product of two infinitesimal operators, which commutes with all infinitesimal operators of the group. Such an operator is known as a Casimir operator and in the case of the angular momentum is called the total angular-momentum operator and defined as

$$\hat{I}^2 = \hat{I}_x^2 + \hat{I}_y^2 + \hat{I}_z^2. \tag{4.44}$$

The fundamental commutation relations

$$[\hat{I}^2,\hat{I}_x] = [\hat{I}^2,\hat{I}_y] = [\hat{I}^2,\hat{I}_z] = 0 \tag{4.45}$$

can easily be verified. The following alternative expressions for $\hat{I}^2$ are immediately derived from the commutation relations and the definition of the ladder operators:

$$\hat{I}^2 = \hat{I}_+\hat{I}_- - \hat{I}_z + \hat{I}_z^2, \tag{4.46}$$

$$\hat{I}^2 = \tfrac{1}{2}(\hat{I}_+\hat{I}_- + \hat{I}_-\hat{I}_+) + \hat{I}_z^2, \tag{4.47}$$

and

$$\hat{I}^2 = \hat{I}_z(\hat{I}_z + 1) + \hat{I}_-\hat{I}_+, \tag{4.48}$$

which are, again, obtained by direct methods.

## 4.4 Eigenfunctions of the Angular-momentum Operators

Let us consider the $2\ell + 1$ manifold of spherical harmonics $Y_{\ell,m}$. The operator of Eq. 4.12, as applied to any of them, will only affect the azimuthal part $e^{im\phi}$ due to the choice of z as the axis of quantization. After a rotation through $\alpha$, the azimuthal part becomes $e^{im(\phi+\alpha)}$; i.e.,

$$R(\alpha,z) \cdot e^{im\phi} = e^{im(\phi+\alpha)} = e^{im\alpha} \cdot e^{im\phi}, \tag{4.49}$$

which permits us to identify $R(\alpha,z)$ with

$$R(\alpha,z) = e^{im\alpha}, \tag{4.50}$$

which is the character of the representation of the rotation through $\alpha$ spanned by $Y_{\ell,m}$ in the continuous group $C_\infty$ of rotations about z. For infinitesimal rotations, we may write

$$R(\alpha,z) \cdot e^{im\phi} = (1 + im\alpha)\, e^{im\phi}, \tag{4.51}$$

which, by comparison with Eq. 4.12, leads to

$$\hat{I}_z e^{im\phi} = m e^{im\phi}, \tag{4.52}$$

or, in simplified notation,

$$\hat{I}_z u_m = m u_m, \tag{4.53}$$

where $u_m$ is a vector spanning the mth representation of the $C_\infty$ group. Equation 4.53 is fundamental and identifies $u_m$ as an eigenfunction of $\hat{I}_z$ with the eigenvalue m.

The advantages of defining the ladder operators $\hat{I}_+$ and $\hat{I}_-$ of Eqs. 4.39 and 4.40 will now be apparent, since in operating on $u_m$ they give rise to a base vector within the same manifold that transforms according to the $(m+1)$th and the $(m-1)$th representations, respectively, namely,

$$\hat{I}_z(\hat{I}_+ u_m) = (\hat{I}_+\hat{I}_z + \hat{I}_+)\, u_m = \hat{I}_+(\hat{I}_z + 1)\, u_m = (m+1)\, \hat{I}_+ u_m, \tag{4.54}$$

and analogously

$$\hat{I}_z(\hat{I}_- u_m) = (m-1)\,\hat{I}_- u_m. \tag{4.55}$$

The vectors $\hat{I}_+ u_m$ and $\hat{I}_- u_m$, although transforming as $u_{m+1}$ and $u_{m-1}$, are not usually normalized. But the transformation properties are not affected by normalization factors. The unnormalized function $U_m = Cu_m$ will always be an eigenfunction if $u_m$ is itself an eigenfunction, since

$$\hat{I}_z U_m = \hat{I}_z(Cu_m) = m(Cu_m) = mU_m. \tag{4.56}$$

By applying Eqs. 4.54 and 4.55 again and again, we will finally arrive at the highest and lowest values of m in the chosen vector space, supposed to be finite. If we call j the highest value of m, it is clear that

$$\hat{I}_z\hat{I}_+ u_j = (j+1)\,\hat{I}_+ u_j \tag{4.57}$$

is inconsistent with the assumption that j is the maximum value of m within the manifold and Eq. 4.57 must vanish. Analogously,

$$\hat{I}_z\hat{I}_- u_{-j} = -(j+1)\,\hat{I}_- u_{-j} = 0, \tag{4.58}$$

and we are left with $2j + 1$ vectors of

$$m = -j, -(j-1), \ldots, (j-1), j \tag{4.59}$$

Since the number of base vectors is necessarily an integer, j may be integer or half-an-odd integer. Half-an-odd values give rise to double groups in which the identity is rotation through an angle of $4\pi$, while rotation through $2\pi$ just reverses the base vectors.

If we look now at the full rotation group in which $\hat{I}_+$ and $\hat{I}_-$ are symmetry elements, the $2j + 1$ vectors, because they are changed into one another by the ladder operators, must span an irreducible representation, which is known as the $D^{(j)}$ representation.

## 4.5 Normalization of the Ladder-operator Eigenfunctions

We have seen that the operators $\hat{I}_+$ and $\hat{I}_-$ raise and lower the eigenfunctions in such a way that

$$\hat{I}_z\hat{I}_+ u_m = (m+1)\,\hat{I}_+ u_m \tag{4.54}$$

and

$$\hat{I}_z\hat{I}_- u_m = (m-1)\,\hat{I}_- u_m, \tag{4.55}$$

and we anticipated that if $u_m$ was normalized, the new eigenfunctions $\hat{I}_+ u_m$ and $\hat{I}_- u_m$ of eigenvalues $(m+1)$ and $(m-1)$ usually were not normalized. Assume that they are normalized after division by N(m); i.e.,

$$\frac{\hat{I}_+ u_m}{N(m)} = u_{m+1}. \tag{4.60}$$

In such a case,

$$\hat{I}_z \frac{\hat{I}_+ u_m}{N(m)} = \hat{I}_z u_{m+1} = (m+1)\, u_{m+1}. \tag{4.61}$$

In the following, we are going to derive the value of N(m). First, however, we have to find the eigenvalue of $u_m$ when operated by $\hat{I}^2$. Let this eigenvalue be x; i.e.,

$$\hat{I}^2 u_m = x u_m. \tag{4.62}$$

The expectation value of $\hat{I}^2$ is, according to Eq. 3.7,

$$\langle I^2 \rangle = \langle u_m | \hat{I}^2 | u_m \rangle = \langle u_m | \hat{I}^2 u_m \rangle, \tag{4.63}$$

which may be expanded, with the help of Eq. 4.48, as

$$\langle u_m | \hat{I}^2 u_m \rangle = m(m+1) + \langle u_m | \hat{I}_- \hat{I}_+ u_m \rangle. \tag{4.64}$$

To solve the second term of the right-hand side of Eq. 4.64, we have to remember that the angular-momentum operators are Hermitian, since they have real eigenvalues. Let us recall that an operator $\hat{P}$ is Hermitian if

$$\int u^* \hat{P} v \, d\tau = \int v \hat{P}^* u^* \, d\tau, \tag{4.65}$$

which in bracket notation is expressed as

$$\langle u | Pv \rangle = \langle v | P^* u \rangle. \tag{4.66}$$

Therefore, since $\hat{I}_-$ is Hermitian and $\hat{I}_-^* = \hat{I}_+$,

$$\int u_m^* \hat{I}_- (\hat{I}_+ u_m) \, d\tau = \int (\hat{I}_+ u_m) \hat{I}_+ u_m^* \, d\tau, \tag{4.67}$$

or, in bracket notation,

$$\langle u_m | \hat{I}_- \hat{I}_+ u_m \rangle = \langle \hat{I}_+ u_m | \hat{I}_+ u_m \rangle = N^2(m) \langle u_{m+1} | u_{m+1} \rangle, \tag{4.68}$$

which, since $u_{m+1}$ is normalized, simplifies to

$$\langle u_m | \hat{I}_- \hat{I}_+ u_m \rangle = N^2(m). \tag{4.69}$$

In view of Eqs. 4.69 and 4.64, we may write

$$\langle u_m|\hat{I}^2 u_m\rangle = m(m+1) + N^2(m). \tag{4.70}$$

The left-hand side is the expectation value of $\hat{I}^2$; therefore, from Eq. 4.62,

$$\langle u_m|\hat{I}^2 u_m\rangle = x\langle u_m|u_m\rangle = x, \tag{4.71}$$

and the normalization coefficient is then given by

$$N^2(m) = x - m(m+1), \tag{4.72}$$

Since $N^2(m)$ cannot be negative, we obtain for the eigenvalue x the general condition

$$x \geq m(m+1), \tag{4.73}$$

even after repeated application of the raising operator in Eq. 4.60. Since

$$\hat{I}_+ u_j = N(j)u_{j+1} = 0, \tag{4.74}$$

if follows that $N(j) = 0$ and then $x = j(j+1)$, which finally gives

$$\hat{I}^2 u_m^{(j)} = j(j+1)\, u_m^{(j)} \tag{4.75}$$

for all $(2j+1)$ $u_m^{(j)}$ vectors that transform according to the $D^{(j)}$ representation of the full rotation group, irrespective of the value of m. The values of N(m) follow from Eq. 4.72. Consequently, the infinitesimal-rotation operators of the full rotation group have eigenfunctions $u_m^{(j)}$ with the following properties:

$$\hat{I}_z u_m^{(j)} = m u_m^{(j)} \quad \text{with } j \geq m \geq -j; \tag{4.76}$$

$$\hat{I}_+ u_m^{(j)} = \{j(j+1) - m(m+1)\}^{\frac{1}{2}} u_{m+1}^{(j)} = \{(j-m)(j+m+1)\}^{\frac{1}{2}} u_{m+1}^{(j)}; \tag{4.77}$$

$$\hat{I}_- u_m^{(j)} = \{j(j+1) - m(m-1)\}^{\frac{1}{2}} u_{m-1}^{(j)} = \{(j+m)(j-m+1)\}^{\frac{1}{2}} u_{m-1}^{(j)}; \tag{4.78}$$

$$\hat{I}^2 u_m^{(j)} = j(j+1)\, u_m^{(j)}. \tag{4.79}$$

# 5. THE PHENOMENON OF RESONANCE

## 5.1 Mechanism of Absorption

When a magnetic field of strength B is applied to a spin system, the spin angular momentum is quantized in the direction of the field and precesses about it in the way described in Section 1.3. There is a difference, however, in that the magnetogyric ratio of Eq. 1.28 must, in the case of the electron, be multiplied by $g_e = 2.0023$. For simplicity, we take $g_e = 2$ and rewrite Eq. 1.28 as

$$\vec{\mu}_e = 2\gamma\vec{G}, \tag{5.1}$$

where the resolved angular momentum is given by

$$G = m_S\hbar. \tag{5.2}$$

Replacing Eq. 1.29 for $\gamma$ and Eq. 5.2 for G, one arrives at

$$\mu_e = 2m_S\left[\frac{\hbar}{2m}q\ (\text{emu})\right] = 2m_S\mu_B, \tag{5.3}$$

where

$$\mu_B = \frac{\hbar}{2m}q\ (\text{emu}) = \frac{\hbar}{2mc}q\ (\text{esu}) = -0.92732 \times 10^{-20}\ \text{erg/G} \tag{5.4}$$

is the Bohr magneton introduced in Eq. 2.5.

In Section 1.3 we anticipated that the angle $\alpha$ of precession, which was fixed in the classical case by the conditions prevailing when the magnetic field was turned on, is, in the quantum-mechanical model, imposed by the conditions of quantization. We may now look at this problem again and remember what we learned in Chapter 4 about angular-momentum operators. Exactly in the same way as we have orbital angular-momentum operators with orbital angular wavefunctions that are eigenfunctions of these operators with the general properties given in Eqs. 4.76-4.79, we may write $\hat{S}$ instead of $\hat{I}$ and take $m = \pm\frac{1}{2}$ for one electron, which gives rise to two base vectors $u_{1/2}^{(1/2)}$ and $u_{-1/2}^{(1/2)}$. Moreover, remembering Eq. 4.31, one may write

$$\dot{\hat{S}} = \hbar\hat{S}, \tag{5.5}$$

where both $\dot{\hat{S}}$ and $\hat{S}$ are operators. We then find their properties very easily, as follows.

Let $|\alpha\rangle = u_{1/2}^{(1/2)}$ and $|\beta\rangle = u_{-1/2}^{(1/2)}$ be the two spin functions of a single unpaired electron introduced in Section 3.4. We find:

$$\hat{S}^2|\alpha> = S(S+1)|\alpha> = \tfrac{3}{4}|\alpha>, \tag{5.6}$$

$$\hat{S}^2|\beta> = S(S+1)|\beta> = \tfrac{3}{4}|\beta>, \tag{5.7}$$

$$\hat{S}_z|\alpha> = \tfrac{1}{2}|\alpha>, \tag{5.8}$$

$$\hat{S}_z|\beta> = -\tfrac{1}{2}|\beta>, \tag{5.9}$$

$$\hat{S}_+|\alpha> = 0, \tag{5.10}$$

$$\hat{S}_-|\alpha> = |\beta>, \tag{5.11}$$

$$\hat{S}_+|\beta> = |\alpha>, \tag{5.12}$$

and

$$\hat{S}_-|\beta> = 0, \tag{5.13}$$

and, using Eq. 5.5, we obtain

$$\dot{\hat{S}}^2|\alpha> = \hbar^2 S(S+1)|\alpha>, \tag{5.14}$$

$$\dot{\hat{S}}^2|\beta> = \hbar^2 S(S+1)|\beta>, \tag{5.15}$$

$$\dot{\hat{S}}_z|\alpha> = \tfrac{1}{2}\hbar|\alpha>, \tag{5.16}$$

and

$$\dot{\hat{S}}_z|\beta> = -\tfrac{1}{2}\hbar|\beta>. \tag{5.17}$$

Thus, the expectation value of the angular momentum $\dot{\hat{S}}_z$ given by $|\alpha>$, for example, is

$$<\alpha|\dot{\hat{S}}_z|\alpha> = <\alpha|\tfrac{1}{2}\hbar|\alpha> = \tfrac{1}{2}\hbar, \tag{5.18}$$

while the expectation value of $\dot{\hat{S}}^2$ is, for $S = \frac{1}{2}$,

$$<\alpha|\dot{\hat{S}}^2|\alpha> = <\beta|\dot{\hat{S}}^2|\beta> = \tfrac{3}{4}\hbar^2. \tag{5.19}$$

The electron spin may be described according to Eqs. 5.18 and 5.19 as an angular momentum $\hbar\sqrt{S(S+1)} = (\sqrt{3/2})\hbar$ with resolved value $m_S\hbar = \pm\frac{1}{2}\hbar$. This latter is the justification for Eq. 5.2; the former explains why the actual magnetic dipole precesses about the direction of quantization, imposing conditions upon the value of the angle of precession.

Let us assume that the precession occurs inside a cavity which is the seat of a standing microwave of magnetic field vector of strength

$$B_{\perp}(t) = B_0 e^{i\omega t} + B_0 e^{-i\omega t} \tag{5.20}$$

in a direction perpendicular to the externally applied, static field $\vec{B}_{ext}$, as illustrated in Fig. 16. Absorption of microwave power will then occur if the microwave frequency is equal to the frequency of precession of the spin angular momentum. This is easily visualized if one considers Eq. 5.20 where the two terms of the right-hand side represent counter-clockwise and clockwise rotating magnetic fields whose resultant, $B_{\perp}(t)$, oscillates in a perpendicular direction to the static magnetic field. One of the two components will have the sense of rotation of the precession and, provided both frequencies are the same, will continuously accompany the spin, forcing it to change its precession angle $\alpha$ to the other quantum-mechanically allowed value. This jump corresponds to a flip of the electron from the low-energy orientation $m_S = -\frac{1}{2}$ to the high-energy orientation $m_S = \frac{1}{2}$ and will be accomplished by absorption of a microwave photon; i.e.,

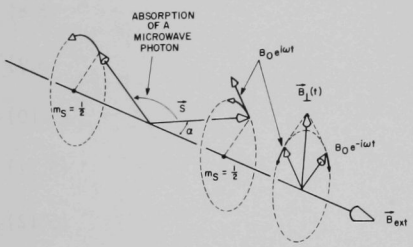


Fig. 16. Precession of the Electron Spin in the Cavity Magnetic Fields

$$\hbar\omega = h\nu = \Delta E = 2\Delta m_S \mu_B B_{ext} = 2\mu_B B_{ext} \tag{5.21}$$

since

$$\Delta m_S = \tfrac{1}{2} - (-\tfrac{1}{2}) = 1. \tag{5.22}$$

The assignment of $m_S = -\frac{1}{2}$ to the low-energy level is due to the negative sign of the electronic charge; the magnetic moment is opposed to $m_S$ and therefore lies parallel to the external magnetic field, corresponding to minimum potential energy. In operator notation, we may write the Hamiltonian as

$$\mathcal{H} = 2\mu_B \hat{S} \cdot \vec{B}, \tag{5.23}$$

where $\vec{B}$ stands for the external field. We may write Eq. 5.23 in terms of the spin operators as

$$\mathcal{H} = 2\mu_B(\hat{S}_x B_x + \hat{S}_y B_y + \hat{S}_z B_z), \tag{5.24}$$

and since, by assumption,

$$B_z = B; \quad B_x = B_y = 0, \tag{5.25}$$

we are left with

$$\mathcal{H} = 2\mu_B \hat{S}_z B. \tag{5.26}$$

Operating on the states $|\alpha\rangle$ and $|\beta\rangle$, we get

$$\langle\alpha|\mathcal{H}|\alpha\rangle = 2\mu_B B\langle\alpha|\hat{S}_z|\alpha\rangle = \mu_B B \tag{5.27}$$

and

$$\langle\beta|\mathcal{H}|\beta\rangle = 2\mu_B B\langle\beta|\hat{S}_z|\beta\rangle = -\mu_B B, \tag{5.28}$$

which are the two energy levels of a free electron in a magnetic field, their difference being given by Eq. 5.21.

## 5.2 Relaxation Processes

In Section 2.4, we saw that steady absorption of power occurs because the electrons promoted to the upper level return to the lower level by radiationless mechanisms. We cited one of these mechanisms: the spin-lattice interaction. In this section, we are going to analyze this and other relaxation processes, as they are generally called. First, we should notice that these processes are exponential in time and lead to "decay" curves of the population in excess over the thermal-equilibrium value which may, and indeed are, measured by pulse techniques. Thus, we may define as relaxation time the time required for a drop of the signal intensity to a conventional fraction of the initial intensity, such as 1 - 1/e. The precise definition is not needed in the argument that follows, which is essentially valid in order of magnitude.

The effect of the spin relaxation on EPR measurements appears in connection with Heisenberg's uncertainty principle. Recall that this principle states that it is impossible to determine, precisely and simultaneously, the momentum p and the position coordinate q of a particle, or any pair of conjugate variables such as, for example, energy and time. The uncertainty $\delta$ in each observable is given by

$$\delta p \cdot \delta q \approx \hbar \tag{5.29}$$

or

$$\delta E \cdot \delta t \approx \hbar. \tag{5.30}$$

If we substitute the relaxation time $\tau$ for $\delta t$, we find

$$\delta \Delta E \cdot \tau \approx \hbar, \tag{5.31}$$

where $\delta \Delta E$ is now the uncertainty in the transition energy. Since this latter is given by

$$\Delta E = \hbar\omega, \tag{5.21}$$

where $\omega$ is $2\pi$ times the microwave frequency, we may write the uncertainty in the transition energy as

$$\delta\Delta E = \hbar\delta\omega, \tag{5.32}$$

which immediately gives

$$\tau\delta\omega \sim 1. \tag{5.33}$$

Interpretation of Eq. 5.33 is straightforward. If the relaxation time is very short, the absorption signal will be very broad, and conversely, if the relaxation time is very long, the absorption signal will be very narrow, assuming absence of other broadening and narrowing mechanisms.

Equation 5.33 may be used for an operational definition of the relaxation time as the value for which

$$\tau\delta\omega = 1 \tag{5.34}$$

after a convention has been adopted to measure $\delta\omega$, such as, for example, the width of the absorption line at half-height.

The physical reason behind the relaxation processes was explained by Bloch as applied to nuclear relaxation processes. His equations describe equally well the behavior of an electron-spin system, as follows.

The basic idea behind Bloch's treatment is that the magnetization of a substance tends exponentially toward its thermal-equilibrium value $M_0$ due to two well-defined processes of interaction. Suppose that in our cavity the electron magnetic moments are precessing about the resultant of the external field and the instantaneous value of the oscillatory field $B_\perp$. Turning off the $B_\perp$ field will, in general, leave the electron magnetic moment pointing in a direction that will <u>not</u> be the direction of the external field $B_{ext}$. The electron magnetic moment will start to precess about $B_{ext}$ in a nonequilibrium cone. If the direction of $B_{ext}$ is taken as the z axis, the component of the magnetization along z will increase as the magnetization vector $\vec{M}$ moves toward the z axis. This process requires the dipole to give up energy to the lattice and is called spin-lattice relaxation. At the same time, the component perpendicular to the z axis will also change, due to a more complex effect. The component of the magnetization perpendicular to the z axis was given, while $B_\perp$ was applied, by the vector sum of all the individual electron magnetic moments along such direction; these electrons were precessing about individual fields arising from $B_\perp$ and $B_{ext}$ and those due to local magnetic interactions. As soon as $B_\perp$ is turned off, the coherence of the individual components is lost and $M_\perp$, the component

of the magnetization perpendicular to z, starts to decay, also exponentially. This process involves spin-spin, rather than spin-lattice, interaction and is likely to have a different relaxation time. If both relaxations are assumed to be exponential, they may be expressed by Bloch's equations

$$(d/dt)M_z = (1/T_1)(M_0 - M_z) \tag{5.35}$$

and

$$(d/dt)M_\perp = -(1/T_2)M_\perp, \tag{5.36}$$

where

$T_1$ = spin-lattice or longitudinal relaxation time,

and

$T_2$ = spin-spin or transverse relaxation time.

In terms of spin operators, $T_1$ is associated with the change in states given by the eigenvalues of $\hat{S}_z$. The transverse relaxation time $T_2$ accounts for the fact that the randomness in equilibrium of the $S_x$ and $S_y$ components of the various spins of a sample is broken down by the microwave field. Randomness is removed because the actual magnetic field acting on each electron is given by the vector sum of the external and the microwave fields and does not in general coincide with the direction of the former. Terms involving $S_x$ and $S_y$ have then to be taken into account, giving rise to various degrees of coherence. The loss of this transverse coherence when the microwave field vanishes determines the relaxation time $T_2$, which in turn affects the line width, through Heisenberg's principle. When $T_2$ is very long, almost perfect coherence is achieved and the line is very narrow. These types of broadening determine, if they are dominant, the shape of the absorption line as Lorentzian, together with other processes such as exchange interaction between like centers, which has no classical analog. This shape is easily recognizable: It narrows the absorption curve in the center and broadens it in the low-absorption tails. When the width of the line is due to random orientation in the presence of anisotropy, it takes the form of a random-distribution function and called Gaussian.

A typical case of exchange narrowing is provided by solid DPPH (1,1-diphenyl-2-pycryl hydrazyl), which is a rather stable radical of structural formula

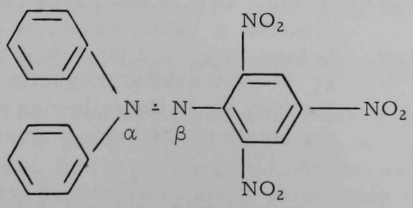


that is widely used in EPR as a standard.

## 5.3 Zeeman Hamiltonian When J Is a Good Quantum Number

When Russell-Saunders coupling is dominant, the vectors $\vec{L}$ and $\vec{S}$ couple together to give a vector $\vec{J}$ according to

$$\vec{J} = \vec{L} + \vec{S}. \tag{5.37}$$

To the vector $\vec{J}$ there corresponds a quantum number J, which is an integer or half-an-integer according to whether S is an integer or half-an-integer, since L is always an integer. When Russell-Saunders coupling occurs, J is a good quantum number. In the absence of an external magnetic field, the 2J + 1 manifold of states of $m_J = -J, -(J-1), \ldots, (J-1), J$ is degenerate. The degeneracy is lifted by the magnetic field, and the Zeeman term of the Hamiltonian takes the form

$$\mathcal{H} = g_J \mu_B \hat{J} \cdot \vec{B}. \tag{5.38}$$

For $B = B_z$, $B_x = B_y = 0$, and the state $|Jm_J\rangle$, we find, in general,

$$\langle Jm_J|\mathcal{H}|Jm_J\rangle = g_J \mu_B B \langle Jm_J|\hat{J}_z|Jm_J\rangle = m_J g_J \mu_B B, \tag{5.39}$$

where $|Jm_J\rangle$ is an eigenfunction of $\hat{J}_z$ with the eigenvalue $m_J$. Next we proceed to evaluate $g_J$.

The vector diagram of angular-momentum coupling in the Russell-Saunders case is illustrated in Fig. 17, at the top. The bottom of the same figure shows the coupling of the associated magnetic moments. Two features strike our attention. On the one hand, the magnetic dipoles are oriented in the opposite direction to that of the angular momenta; this is due, as we have already seen, to the negative sign of the electronic charge. On the other hand, we notice that the magnetic moment of the electron is twice the length of its angular momentum in the arbitrary units in which both orbital angular momentum and magnetic moment have the same length. This is due to the anomalous electron g value, which, as anticipated before, is $g_S = 2.0023 \approx 2$, instead of $g_L = 1$ for orbital magnetic moments. We may write the following values for the length of the vectors quantities of Fig. 17:

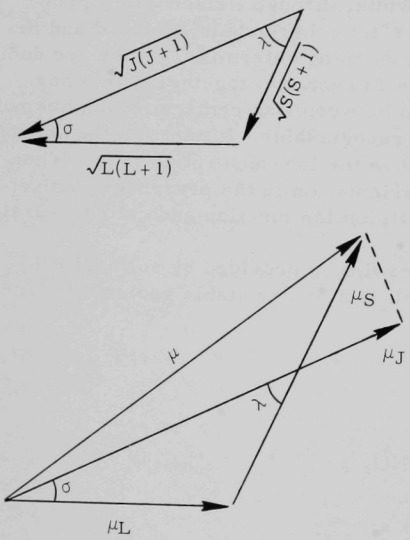


Fig. 17. Association of Magnetic Moments in Russell-Saunders Coupling

$$\text{Length of spin vector} = \hbar\sqrt{S(S+1)}; \tag{5.40}$$

$$\text{Length of orbital vector} = \hbar\sqrt{L(L+1)}; \tag{5.41}$$

$$\text{Length of J vector} = \hbar\sqrt{J(J+1)}. \tag{5.42}$$

In turn, the magnetic moments are given by

$$\mu_S = g_S\mu_B\sqrt{S(S+1)} \tag{5.43}$$

and

$$\mu_L = g_L\mu_B\sqrt{L(L+1)}, \tag{5.44}$$

and that in the direction of $\vec{J}$, which is the one in which we are interested, is

$$\mu_J = \mu_L \cos\sigma + \mu_S \cos\lambda. \tag{5.45}$$

If we use Eqs. 5.40-5.42 and the property of the triangles of sides a, b, and c,

$$a^2 + b^2 - 2ab\cos(a,b) = c^2, \tag{5.46}$$

the trigonometric functions are given by

$$\cos\sigma = \frac{L(L+1) + J(J+1) - S(S+1)}{2\sqrt{L(L+1)\,J(J+1)}} \tag{5.47}$$

and

$$\cos\lambda = \frac{S(S+1) + J(J+1) - L(L+1)}{2\sqrt{S(S+1)\,J(J+1)}}. \tag{5.48}$$

Remembering that $g_L = 1$ and $g_S = 2$, and making

$$\mu_J = g_J\mu_B\sqrt{J(J+1)} \tag{5.49}$$

for notation consistency, one finally arrives at

$$g_J = 1 + \frac{J(J+1) + S(S+1) - L(L+1)}{2J(J+1)}. \tag{5.50}$$

Departures from this value are usually due to admixture of excited states.

## 5.4 The General Case: Effective-spin Hamiltonian

The Zeeman Hamiltonian when spin-only paramagnetism exists and when J is a good quantum number is isotropic and the g value is a scalar. This is not, however, the general case; admixture of excited states not only imposes a departure of the g value from the ground state one, but also

determines in most cases the appearance of anisotropy, as explained in Section 2.4. We are now going to consider the general problem of constructing a Hamiltonian suitable for computation. We assume that the paramagnetic ion is in a known environment. In other words, we assume that we have solved the crystal-field problem and know, in consequence, the splitting of the electronic levels.

There are in a paramagnetic system three magnetic operators: the electron-spin operator $\hat{S}$, the electron-orbital angular-momentum operator $\hat{L}$, and the nuclear-spin operator $\hat{I}$. In all three, we define operators along x, y, and z, as well as the raising and lowering operators defined in Eqs. 4.39 and 4.40. We notice, incidentally, that the formalism of these operators is exactly the same in all cases; their difference consists in the type of eigenfunctions they have, as indicated by the letter used as their symbol. Thus, $\hat{S}$ operators operate on electron-spin coordinates and commute with all others, $\hat{L}$ operators on angular functions of the spatial coordinates and commute with all others, and $\hat{I}$ operators on the nuclear-spin coordinates and commute with all others. Therefore, when we have, for example, an expression such as $\hat{L} \cdot \hat{S}$ it is supposed to operate on the wavefunction $|\ell m \alpha\rangle$ in the following way:

$$\langle \ell m \alpha | \hat{L}_z \cdot \hat{S}_z | \ell m \alpha \rangle = \langle \ell m | \hat{L}_z | \ell m \rangle \langle \alpha | \hat{S}_z | \alpha \rangle = \tfrac{1}{2} m, \tag{5.51}$$

because $\hat{L}$ commutes with $|\alpha\rangle$ and $\hat{S}$ commutes with $|\ell m\rangle$.

In the magnetic experiment, we have to consider six terms in addition to the crystal-field terms to be discussed later: the three terms arising from coupling of $\hat{S}$, $\hat{L}$, and $\hat{I}$ with the external magnetic field $\vec{B}$, and the three interaction terms $\hat{S} \cdot \hat{L}$, $\hat{L} \cdot \hat{I}$, and $\hat{S} \cdot \hat{I}$. They are usually written

$$\mathcal{H}_{ZE} = \mu_B (\hat{L} + 2\hat{S}) \cdot \vec{B}, \tag{5.52}$$

$$\mathcal{H}_{ZN} = -g_N \mu_N \hat{I} \cdot \vec{B}, \tag{5.53}$$

$$\mathcal{H}_{HF} = K \hat{S} \cdot \hat{I} + 2\mu_B g_N \mu_N \left\{ 3 \frac{(\hat{S} \cdot \vec{r})(\hat{I} \cdot \vec{r})}{r^5} - \frac{\hat{S} \cdot \hat{I}}{r^3} \right\}, \tag{5.54}$$

$$\mathcal{H}_{LS} = \hat{S} \cdot \hat{\lambda}(r) \cdot \hat{I} = \lambda \hat{S} \cdot \hat{I}, \tag{5.55}$$

and

$$\mathcal{H}_{LI} = 2\mu_B g_N \mu_N \frac{L \cdot I}{r^3}. \tag{5.56}$$

Both electron orbital and spin Zeeman coupling are taken together. The negative sign affecting Eq. 5.53 arises from the fact that the nuclear magnetic moment is generally positive, as opposed to the electronic charge.

Therefore $m_I$ and the resolved magnetic moment have the same sign. All the terms, on the other hand, correspond to a decrease in the potential energy. Another way to look at it is to state that $\mu_N$, the nuclear magneton, is defined as a positive constant, while the Bohr magneton $\mu_B$ is negative, according to Eq. 5.4. The $g_N$ value for the nucleus is introduced because of the use of the nuclear magneton. The magnetic moment of the nucleus is then

$$\text{nuclear magnetic moment} = g_N \mu_N \sqrt{I(I+1)}, \tag{5.57}$$

and its resolved values in the magnetic experiment are, in complete analogy with $\hat{L}$ and $\hat{S}$,

$$m_I g_N \mu_N. \tag{5.58}$$

We may therefore define nuclear-spin wavefunctions that are eigenfunctions of the $\hat{I}$ operator. For convenience of notation, when $I = \frac{1}{2}$, these wavefunctions are called $|\alpha_N>$ and $|\beta_N>$. Thus, the properties of the $\hat{I}$ operators are:

$$\hat{I}^2|\alpha_N> = I(I+1)|\alpha_N>; \tag{5.59}$$

$$\hat{I}^2|\beta_N> = I(I+1)|\beta_N>; \tag{5.60}$$

$$\hat{I}_z|\alpha_N> = \tfrac{1}{2}|\alpha_N>; \tag{5.61}$$

$$\hat{I}_z|\beta_N> = -\tfrac{1}{2}|\beta_N>; \tag{5.62}$$

$$\hat{I}_+|\alpha_N> = 0; \tag{5.63}$$

$$\hat{I}_-|\alpha_N> = |\beta_N>; \tag{5.64}$$

$$\hat{I}_+|\beta_N> = |\alpha_N>; \tag{5.65}$$

$$\hat{I}_-|\beta_N> = 0. \tag{5.66}$$

When Eqs. 5.52 and 5.54-5.56 are worked out with perturbation theory, as we see in Chapters 6 and 7, it is possible to gather the different effects in two terms:

$$\mathcal{H} = \mu_B \hat{S} \cdot \hat{g} \cdot \vec{B} + \hat{S} \cdot \hat{A} \cdot \hat{I}, \tag{2.35}$$

which is the Hamiltonian introduced in Section 2.4. We have now to add the nuclear Zeeman term of Eq. 5.53 and at least three other terms that will be discussed in Chapter 8. We finally obtain

$$\mathcal{H} = \mu_B \hat{S} \cdot \hat{g} \cdot \vec{B} + \hat{S} \cdot \hat{A} \cdot \hat{I} - 2\mu_B g_N \mu_N \hat{I} \cdot \hat{B} + D[\hat{S}_z^2 - \tfrac{1}{3}S(S+1)]$$

$$+ E(\hat{S}_x^2 - \hat{S}_y^2) + P[\hat{I}_z^2 - \tfrac{1}{3}I(I+1)] + P'(\hat{I}_x^2 - \hat{I}_y^2), \qquad (2.36)$$

where D and E are crystal-field terms that vanish when $S = \frac{1}{2}$ and P and P' are nuclear electric-quadrupole terms that vanish when $I = \frac{1}{2}$, discussed in Sections 8.1 and 8.3.

The first term includes spin and orbital Zeeman coupling. The second term includes hyperfine interaction and orbital effects. The spin-orbit coupling term of Eq. 5.55 is now hidden in the first two terms and in the crystal-field terms. Therefore, most of the individual effects listed in Eqs. 5.52-5.56 have lost their identity in the new Hamiltonian, to the extent that the spin operator $\hat{S}$ that appears in Eq. 5.67 can no longer be taken as the spin operator of Section 5.1. The new operator, called effective-spin operator, not only operates on the spin coordinates, but also, as anticipated in Section 2.4, on the unquenched orbital angular momentum. Strictly, one should use a different symbol for this operator, but the fact that it approaches the ordinary spin operator as the admixture of excited states decreases has imposed the use of the same symbol. In the following chapters, we are going to discuss separately the various terms of the spin Hamiltonian of Eq. 5.67.

# 6. THEORY OF THE $\hat{g}$ TENSOR

## 6.1 Crystal-field Splitting of Electronic Levels

By crystal field we mean any environment about a paramagnetic ion or an inorganic radical arising from the more or less regular distribution of electric charges (ions) or electric dipoles (for example, water of hydration) around it. The crystal-field approach strictly applies when there is no overlapping between the central ion atomic orbitals (AO) and the immediate neighbors, which we refer to from now on as ligand molecules. In the presence of various degrees of covalency, it is necessary to make linear combinations of AO's of the central atoms and the ligand molecules to form molecular orbitals (MO's). In all cases, the symmetry requirements remain exactly the same. For simplicity, we are going to review quickly the results of crystal-field theory as applied to paramagnetic ions and leave the MO approach for later discussion.

The nature of the crystal field lies in the creation of an electric field around the central ion. As we have seen in Section 1.6, the point group of a uniform electric field is $C_{\infty v}$ ($\infty$m), containing therefore infinite planes of symmetry whose intersection determines the $\infty$-fold axis of symmetry, $C_{\infty}$. The problem for a paramagnetic ion surrounded by a more or less regular, three-dimensional array of immediate neighbors reduces to finding the symmetry point group of the configuration and the strength of the electrostatic interactions.

It is convenient to start by studying a regular-octahedron arrangement of ligands which belongs to the symmetry point group $O_h$ (m3m). Appropriate distortion along the diagonal intersecting the centers of any pair of parallel faces in the octahedron will descend the symmetry to the trigonal point groups. Analogously, a distortion along opposed vertices will lead to the tetragonal groups. Further distortions will eventually give rise to the point groups of lower symmetry.

Let us first consider the regular octahedron. Having solved the Schroedinger equation taking the z axis as the axis of quantization, which is one of the three equivalent octahedral axes, we find ourselves with several manifolds of different $\ell$, according to what was discussed at length in Chapter 3. The existence of planes of symmetry containing the z axis makes the pairs of complex wavefunctions $(x+iy)^n$ and $(x-iy)^n$ equivalent since they represent states of +m and -m, and the magnetic moments are reversed by planes of symmetry parallel to them. The equivalence of $(x+iy)^n$ and $(x-iy)^n$ becomes obvious when one considers the xz plane of symmetry, which only changes y into -y. We have then to take linear combinations of both wavefunctions, such as those given in Eqs. 3.16 and 3.17, which are no longer complex, or, simply enough, the real orthogonal solutions studied in Section 3.3.

An inspection of Fig. 18 and Table II will convince us that for a $d^1$ ion, the fivefold manifold of d orbitals splits into a threefold manifold of orbitally degenerate orbitals of low energy (because the electronic repulsion is minimum) and a twofold manifold of orbitally degenerate orbitals of high energy (because the electrostatic repulsion is maximum). In a $d^9$ ion, on the other hand, the splitting will be reversed, as indicated in Fig. 19 because promotion of an unpaired electron can only correspond to the unpairing of a paired one, a process that may be described as promotion of a positive hole in the opposite direction. In the hole formalism, which is rigorous, the sign of the crystal field changes, and the splitting of levels is reversed.

We may now effect a tetragonal distortion in the octahedron of the $d^9$ configuration by either compressing or elongating the octahedron about z. Both cases are illustrated in Fig. 20. A strong distortion by elongation leads to the square planar configuration so common in $Cu^{2+}(3d^9,{}^2D)$ and $Ag^{2+}(4d^9,{}^2D)$ complex ions. A further orthorhombic distortion, also indicated in Fig. 20, removes all orbital degeneracies. This is a natural consequence of the fact that all orthorhombic and less-symmetric point groups are Abelian; all the representations are therefore one-dimensional, and all bases have to be taken separately. Abelian groups that are not cyclic cannot have orbital degeneracy. There is, however, spin degeneracy, as stated by Kramers' theorem, which is considered in the next section.

## 6.2 Kramers' Theorem of Spin Degeneracy

Kramers' theorem states that the energy levels of a system of atoms in an external field of purely electrical origin are necessarily twice degenerate if the number of electrons in the system is odd. This is the basic theorem of EPR, for the magnetic field lifts the spin degeneracy left by the crystal field, thereby creating magnetic levels between which electronic transitions may be observed.

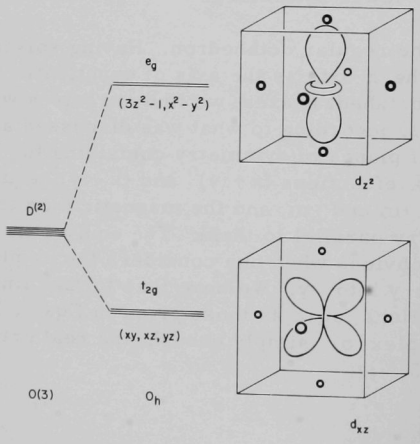


Fig. 18

Octahedral Splitting of the Manifold of d Orbitals

TABLE II. Character Table and Bases for the Representation of the $O_h$ Group

$O_h$ = m3m,
cubic.

| $O_h$ | E | $8C_3$ | $6C_2$ | $6C_4$ | $3C_2(=C_4^2)$ | i | $6S_4$ | $8S_6$ | $3\sigma_h$ | $6\sigma_d$ |
|---|---|---|---|---|---|---|---|---|---|---|
| $A_{1g}$ | 1 | 1 | 1 | 1 | 1 | 1 | 1 | 1 | 1 | 1 |
| $A_{2g}$ | 1 | 1 | -1 | -1 | 1 | 1 | -1 | 1 | 1 | -1 |
| $E_g$ | 2 | -1 | 0 | 0 | 2 | 2 | 0 | -1 | 2 | 0 |
| $T_{1g}$ | 3 | 0 | -1 | 1 | -1 | 3 | 1 | 0 | -1 | -1 |
| $T_{2g}$ | 3 | 0 | 1 | -1 | -1 | 3 | -1 | 0 | -1 | 1 |
| $A_{1u}$ | 1 | 1 | 1 | 1 | 1 | -1 | -1 | -1 | -1 | -1 |
| $A_{2u}$ | 1 | 1 | -1 | -1 | 1 | -1 | 1 | -1 | -1 | 1 |
| $E_u$ | 2 | -1 | 0 | 0 | 2 | -2 | 0 | 1 | -2 | 0 |
| $T_{1u}$ | 3 | 0 | -1 | 1 | -1 | -3 | -1 | 0 | 1 | 1 |
| $T_{2u}$ | 3 | 0 | 1 | -1 | -1 | -3 | 1 | 0 | 1 | -1 |

Bases:

| | | | | |
|---|---|---|---|---|
| $A_{1g}$ | | | $x^2 + y^2 + z^2$ | |
| $E_g$ | | | $(2z^2 - x^2 - y^2, x^2 - y^2)$ | |
| $T_{1g}$ | $(R_x, R_y, R_z)$ | | | |
| $T_{2g}$ | | | $(xy, yz, xz)$ | |
| $A_{2u}$ | | | | $xyz$ |
| $T_{1u}$ | | $(x, y, z)$ | | $[x(2x^2 - 3y^2 - 3z^2), y(2y^2 - 3z^2 - 3x^2), z(2z^2 - 3x^2 - 3y^2)]$ |
| $T_{2u}$ | | | | $[x(y^2 - z^2), y(z^2 - x^2), z(x^2 - y^2)]$ |

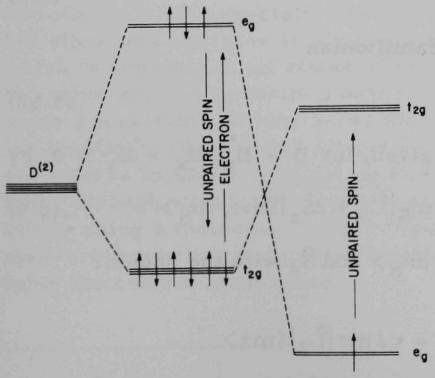


Fig. 19. Equivalence of the Hole Formalism

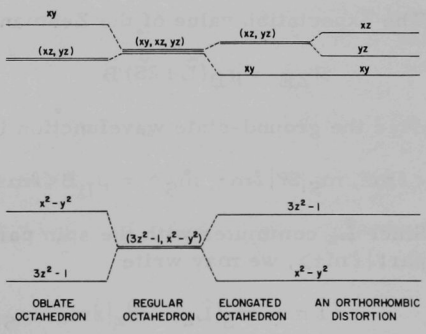


Fig. 20. Crystal-field Splitting of the $d^9$ Configuration in Various Symmetries

Kramers' theorem appears as a consequence of the polar character of the electric vector and the axial character of the magnetic vector. In a system of an odd number of electrons, at least one of them must have its spin uncompensated. Let it be represented by the spin vector $\vec{S}$. We apply an electric field which is characterized by infinite planes of symmetry containing the $\infty$-fold axis. The spin vector will lie in one of them. Since the spin vector is axial, it will be reversed by such a plane, with the result

$$-\vec{S} = \sigma_v \cdot \vec{S}. \tag{6.1}$$

Since $\sigma_v$ is an operation of symmetry in the electric field, $-\vec{S}$ and $\vec{S}$ must have the same energy and the level is then twofold degenerate. This degeneracy is lifted by the magnetic field, which quantizes the spin vector and does not contain $\sigma_v$. In the new system, $\vec{S}$ and $-\vec{S}$ have different energies, giving rise to the splitting of levels that allows electron transitions to occur.

## 6.3 Zeeman Term of an Orbital-singlet Ground State

Let us see what happens if the lowest-lying crystal-field level with an unpaired electron is an orbital singlet, in other words, if the unpaired electron is in an orbitally nondegenerate orbital. In the presence of the crystal field, we know that a single level corresponds to a real (or imaginary, but never complex) wavefunction

$$\frac{1}{\sqrt{2}}\left(Y_{\ell,m} \pm Y_{\ell,-m}\right) = |\ell m\pm\rangle, \tag{6.2}$$

or, if $m = 0$, to

$$Y_{\ell,0} = |\ell 0\rangle. \tag{6.3}$$

The expectation value of the Zeeman Hamiltonian

$$\mathcal{H}_{ZE} = \mu_B(\hat{L} + 2\hat{S})\,\vec{B} \tag{5.52}$$

over the ground-state wavefunction is given, for $B = B_z$, $B_x = B_y = 0$, by

$$\langle \ell m\pm, m_S|\mathcal{H}|\ell m\pm, m_S\rangle = \mu_B B\langle \ell m\pm, m_S|\hat{L}_z + 2\hat{S}_z|\ell m\pm, m_S\rangle. \tag{6.4}$$

Since $\hat{L}_z$ commutes with the spin part $|m_S\rangle$ and $\hat{S}_z$ with the angular part $|\ell m\pm\rangle$, we may write

$$\langle \ell m\pm, m_S|\hat{L}_z + 2\hat{S}_z|\ell m\pm, m_S\rangle = \langle \ell m\pm|\hat{L}_z|\ell m\pm\rangle + 2\langle m_S|\hat{S}_z|m_S\rangle. \tag{6.5}$$

First we notice that

$$\langle \ell m\pm|\hat{L}_z|\ell m\pm\rangle = \langle \ell m\pm|m|\ell m\mp\rangle \tag{6.6}$$

since

$$\hat{L}_z(Y_{\ell,m} \pm Y_{\ell,-m}) = m(Y_{\ell,m} \mp Y_{\ell,-m}). \tag{6.7}$$

Because $|\ell m+\rangle$ and $|\ell m-\rangle$ are orthogonal, we find

$$\langle \ell m\pm|\hat{L}_z|\ell m\pm\rangle = 0, \tag{6.8}$$

with the meaning that an orbital singlet has no angular momentum. Solution of the spin part is straightforward:

$$\langle m_S|\hat{S}_z|m_S\rangle = m_S, \tag{6.9}$$

and the values of the Zeeman Hamiltonian reduce to the already well-known energies of Eqs. 2.3 and 2.4.

## 6.4 Orbital Admixture: Perturbed Ground State

To account for departures of the g values from the free-electron one, we must consider admixture of excited states $|n\rangle$ into the ground state $|0\rangle$. Admixture occurs through spin-orbit coupling to a degree determined by the crystal-field splitting. This is the only way an unpaired electron in the ground state may acquire some orbital angular momentum and is represented by the term

$$\mathcal{H}_{LS} = \lambda \hat{L} \cdot \hat{S}. \tag{5.55}$$

Strictly, $\lambda$ is the expectation value of the spin-orbit coupling operator $\hat{\lambda}(r)$,* but since this operator is averaged over the radial part of the wavefunction, which is common to all states of the same principal quantum number n and the same angular quantum number $\ell$, it is a constant for all electrons of the same $\ell$ manifold and may be written as a scalar in Eq. 5.55. Therefore, the treatment that follows should be applied in cases in which the unpaired electron is localized completely in the central atom. Introduction of covalency through wavefunction overlapping may be handled in a similar way, but by using a molecular rather than an atomic orbital, in which case the spin-orbit coupling parameter loses its identity of a parameter characterizing the central atom alone.

---

*$\lambda(r) = \dfrac{e\hbar^2}{2m^2c^2}\left[\dfrac{1}{r}\dfrac{\partial}{\partial r}V(r)\right]$.

Perturbation theory gives, for the perturbed wavefunction that we call $|\pm\rangle$, the expression

$$|\pm\rangle = |0\rangle - \sum_n \frac{\lambda\langle n|\hat{L}\cdot\hat{S}|0\rangle}{E_n - E_0}|n\rangle, \tag{6.10}$$

which is a good approximation, provided $\lambda$ is much smaller than $E_n - E_0$. For computation, the operator $\hat{L}\cdot\hat{S}$ may be put in the more useful form

$$\hat{L}\cdot\hat{S} = \hat{L}_z\hat{S}_z + \tfrac{1}{2}(\hat{L}_+\hat{S}_- + \hat{L}_-\hat{S}_+). \tag{6.11}$$

The physical interpretation of Eq. 6.11 is interesting. $\hat{L}_z\hat{S}_z$ will mix excited states of the spin of the ground state, while the ladder operators will mix $|0\alpha\rangle$ with $|n\beta\rangle$ and $|0\beta\rangle$ with $|n\alpha\rangle$. When the perturbation of Eq. 6.10 is applied to $|0\alpha\rangle$ and $|0\beta\rangle$ it is found, by using Eq. 6.11, that

$$|+\rangle = |0\alpha\rangle - \tfrac{1}{2}\lambda\sum_n \frac{\langle n|\hat{L}_z|0\rangle}{E_n - E_0}|n\alpha\rangle - \tfrac{1}{2}\lambda\sum_n \frac{\langle n|\hat{L}_+|0\rangle}{E_n - E_0}|n\beta\rangle \tag{6.12}$$

and

$$|-\rangle = |0\beta\rangle + \tfrac{1}{2}\lambda\sum_n \frac{\langle n|\hat{L}_z|0\rangle}{E_n - E_0}|n\beta\rangle - \tfrac{1}{2}\lambda\sum_n \frac{\langle n|\hat{L}_-|0\rangle}{E_n - E_0}|n\alpha\rangle. \tag{6.13}$$

We now define effective-spin operators such that

$$\hat{S}_z|+\rangle = \tfrac{1}{2}|+\rangle; \tag{6.14}$$

$$\hat{S}_z|-\rangle = -\tfrac{1}{2}|-\rangle; \tag{6.15}$$

$$\hat{S}_+|+\rangle = 0; \tag{6.16}$$

$$\hat{S}_-|+\rangle = |-\rangle; \tag{6.17}$$

$$\hat{S}_+|-\rangle = |+\rangle; \tag{6.18}$$

$$\hat{S}_-|-\rangle = 0. \tag{6.19}$$

Notice that $|+\rangle$ and $|-\rangle$ are no longer eigenfunctions of the true spin operator $\hat{S}_z$ for which no different symbol is used.

In general, the effective-spin Hamiltonian we want to solve will have nondiagonal elements in an arbitrary frame, i.e.,

$$\mathcal{H} = \mu_B \hat{S} \cdot \begin{pmatrix} g_{xx} & g_{xy} & g_{xz} \\ g_{xy} & g_{yy} & g_{yz} \\ g_{xz} & g_{yz} & g_{zz} \end{pmatrix} \cdot \vec{B}, \tag{6.20}$$

and for $B = B_z$, $B_x = B_y = 0$, we may write

$$\mathcal{H} = \mu_B B(g_{zx}\hat{S}_x + g_{zy}\hat{S}_y + g_{zz}\hat{S}_z), \tag{6.21}$$

since $\vec{B}$ and $\hat{S}$ commute and $g_{ij} = g_{ji}$. We have now to find expressions for $\hat{S}_x$ and $\hat{S}_y$. They may be put in the form

$$\hat{S}_x = \tfrac{1}{2}(\hat{S}_+ + \hat{S}_-) \tag{6.22}$$

and

$$\hat{S}_y = -(i/2)(\hat{S}_+ - \hat{S}_-), \tag{6.23}$$

which, by using Eqs. 6.16 to 6.19, lead to

$$\hat{S}_x|+> = \tfrac{1}{2}|->; \tag{6.24}$$

$$\hat{S}_y|+> = (i/2)|->; \tag{6.25}$$

$$\hat{S}_x|-> = \tfrac{1}{2}|+>; \tag{6.26}$$

$$\hat{S}_y|-> = -(i/2)|+>. \tag{6.27}$$

Operation on $|+>$ and $|->$ by Eq. 6.21 results in the following 2 x 2 matrix:

$$\begin{array}{c|cc} & |+> & |-> \\ \hline <+| & \tfrac{1}{2}\mu_B B g_{zz} & \tfrac{1}{2}\mu_B B(g_{zx} - ig_{zy}) \\ <-| & \tfrac{1}{2}\mu_B B(g_{zx} + ig_{zy}) & -\tfrac{1}{2}\mu_B B g_{zz} \end{array} \tag{6.28}$$

On the other hand, if we solve for the true Zeeman Hamiltonian of Eq. 5.52, we obtain the 2 x 2 matrix

$$\mu_B B \begin{pmatrix} <+|\hat{L}_z + 2\hat{S}_z|+> & <+|\hat{L}_z + 2\hat{S}_z|-> \\ <-|\hat{L}_z + 2\hat{S}_z|+> & <-|\hat{L}_z + 2\hat{S}_z|-> \end{pmatrix}. \tag{6.29}$$

The matrices of Eqs. 6.28 and 6.29 are just two different expressions of the same physical phenomenon and must therefore be identical, which can only be true if

$$g_{zz} = 2\langle +|\hat{L}_z + 2\hat{S}_z|+\rangle = -2\langle -|\hat{L}_z + 2\hat{S}_z|-\rangle, \tag{6.30}$$

$$g_{zx} + ig_{zy} = 2\langle -|\hat{L}_z + 2\hat{S}_z|+\rangle, \tag{6.31}$$

and

$$g_{zx} - ig_{zy} = -2\langle +|\hat{L}_z + 2\hat{S}_z|-\rangle. \tag{6.32}$$

After direct computation of Eq. 6.30, we obtain

$$g_{zz} = 2 - 2\lambda \sum_n \frac{\langle 0|\hat{L}_z|n\rangle\langle n|\hat{L}_z|0\rangle}{E_n - E_0}. \tag{6.33}$$

From Eqs. 6.31 and 6.32, the off-diagonal matrix elements become

$$g_{ij} = 2\delta_{ij} - 2\lambda \sum_n \frac{\langle 0|\hat{L}_i|n\rangle\langle n|\hat{L}_j|0\rangle}{E_n - E_0}. \tag{6.34}$$

The physical meaning of these equations is not immediately obvious; in the next section, we are going to try to find such a meaning.

## 6.5 Physical Meaning of Admixture

Equation 6.32 will now be solved for a $d^9$ ion in square planar configuration, such as $Cu^{2+}$, whose crystal-field splitting is illustrated in Fig. 21. Since the square planar configuration has axial symmetry, we may write

$$g_{\parallel} = 2 - 2\lambda \frac{\langle x^2 - y^2|\hat{L}_z|xy\rangle\langle xy|\hat{L}_z|x^2 - y^2\rangle}{E_{xy} - E_{x^2-y^2}} \tag{6.35}$$

and, for example,

$$g_{\perp} = 2 - 2\lambda \frac{\langle x^2 - y^2|\hat{L}_x|xz,\, yz\rangle\langle xz,\, yz|\hat{L}_x|x^2 - y^2\rangle}{E_{(xz,yz)} - E_{x^2-y^2}}, \tag{6.36}$$

which readily lead to

$$g_{\parallel} = 2 - 8\frac{\lambda}{\Delta_{\parallel}} \tag{6.37}$$

and

$$g_{\perp} = 2 - 2\,\frac{\lambda}{\Delta_{\perp}}, \tag{6.38}$$

known as Polder's relations. For simplicity of notation, we have written

$$\Delta_{\parallel} = E_{xy} - E_{x^2-y^2}; \quad \Delta_{\perp} = E_{(xz,yz)} - E_{x^2-y^2}. \tag{6.39}$$

The choice of excited states in Eqs. 6.35 and 6.36 may be done on the basis of group theoretical considerations, as follows.

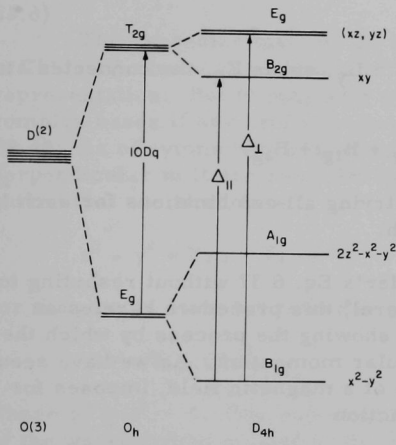


Fig. 21

Crystal-field Splitting of a $d^9$ Electron System in Square Planar Configuration, as Obtained by a 10% Distortion of a Regular Octahedron

Table III shows the character table and representation bases of the $D_{4h}$ group, which is the point group of the square planar configuration.

TABLE III. Character Table of the $D_{4h}$ Point Group

| $D_{4h}$ | E | $2C_4$ | $C_2$ | $2C_2'$ | $2C_2''$ | i | $2S_4$ | $\sigma_h$ | $2\sigma_v$ | $2\sigma_d$ | Bases | | |
|---|---|---|---|---|---|---|---|---|---|---|---|---|---|
| $A_{1g}$ | 1 | 1 | 1 | 1 | 1 | 1 | 1 | 1 | 1 | 1 | | | $x^2 + y^2, z^2$ |
| $A_{2g}$ | 1 | 1 | 1 | -1 | -1 | 1 | 1 | 1 | -1 | -1 | | $L_z$ | |
| $B_{1g}$ | 1 | -1 | 1 | 1 | -1 | 1 | -1 | 1 | 1 | -1 | | | $x^2 - y^2$ |
| $B_{2g}$ | 1 | -1 | 1 | -1 | 1 | 1 | -1 | 1 | -1 | 1 | | | xy |
| $E_g$ | 2 | 0 | -2 | 0 | 0 | 2 | 0 | -2 | 0 | 0 | | $(L_x, L_y)$ | (xz, yz) |
| $A_{1u}$ | 1 | 1 | 1 | 1 | 1 | -1 | -1 | -1 | -1 | -1 | | | |
| $A_{2u}$ | 1 | 1 | 1 | -1 | -1 | -1 | -1 | -1 | 1 | 1 | z | | |
| $B_{1u}$ | 1 | -1 | 1 | 1 | -1 | -1 | 1 | -1 | -1 | 1 | | | |
| $B_{2u}$ | 1 | -1 | 1 | -1 | 1 | -1 | 1 | -1 | 1 | -1 | | | |
| $E_u$ | 2 | 0 | -2 | 0 | 0 | -2 | 0 | 2 | 0 | 0 | (x,y) | | |

If admixture of state $|n\rangle$ is to take place, the expectation value

$$\langle n|\hat{L}_i|0\rangle \tag{6.40}$$

cannot be zero. Remembering Eq. 3.8, we may write as a general requirement

$$\Gamma_1 \in \Gamma_{|n\rangle} \times \Gamma_{\hat{L}_i} \times \Gamma_{|0\rangle}. \tag{6.41}$$

We immediately find that $\hat{L}_z$ must connect the ground state ($B_{1g}$) with $B_{2g}$, which is spanned by $d_{xy}$, since $\hat{L}_z$ spans $A_{2g}$ and

$$B_{2g} \times A_{2g} \times B_{1g} = A_{1g}. \tag{6.42}$$

Analogously, for $\hat{L}_x$, which, together with $\hat{L}_y$, spans $E_g$, the connected state is $E_g(xz, yz)$, since

$$A_{1g} \in E_g \times E_g \times B_{1g} = A_{1g} + A_{2g} + B_{1g} + B_{2g}. \tag{6.43}$$

The group theoretical argument avoids trying all combinations for each $\hat{L}_i$ to select that or those that do not vanish.

Now we are going to derive Polder's Eq. 6.37 without resorting to perturbation theory. Although less general, this procedure carries an immediate physical meaning by clearly showing the process by which the ground state acquires some orbital angular momentum. As we have seen before, the crystal field, in the absence of a magnetic field, imposes for the ground state the use of the real wavefunction

$$d_{x^2-y^2} = |2, 2+\rangle = \frac{1}{\sqrt{2}}(Y_{2,2} + Y_{2,-2}). \tag{6.44}$$

Application of a magnetic field changes the situation completely, since its superposition to the crystal field descends the symmetry of the configuration by removing all operations that would lead to magnetic degeneracy, as explained in detail in Appendix A. The symmetry of the experiment will depend on the orientation of the magnetic field with respect to the crystal-field reference frame. Figure 22 illustrates the descent of symmetry due to a magnetic field parallel to z and to y. The intersection groups are

$$D_{4h} \cap C_{\infty h}(z) = C_{4h}(z); \tag{6.45}$$

$$\left.\begin{aligned} D_{4h} \cap C_{\infty h}(x) &= C_{2h}(x); \\ D_{4h} \cap C_{\infty h}(y) &= C_{2h}(y). \end{aligned}\right\} \tag{6.46}$$

The analysis that follows will be limited to Eq. 6.45, in the understanding that it may be applied in the same manner to other orientations as well.

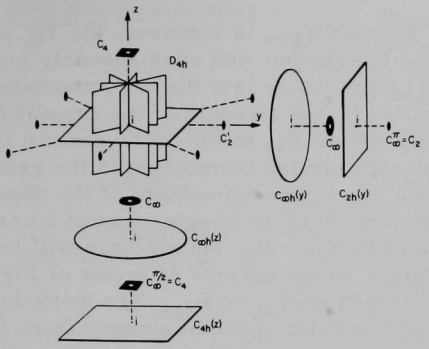


Fig. 22

Magnetic Intersection Groups of $D_{4h}$ for Selected Orientations of the Magnetic Field

The character table of the intersection group $C_{4h}(z)$ is displayed in Table IV. In most applications, it suffices to use real bases for group representation. But in magnetic problems, it is important to use the complex bases if any orbital angular momentum is to be considered. Since the planes of symmetry containing the fourfold axis and the twofold axes perpendicular to it are removed by the magnetic field, it is no longer required that one shall take

$$x^2 - y^2 \propto Y_{2,2} + Y_{2,-2} \tag{6.47}$$

for the ground state but rather any energetically favorable combination

$$\psi = aY_{2,2} + bY_{2,-2}, \tag{6.48}$$

where $a^2 + b^2 = 1$. The expectation value of the orbital angular momentum of the wavefunction defined in Eq. 6.48 is no longer zero but

$$\langle \psi | \hat{L}_z | \psi \rangle = 2(a^2 - b^2), \tag{6.49}$$

which produces a shift in the g value to be calculated in the following paragraphs.

TABLE IV. Character Table of the $C_{4h}$ Point Group

| $C_4$ | E | $C_4$ | $C_2$ | $C_4^3$ | i | $S_4^3$ | h | $S_4$ | Bases | | |
|---|---|---|---|---|---|---|---|---|---|---|---|
| $A_g$ | 1 | 1 | 1 | 1 | 1 | 1 | 1 | 1 | | $L_z$ | $x^2 + y^2$, $z^2$ |
| $B_g$ | 1 | -1 | 1 | -1 | 1 | -1 | 1 | -1 | | | $(x+iy)^2$, $(x-iy)^2$ |
| $E_g$ | 1 | i | -1 | -i | 1 | i | -1 | -i | | $L_+$ | $z(x+iy)$ |
| | 1 | -i | -1 | i | 1 | -i | -1 | i | | $L_-$ | $z(x-iy)$ |
| $A_u$ | 1 | 1 | 1 | 1 | -1 | -1 | -1 | -1 | z | | |
| $B_u$ | 1 | -1 | 1 | -1 | -1 | 1 | -1 | 1 | | | |
| $E_u$ | 1 | i | -1 | -i | -1 | -i | 1 | i | x + iy | | |
| | 1 | -i | -1 | i | -1 | i | 1 | -i | x - iy | | |

In the E representations, $\pm i$ stands for $e^{\pm im\phi}$ ($m = 1$, $\phi = \pi/2$).

After the degeneracy of $Y_{2,2}$ and $Y_{2,-2}$ is removed, the $Y_{2,-2}$ state will be energetically favored, and the system will spontaneously evolve to introduce as much additional $Y_{2,-2}$ admixture into the new, magnetically perturbed ground state as permitted by the strength of the crystal field. The additional $Y_{2,-2}$ has to be taken from $B_{2g}$ to which the excess $Y_{2,2}$ must be returned. Thus the appearance of angular momentum in the ground state is compensated by the appearance of angular momentum of the opposite sign in the excited state. It is now possible to imagine that at a certain, probably very large magnetic field strength $B_\infty$, the electron will be in a pure $Y_{2,-2}$ state, which is equivalent, in the scheme of levels of Fig. 21, to having transferred one-half electron from $B_{1g}$ to $B_{2g}$. The work done by the magnetic field in changing the magnetic quantum number from $m_L = 0$ in the absence of a magnetic field to $m_L$, which is $\Delta m_L g_L \mu_B B_\infty$, must be equal to one-half the crystal-field splitting, since this latter is referred to one electronic charge; i.e.,

$$\Delta m_L g_L \mu_B B_\infty = \tfrac{1}{2}\Delta_{\|}. \tag{6.50}$$

In the same field $B_\infty$, the additional decrease of magnetic energy provides the necessary energy to flip the orbital angular momentum from zero to $m_L$, which is work that must be done by the coupling between spin and orbit. For $\Delta m_S = 1$ and $\Delta m_L = m_L$, this work is

$$-\Delta g_{\|} \mu_B B_\infty = m_L \lambda. \tag{6.51}$$

Eliminating $\mu_B B_\infty$ between Eqs. 6.50 and 6.51, one arrives at, after setting $g_L = 1$,

$$\Delta g_{\|} = -2\frac{m_L^2 \lambda}{\Delta_{\|}}, \tag{6.52}$$

which, for $m_L = -2$, gives Polder's relation,

$$g_{\|} = g_e + \Delta g_{\|} = 2 - 8\frac{\lambda}{\Delta_{\|}}. \tag{6.53}$$

It is of some interest to calculate the values of the coefficients a and b of Eq. 6.49 for conventional magnetic fields such as those used in paramagnetic experiments. For a field of 10 kG and crystal-field splittings in the optical region (12,500 to 25,000 $cm^{-1}$), $a^2 - b^2$ is of the order of $10^{-4}$. Its absolute value increases linearly and reaches unity (a = 0, b = 1) for magnetic fields between 50 and 100 MG, clearly unattainable under normal laboratory conditions. That the admixture of excited state is proportional to the magnetic field does not need to upset us since $\Delta g$, which is field-independent, actually represents the admixture per unit magnetic field.

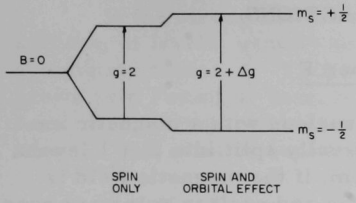


Fig. 23. Influence of Orbital Effects in the Zeeman Splitting

Since $\lambda$ is negative for more-than-half-filled shells (which is the case of $d^9$ ions), $\Delta g_{\parallel}$, as well as $\Delta g_{\perp}$, is positive and the Zeeman splitting takes the form indicated in Fig. 23.

Interpretation of Eq. 6.52 is interesting. For values of the crystal-field splitting small enough to admix as much excited state as possible, Eq. 6.52 ceases to be valid. If we assume Russell-Saunders coupling $J = L + S$ and call $g_J$ the electron g value in this system, there is a value of the crystal-field splitting, $\Delta_0$, such that

$$g_J - 2.0023 = -2\frac{m_L^2 \lambda}{\Delta_0}, \tag{6.54}$$

which means that the maximum angular momentum will appear for

$$\Delta_0 \leq 2\frac{m_L^2 \lambda}{2.0023 - g_J}. \tag{6.55}$$

This condition immediately identifies with the requirement of second-order perturbation that the spin-orbit coupling coefficient $\lambda$ shall be small as compared with the crystal-field splitting. Moreover, Eq. 6.55 establishes the limit of the crystal-field splitting below which Polder's relations are no longer valid, of order $10\lambda$ in absolute value.

# 7. HYPERFINE INTERACTIONS

## 7.1 Hyperfine Splitting: The Quantum Number F

When an unpaired electron is near a nucleus with a magnetic moment, the energy levels of the electron are usually split into 2I + 1 levels, where I is the nuclear spin. In such a system, if the magnetic field is large enough, one assumes that both electronic and nuclear spins are quantized in the external field. However, each one of them experiences a magnetic field which results from the external one and the field due to the other. Since the nuclear transitions would occur at much lower frequency at the same field (about three orders of magnitude lower), the electronic transitions occur at constant orientation of the nuclei, which is expressed by the conditions

$$\Delta m_S = 1, \Delta m_I = 0. \tag{7.1}$$

This is not always true; in some cases, weak lines are observed that correspond to $\Delta m_S = \Delta m_I = 1$ transitions, called satellites. But for our purpose, we only consider those transitions satisfying conditions 7.1. We will later see that simultaneously induced nuclear transitions by use of dual-resonance techniques (ENDOR) constitute a very powerful technique for the elucidation of ambiguous hyperfine structures.

An interesting effect occurs when the external field becomes smaller. Independent quantization of $\vec{S}$ and $\vec{I}$ and $\vec{I}$-$\vec{S}$ coupling become competitive processes until the latter becomes dominant. At $\vec{B} = 0$, $\vec{S}$-$\vec{I}$ coupling imposes the use of a new quantum number F defined as

$$\vec{F} = \vec{S} + \vec{I}. \tag{7.2}$$

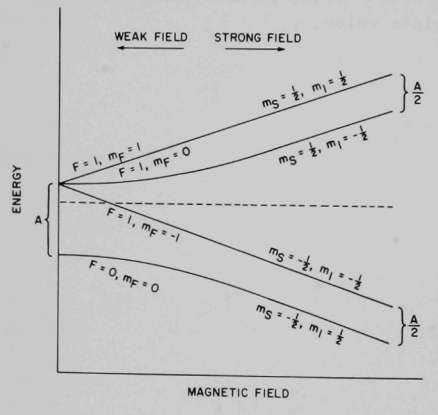


Fig. 24. Breit-Rabi Levels for $S = I = \frac{1}{2}$

This state of affairs leads to the zero-field splitting illustrated in Fig. 24 for a system of $S = I = \frac{1}{2}$. Diagrams of this type were introduced by Breit and Rabi and are available in the literature for various values of S and I.

We discuss only the strong-field case, when the I-S coupling can be treated as a perturbation and I and S are good quantum numbers. Interpretation of spectra at low fields, where S, I, and F transitions may be observed according to the direction of the microwave magnetic field with respect to the external one, is difficult and has not received much attention.

In the strong-field case, the hyperfine interaction appears as a splitting of levels, usually anisotropic. It is represented by a second-rank, symmetric tensor $\hat{A}$. This effect can be decomposed into an isotropic part, known as a Fermi or contact term, customarily symbolized K, and a traceless, second-rank symmetric tensor $\hat{T}$, known as a dipole-dipole interaction tensor. The relation between $\hat{A}$, K, and $\hat{T}$ is then

$$\hat{A} = K + \hat{T}, \tag{7.3}$$

with

$$\mathrm{Tr}\ \hat{T} = \sum_j T_{jj} = 0. \tag{7.4}$$

The former is due to unpaired electron density inside the nucleus; the latter is due to interaction between the nuclear magnetic moment and the spin magnetic moment outside the nucleus. We discuss each case separately in the following sections.

## 7.2 Interaction between Nuclear and Electronic Spins

Consider Fig. 25, where a nucleus has been represented by a positive charge q going in a circular path of radius a at constant linear velocity v. The velocity v is, as we know, related to the period T by

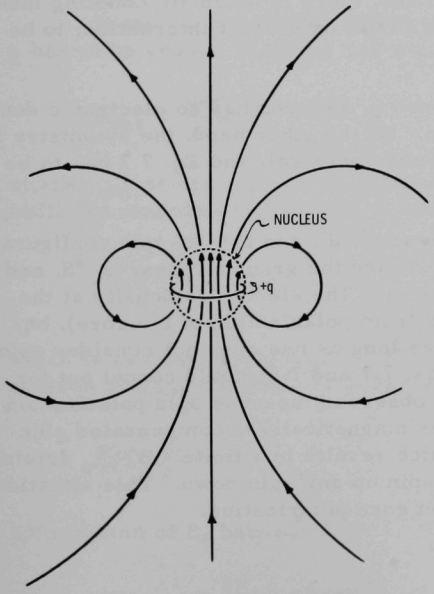


Fig. 25. Magnetic Field of a Nucleus

$$v = 2\pi a \frac{1}{T}. \tag{7.5}$$

This current loop is equivalent to a magnetic moment, after solving Eq. 1.4,

$$\mu_{nuc} = \frac{1}{c}\frac{q}{T}\pi a^2 = \frac{qav}{2c} \tag{7.6}$$

normal to the ring, whose direction is given by the right-handed convention. In other words, looking at the loop from the positive end of the magnetic-field vector inside the loop, one sees the positive charge circulating counterclockwise. Consider now the magnetic lines also drawn in Fig. 25, and imagine that the nucleus is imbedded in an electron cloud with center in the nucleus, of wavefunction $\psi(\vec{r})$. Notice that the symbol

$\psi(\vec{r})$ is a short symbol for $\psi(r,\theta,\phi)$. Consider a volume element dV, outside the nucleus, of electronic density $|\psi(\vec{r})|^2$ dV. The magnetic field $\vec{B}(\vec{r})$ acting on this volume element is given by Eq. 1.54 as proportional to $(3\cos^2\theta - 1)/r^3$. Its average seen by the electron outside the sphere of radius a (indicated in Fig. 25 in dotted lines) representing the nuclear volume is given by the expectation value

$$\langle B\rangle_{r>a} = \int_a^\infty \psi^*(\vec{r})B(\vec{r})\psi(\vec{r})\ dV, \tag{7.7}$$

where integration over the nuclear sphere has been excluded. Inside the sphere, we have, on the other hand,

$$\langle B\rangle_{r<a} = \int_0^a \psi^*(\vec{r})B(\vec{r})\psi(\vec{r})\ dV. \tag{7.8}$$

Two cases have now to be considered: s and non s electrons.

For s electrons: Due to spherical symmetry, the average of Eq. 7.7 is zero, while the average of Eq. 7.8 is not, as seen in Fig. 25, where the magnetic lines all point up inside the nucleus. Since an s electron has a finite electronic density inside the nucleus, there is magnetic coupling independent of the orientation. This is the Fermi or contact interaction, to be studied in Section 7.3.

For non s electrons: Since a non s electron has no electronic density inside the nucleus, Eq. 7.8 is zero. On the other hand, the symmetry of a single non s electron is not necessarily spherical, and Eq. 7.7 has to be calculated in each particular case.

In many-electron systems such as $p^3$, $d^5$, and $f^7$ high-spin configurations, the angular momentum cancels out and the ground states, $^4S$, $^6S$, and $^8S$, respectively, have spherical symmetry. The electronic density at the nucleus remains, however, zero (aside from polarization of the core), because the electrons are not s. Thus, as long as one does not consider spin polarization of inner s shells, both Eqs. 7.7 and 7.8 should cancel out for S states. This extreme case is never observed, because spin polarization of the inner s shells always introduces magnetically uncompensated electronic densities inside the nucleus, which results in a finite $\langle B\rangle_{r<a}$ arising from the difference between states of spin up and spin down. This situation is considered in detail in Section 7.5 on core polarization.

## 7.3 Contact Term of s Electrons

The magnetic energy of an s electron due to coupling with a nucleus of magnetic moment $\mu_{nuc}$ is, according to what we already know, given by

$$E = g_e \mu_B \langle B \rangle_{r<a}. \tag{7.9}$$

To solve Eq. 7.9, we have to evaluate $\langle B \rangle_{r<a}$, which is given by Eq. 7.8. We assume that within the sphere of radius a the value of the magnetic field may be taken as the value at the center of the loop, $B_0$, and that the value of $\psi(\vec{r})$ for $r < a$ is constant and equal to $\psi(0)$. We may then write

$$\langle B \rangle_{r<a} = \int_0^a B_0 |\psi(0)|^2 \, dV = B_0 |\psi(0)|^2 \int_0^a dV = B_0 |\psi(0)|^2 \left(\frac{4\pi}{3}\right) a^3, \tag{7.10}$$

since $dV = r^2 \sin\theta \, dr \, d\theta \, d\phi$ in spherical polar coordinates, and the integration gives

$$\int_0^{V_n} dV = \int_0^{2\pi} \int_0^{\pi} \int_0^a r^2 \, dr \sin\theta \, d\theta \, d\phi = \frac{4\pi}{3} a^3. \tag{7.11}$$

Actual departures from these assumptions lead to higher-order isotopic effects called hyperfine anomalies, which arise from the fact that two isotopes may have different current distributions, in which case they will exhibit coupling energies that are not simply in the ratio of their nuclear moments.

In the representation of the nucleus by a ring current, the value of a has to be chosen to fit the expression given in Eq. 7.6; i.e.,

$$\mu_{nuc} = \frac{qav}{2c}, \tag{7.6}$$

where $\mu_{nuc}$ is the nuclear magnetic moment, which is normal to the loop, while the magnetic field at the center of the loop is in turn given by

$$B_0 = \frac{qv}{ca^2}, \tag{7.12}$$

which is obtained from Eq. 1.5 after making $v = 2\pi a/T$ and $i = q/T$. Comparison of Eqs. 7.6 and 7.12 leads to

$$B_0 = \frac{2c}{a^3} \mu_{nuc}. \tag{7.13}$$

Elimination of $B_0$ between Eqs. 7.10 and 7.13 leads to

$$\langle B \rangle_{r<a} = \frac{8\pi}{3} \mu_{nuc} |\psi(0)|^2, \tag{7.14}$$

and Eq. 7.9 becomes

$$E = \frac{8\pi}{3} g_e \vec{\mu}_B \cdot \vec{\mu}_{nuc} |\psi(0)|^2. \tag{7.15}$$

Expressed in terms of spin vector operators, Eq. 7.15 takes the general form

$$K\hat{S} \cdot \hat{I} = \frac{8\pi}{3} g_e \mu_B g_N \mu_N \hat{S} \cdot \hat{I}\, \delta(r), \tag{7.16}$$

where $\mu_N$ is the nuclear magneton, $g_N$ the nuclear g factor, their product being equal to $\mu_{nuc}$, and $\delta(r)$ is Dirac's delta function.

In general,

$$\hat{S} \cdot \hat{I} = \hat{S}_x \hat{I}_x + \hat{S}_y \hat{I}_y + \hat{S}_z \hat{I}_z. \tag{7.17}$$

Because of the symmetry of the system and because the Larmor precession frequencies of nucleus and electron are very different, $\hat{S}_x \hat{I}_x$ and $\hat{S}_y \hat{I}_y$ cancel out in the strong-field case, where nucleus and electron are assumed to be independently quantized in the external field. Equation 7.16 then takes the form

$$K\hat{S} \cdot \hat{I} = \frac{8\pi}{3} g_e \mu_B g_N \mu_N |\psi(0)|^2 \hat{S}_z \hat{I}_z, \tag{7.18}$$

and the eigenvalues are

$$E = \frac{8\pi}{3} g_e \mu_B g_N \mu_N |\psi(0)|^2 m_S m_I. \tag{7.19}$$

That $\hat{S}_x \hat{I}_x$ and $\hat{S}_y \hat{I}_y$ cancel out in the strong-field case can also be proved by setting

$$\hat{S} \cdot \hat{I} = \hat{S}_z \hat{I}_z + \tfrac{1}{2}(\hat{S}_+ \hat{I}_- + \hat{S}_- \hat{I}_+). \tag{7.20}$$

We now operate on the state $|m_S m_I\rangle$ with the Hamiltonian of Eq. 7.16 and find

$$\langle m_S m_I | \hat{S}_z \hat{I}_z | m_S m_I \rangle = m_S m_I \tag{7.21}$$

and

$$\langle m_S m_I | \hat{S}_+ \hat{I}_- | m_S m_I \rangle = \langle m_S m_I | \hat{S}_- \hat{I}_+ | m_S m_I \rangle = 0, \tag{7.22}$$

arriving, again, at the eigenvalues of Eq. 7.19.

Values of the contact term for full localization are given in Table B.I for atoms helium to bismuth as calculated by Hartree-Fock (H-F) theory. The value for hydrogen, which is by far more accurate, because the hydrogen atom is a two-body system and can be exactly solved, compares extremely well with the experimental one. In the other cases, especially in the heavier atoms, the H-F values cannot be expected to be better than within 20-30% of the experimental values as obtained by atomic-beam studies.

## 7.4 Dipole-Dipole Interaction

The dipole-dipole interaction term $\hat{S} \cdot \hat{T} \cdot \hat{I}$ may be written in the form

$$\hat{S} \cdot \hat{T} \cdot \hat{I} = g_e \mu_B g_N \mu_N \left\{ \frac{3(\hat{S} \cdot \vec{r})(\hat{I} \cdot \vec{r})}{r^5} - \frac{\hat{S} \cdot \hat{I}}{r^3} \right\}. \tag{7.23}$$

In the strong-field approximation, S and I are supposed to be quantized in the applied magnetic field.

The principal values of the $\hat{T}$ tensor are given by

$$T_{xx} = g_e \mu_B g_N \mu_N \int \psi^* \frac{3 \sin^2 \theta \cos^2 \phi - 1}{r^3} \psi \, dV, \tag{7.24}$$

$$T_{yy} = g_e \mu_B g_N \mu_N \int \psi^* \frac{3 \sin^2 \theta \sin^2 \phi - 1}{r^3} \psi \, dV, \tag{7.25}$$

and

$$T_{zz} = g_e \mu_B g_N \mu_N \int \psi^* \frac{3 \cos^2 \theta - 1}{r^3} \psi \, dV, \tag{7.26}$$

where $\psi$ is the electron wavefunction. The integration has to be performed over the range of r, $\theta$, and $\phi$. Since in spherical polar coordinates the variables of an atomic wavefunction are separable, Eqs. 7.24-7.26 are readily solved. The radial part separates in all three to give

$$\langle r^{-3} \rangle = \int_0^\infty R^*(r) \cdot R(r) \cdot (r^{-3}) r^2 \, dr, \tag{7.27}$$

whose value is found in Hartree-Fock tables. The angular part is given by the spherical harmonics of Eq. 3.12. After integration of the radial part, Eqs. 7.24-7.26 become

$$T_{xx} = g_e \mu_B g_N \mu_N \langle r^{-3} \rangle \int_0^{2\pi} \int_0^{\pi} |\psi(\theta, \phi)|^2 (3 \sin^2 \theta \cos^2 \phi - 1) \sin \theta \, d\theta \, d\phi, \tag{7.28}$$

$$T_{yy} = g_e\mu_B g_N\mu_N \langle r^{-3}\rangle \int_0^{2\pi}\int_0^{\pi} |\psi(\theta, \phi)|^2 (3 \sin^2\theta \sin^2\phi - 1) \sin\theta \, d\theta \, d\phi, \tag{7.29}$$

and

$$T_{zz} = g_e\mu_B g_N\mu_N \langle r^{-3}\rangle \int_0^{2\pi}\int_0^{\pi} |\psi(\theta, \phi)|^2 (3 \cos^2\theta - 1) \sin\theta \, d\theta \, d\phi. \tag{7.30}$$

After substitution of

$$\cos\theta = z, \quad \sin\theta \, d\theta = -dz, \tag{7.31}$$

the integrals

$$t_{ii} = \frac{T_{ii}}{g_e\mu_B g_N\mu_N \langle r^{-3}\rangle}, \tag{7.32}$$

which are now functions of the polar and azimuthal coordinates only, are easily reduced to

$$t_{xx} = 3A - 3B - 1, \tag{7.33}$$

$$t_{yy} = 2 - 3A + 3B - 3C, \tag{7.34}$$

and

$$t_{zz} = 3C - 1, \tag{7.35}$$

with

$$A = \int_0^{2\pi}\int_{-1}^{1} \psi^2 \cos^2\phi \, dz \, d\phi, \tag{7.36}$$

$$B = \int_0^{2\pi}\int_{-1}^{1} \psi^2 z^2 \cos^2\phi \, dz \, d\phi, \tag{7.37}$$

and

$$C = \int_0^{2\pi}\int_{-1}^{1} \psi^2 z^2 \, dz \, d\phi. \tag{7.38}$$

The traceless character of the $\hat{T}$ tensor is clearly shown in Eqs. 7.33-7.35. The values of $t_{xx}$, $t_{yy}$, and $t_{zz}$ for each p and d orbital are given in Table B.II.

## 7.5 Core Polarization

As we anticipated in the last paragraph of Section 7.2, in spherically symmetric states such as ($p^3$, $^4S$), ($d^5$, $^6S$), and ($f^7$, $^8S$) the dipole-dipole interaction cancels out and, since the electrons are not in s states, the contact term should vanish as well. A typical case would be $^{55}Mn^{2+}$ in high-spin configuration, with five d electrons in $^6S$ ground state. Natural manganese is 100% $^{55}Mn$ of $I = 5/2$. If what we said were strictly true and we had not overlooked any other effect, the spectrum of $^{55}Mn^{2+}$ in the $^6S$ ground state should exhibit only one transition at the free-electron g value, without hyperfine structure. The spectrum of $Mn^{2+}$, however, consists of six equally spaced lines spread over some 400 G, practically independent of the nature of the compound, provided, of course, that the sample be magnetically diluted. At one time, it was thought that the hyperfine splitting was due to some s character admixed by configuration interaction. It was difficult, however, to explain why the admixture was practically independent of the crystal field. It was then found that the appearance of a contact term was not due to admixture of some excited s states but to differential polarization of the inner s shells, produced by the unpaired spins of the d electrons. Such an effect, involving inner shells which are insensitive to the crystal field, should be independent of the compound as long as the localization of the d electrons did not change. This type of polarization of the core is of course not restricted to $Mn^{2+}$ and is present in all paramagnetic ions. The theoretical basis of the effect lies in exchange and has no classical analog. We are quickly going to review the situation.

In conventional Hartree-Fock theory, the polarization of the spin wavefunction is not considered. The radial wavefunctions do not depend on the spin quantum number, and the net electronic spin at the nucleus cancels out for all filled s shells. As soon as such a restriction is lifted, by developing a spin-polarized Hartree-Fock theory (SPHF), the radial wavefunctions are slightly modified due to exchange, according to whether the inner spins are parallel or antiparallel to the outer-shell unpaired electrons. As a consequence, the electronic density at the nucleus of the same ns orbital is different for $m_S = +\frac{1}{2}$ (spin "up") and for $m_S = -\frac{1}{2}$ (spin "down"), resulting in a net magnetic polarization of the electronic density given by

$$|\psi(0)\uparrow|^2 - |\psi(0)\downarrow|^2. \tag{7.39}$$

The effect of exchange actually consists in the appearance of opposite polarization at the nucleus. Exchange forces generally separate the ns electron of the same spin away from the nucleus, thus decreasing the density of equal spin. Since the sign of the exchange force is determined by the relative position of the nodes of the interacting wavefunctions, it is found that, although the net polarization is opposed to the outer spin, the effect changes sign for different ns shells. It is somewhat surprising that SPHF theory predicts values in good agreement with experimental results, since the differences of Eq. 7.39 are small when compared with the values of $|\psi(0)|^2$ and HF parameters are not better than within 20% of experimental findings. However, this

agreement is no longer surprising if one considers that the HF errors are likely to be systematic; the relative error is therefore propagated to the difference without significant change. An analysis of the literature involving nearly 100 compounds gives the results displayed in Table V.

TABLE V. Summary of Experimental Values of Core Polarization of Several Transition Ions as Compared with Theoretical Estimates

| Ion | $\chi_{exp}$, a.u. | $\chi_{SPHF}$, a.u. |
|---|---|---|
| $Ag^{2+}$ in frozen acid solutions | 10.1 | 9[a] |
| $Ag^{2+}$ in organic ligands | 10.8 | |
| $Mo^{5+}$ in mixed oxohalides | 9.23 | 8.7[b] |
| $Nb^{3+}$ in alkyl oxohalides | 6.84 | 8.36[c] |
| $Cu^{2+}$ collective treatment | 4.89 | 3.75[d] |
| $VO^{2+}$ collective treatment | 3.84 | 3[e] |

[a] Extrapolated from $Y^{2+}$-$Pd^{2+}$ series.
[b] $Mo^{+}$.
[c] $Nb^{3+}$.
[d] $3d^9$ ion.
[e] $3d^1$ ion.

The theory predicts a magnetic field at the nucleus due to core polarization per unpaired electron

$$B_{cp} = m_S \frac{K}{g_N \mu_N} \tag{7.40}$$

for $m_S = +\frac{1}{2}$, of -125, -375, and -700 kG for 3d, 4d, and 5d ions, respectively, practically independent of the nature and charge of the ion within each series. The contact term K is given by

$$K = \frac{8\pi}{3} g_e \mu_B g_N \mu_N \sum_n \left\{ |\psi_{ns}(0)\uparrow|^2 - |\psi_{ns}(0)\downarrow|^2 \right\}. \tag{7.41}$$

The value $\chi$ (in a.u.) used in Table V is the parameter calculated by SPHF theory

$$\sum_n \lim_{r \to 0} \left\{ \left| \frac{P(r)}{r} \right|^2_{ns} - \left| \frac{P(r)}{r} \right|^2_{ns} \right\} = \chi \text{ (in a.u.)}. \tag{7.42}$$

The polarization of the core is then expressed as

$$\chi = \sum_n \chi_{ns}. \tag{7.43}$$

The magnetic field is obtained by the conversion factor 41.2 kG/a.u.

## 7.6 Orbital Contribution to the Hyperfine Interaction

The complete Hamiltonian of hyperfine interaction is obtained by summing Eqs. 5.54 and 5.56:

$$\mathcal{H}_{hf} = K\hat{S} \cdot \hat{I} + 2\mu_B g_N \mu_N \left\{ \frac{3\hat{S} \cdot \vec{rr} \cdot \hat{I}}{r^5} - \frac{\hat{S} \cdot \hat{I}}{r^3} \right\} + 2\mu_B g_N \mu_N \frac{\hat{L} \cdot \hat{I}}{r^3}. \tag{7.44}$$

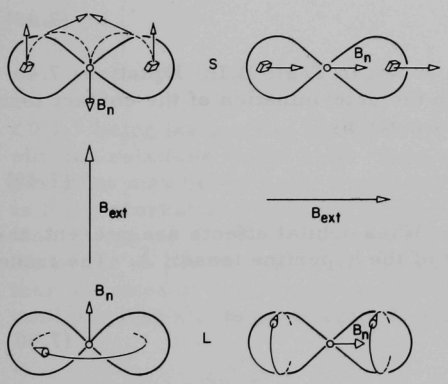


Fig. 26. Magnetic Field at the Nucleus due to Polarization of the Spin and Orbital Momenta for Two Orientations of the External Field

An inspection of this Hamiltonian immediately reveals a striking difference between the dipole-dipole terms involving $\hat{S}$ and $\hat{L}$. For certain orientations of the magnetic field, the electron spin term may vanish or reverse sign, while the electron orbital term does not. This is due to the permanent character of the spin magnetic dipole, as opposed to the electromagnetic character of the orbital one that may be thought of as the magnetic field at the nucleus due to the electron current. While in the former case to each volume element there corresponds an infinitesimal magnetic moment, in the latter case to each volume element there corresponds an infinitesimal current. Figure 26 illustrates the two behaviors, showing how the magnetic field at the nucleus ($B_n$) due to spin and orbital moments changes with the orientation of the applied external field. The choice of the electron state is arbitrary and need not be labeled, provided, of course, it is not spherically symmetric.

Gathering the two anisotropic interactions into the same tensor term leads to

$$2\mu_B g_N \mu_N \left( \frac{3\hat{S} \cdot \vec{rr} \cdot \hat{I}}{r^5} + \frac{\hat{L} \cdot \hat{I} - \hat{S} \cdot \hat{I}}{r^3} \right) = \hat{S} \cdot \hat{T} \cdot \hat{I}, \tag{7.45}$$

where $\hat{T}$ is no longer traceless because of the orbital contribution.

The Hamiltonian of Eq. 7.45 has to be solved by perturbation theory for each electronic configuration, following the line of argument used for the g tensor. For a $d^9$ configuration in square planar coordination, for example, one obtains

$$t_{\parallel} = \Delta g_{\parallel} + (3/7)\Delta g_{\perp} - 4/7 \tag{7.46}$$

and

$$t_{\perp} = \Delta g_{\perp} - (3/14)\Delta g_{\perp} + 2/7, \tag{7.47}$$

where $\Delta g_{\parallel}$ and $\Delta g_{\perp}$ are related to the spin-orbit coupling coefficient and the crystal-field splittings by Polder's relation Eqs. 6.37 and 6.38. When $\Delta g_{\parallel} = \Delta g_{\perp} = 0$, one obtains the principal values

$$t_{\parallel} = -4/7;\ t_{\perp} = 2/7 \tag{7.48}$$

of the traceless tensor for $d_{x^2-y^2}$, as shown in Table B.II. Equations 7.46 and 7.47 are particularly important in the determination of the contact term. In the absence of orbital effects, K is given by

$$K = \tfrac{1}{3}\mathrm{Tr}\hat{A}, \tag{7.49}$$

since $\hat{A} = K + \hat{T}$ and $\hat{T}$ is traceless. When orbital effects are present, they contribute to the isotropic component of the hyperfine tensor $\hat{A}$. The trace of $\hat{A}$ is then

$$\mathrm{Tr}\hat{A} = 3K + (\Delta g_{\parallel} + 2\Delta g_{\perp})\Omega, \tag{7.50}$$

where

$$\Omega = 2\mu_B g_N \mu_N \langle r^{-3} \rangle \tag{7.51}$$

and, in general,

$$K = \tfrac{1}{3}\mathrm{Tr}\hat{A} - \langle \Delta g \rangle \Omega. \tag{7.52}$$

To avoid false assignments, it is particularly important to consider signs in Eq. 7.52. For example, if K is due to core polarization, it has to be taken as negative, while, in $d^9$ configurations, $\langle \Delta g \rangle$ is positive. The sign of $\mathrm{Tr}\hat{A}$ in these configurations is usually negative, so that overlooking of orbital effects leads to absolute values of K smaller than the actual ones. In many cases, however, the orbital correction may be neglected in first approximation, especially in free radicals where the spin-orbit coupling is small and the separation of the excited states large.

## 7.7 Electron Localization and Chemical Bond

The degree of covalency is related to the overlapping of the central-ion and ligand AO's. This overlapping results in a delocalization of the unpaired electron that determines: (1) a smaller splitting due to hyperfine interaction with the central nucleus, and (2) the appearance of superhyperfine structure due to interaction with the ligand nuclei.

In the MO approach, the electron wavefunction is represented by a linear combination of the central-ion AO $\psi_0$ and the ligand orbital $\psi_L$. In transition ions, the unpaired electron usually occupies an antibonding orbital given by

$$\psi = a\psi_0 - b\psi_L, \tag{7.53}$$

where

$$a^2 + b^2 - 2ab\langle 0|L\rangle = 1 \tag{7.54}$$

$\langle 0|L\rangle$ being the overlap integral. If $a$ is not close to unity, Polder's and similar relations do not hold. However, agreement between theory and experiment may be partially restored if one uses the wavefunction of Eq. 7.53 in the perturbation treatment of Section 6.4. If the ligands contain light atoms such as O and N, their spin-orbit coupling contribution, which is of the order of 100 $cm^{-1}$ for total localization, may be neglected and, if one further assumes $a^2 = 1$ for the excited states, Polder-type relations must be multiplied by $a^2$. In particular, Polder's relations become

$$g_{\parallel} = 2 - 8\frac{a^2\lambda_0}{\Delta_{\parallel}} \tag{7.55}$$

and

$$g_{\perp} = 2 - 2\frac{a^2\lambda_0}{\Delta_{\perp}}. \tag{7.56}$$

If the splittings are known from optical data, the determination of $a^2$ is possible. On the other hand, if one compares the experimental principal values of the $\hat{T}$ tensor with the theoretical ones, listed in Table B.I, their ratio is also $a^2$, e.g.,

$$\frac{T_{\parallel}^{(exp)}}{T_{\parallel}^{(th)}} = a^2, \tag{7.57}$$

after correction for orbital effects, if necessary. This procedure, although only approximate, leads to reasonable internal consistency. The field, however, is just beginning, and much theoretical and experimental work lies ahead.

Numerous workers have explored the field of organic free radicals, and current methods for dealing with organic configurations are extensively treated in the literature.

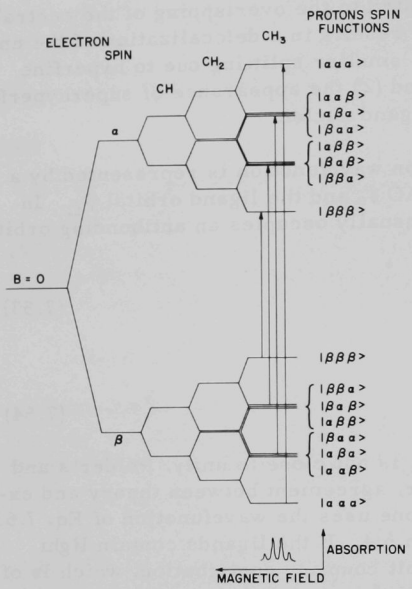


Fig. 27. Hyperfine Splitting of Methyl Radical

## 7.8 Hyperfine Interaction with Equivalent Nuclei

When several ligand molecules are equivalent, such as four pyridine rings in square planar configuration, or when several equivalent atoms share the density of the unpaired electron, as, for example, in the case of the methyl radical $\dot{C}H_3$, the magnetic levels are further split by multiple interaction. The latter case is illustrated in Fig. 27. All protons being equivalent, the total number of levels is given by N + 1, since $I = \frac{1}{2}$, where N is the number of protons. The population of the levels is determined by the number of microstates; thereby the intensity ratio, 1:3:3:1, is given by the coefficients of Newton's binomial. In general, for an arbitrary number N of equivalent nuclei of spin I, the hyperfine multiplicity is given by 2(I + N) - 1.

## 7.9 Hyperfine Interaction in Liquids

The spin Hamiltonian studied so far applies to magnetic units that are "at rest" with respect to the static magnetic field, namely, when the motions are slow when compared with the microwave frequency, or when the amplitude of the vibrations is very small, thus involving a very small uncertainty in the orientation. This is the case for most solids and frozen solutions, and the situation usually improves at lower temperatures. Resonance in low-viscosity liquids, on the other hand, poses a very different problem. The paramagnetic units are tumbling with frequencies larger than the microwave frequency, and the spectra are very different. In this case, only the trace of the magnetic tensors is observed and the spectrum is isotropic. The situation is different from the usually broad isotropic spectra observed in solids and glasses where <u>all</u> orientations contribute to the resonance.

To develop a mathematical theory of the spectra in liquids, we are going to consider the hyperfine term

$$\mathcal{H}_{hf} = \hat{S} \cdot \hat{A} \cdot \hat{I}. \qquad (7.58)$$

The treatment that follows applies to all second-rank, symmetric tensors and therefore covers the $\hat{g}$ and the crystal-field tensors as well.

In the liquid, $\hat{A}$ is a function of time in the laboratory reference frame, for each paramagnetic unit. If $\hat{A}_0$ is the tensor at time $t = 0$, the expression of $\hat{A}$ at time $t$ is given by

$$\hat{A}(t) = \hat{R}^{-1}(t) \cdot \hat{A}_0 \cdot \hat{R}(t), \tag{7.59}$$

where $\hat{R}(t)$ is a real orthogonal matrix. Of course,

$$\hat{R}(0) = \hat{E}, \tag{7.60}$$

where $\hat{E}$ is the identity matrix.

The elements of the matrix $\hat{R}(t)$ are time-dependent direction cosines $\ell_1, \ell_2, \ldots, n_2, n_3$; i.e.,

$$\hat{R}(t) = \begin{pmatrix} \ell_1(t) & \ell_2(t) & \ell_3(t) \\ m_1(t) & m_2(t) & m_3(t) \\ n_1(t) & n_2(t) & n_3(t) \end{pmatrix}, \tag{7.61}$$

and $\hat{R}^{-1}(t)$ is obtained by exchanging rows and columns. The $\hat{R}(t)$ matrix is clearly a mathematical description of the motions.

For the purpose of computation, the development of the similarity transformation of Eq. 7.59 may be put as a matrix multiplication in the six-dimensional space of the tensor parameters as

$$\begin{pmatrix} A'_{11} \\ A'_{22} \\ A'_{33} \\ A'_{23} \\ A'_{31} \\ A'_{12} \end{pmatrix} = \begin{pmatrix} \ell_1^2 & m_1^2 & n_1^2 & 2m_1n_1 & 2n_1\ell_1 & 2\ell_1m_1 \\ \ell_2^2 & m_2^2 & n_2^2 & 2m_2n_2 & 2n_2\ell_2 & 2\ell_2m_2 \\ \ell_3^2 & m_3^2 & n_3^2 & 2m_3n_3 & 2n_3\ell_3 & 2\ell_3m_3 \\ \ell_2\ell_3 & m_2m_3 & n_2n_3 & (m_2n_3+n_2m_3) & (\ell_2n_3+\ell_3n_2) & (\ell_2m_3+\ell_3m_2) \\ \ell_3\ell_1 & m_3m_1 & n_3n_1 & (m_3n_1+n_3m_1) & (\ell_1n_3+\ell_3n_1) & (\ell_1m_3+\ell_3m_1) \\ \ell_1\ell_2 & m_1m_2 & n_1n_2 & (m_1n_2+m_2n_1) & (\ell_1n_2+\ell_2n_1) & (\ell_1m_2+\ell_2m_1) \end{pmatrix} \cdot \begin{pmatrix} A_{11} \\ A_{22} \\ A_{33} \\ A_{23} \\ A_{31} \\ A_{12} \end{pmatrix}. \tag{7.62}$$

We now consider the time average

$$\frac{1}{t} \int_0^t \hat{R}^{-1}(t) \cdot \hat{A}_0 \cdot \hat{R}(t)\, dt \tag{7.63}$$

for an interval $t$ much larger than the inverse frequency of the motions. Under this condition, we may safely represent all motions by the same frequency $1/T$ and solve Eq. 7.63 for $t \gg T$ after setting

$$\hat{R}(t) = \hat{R}(t + T), \tag{7.64}$$

taking the space average of the matrix elements of Eq. 7.62. All odd powers of the direction cosines average to zero, while the even powers give

$$\langle \ell_1^2 \rangle = \langle \ell_2^2 \rangle = \ldots = \langle n_3^2 \rangle = 1/3. \tag{7.65}$$

Equation 7.63 then reduces to

$$\begin{pmatrix} A'_{11} \\ A'_{22} \\ A'_{33} \\ A'_{23} \\ A'_{31} \\ A'_{12} \end{pmatrix} = \left(\begin{array}{ccc|cc} 1/3 & 1/3 & 1/3 & & \\ 1/3 & 1/3 & 1/3 & 0 & \\ 1/3 & 1/3 & 1/3 & & \\ \hline & & & & \\ 0 & & & 0 & \end{array}\right) \cdot \begin{pmatrix} A_{11} \\ A_{22} \\ A_{33} \\ A_{23} \\ A_{31} \\ A_{12} \end{pmatrix}, \tag{7.66}$$

with the results

$$\left.\begin{aligned} A'_{11} = A'_{22} = A'_{33} = \tfrac{1}{3}\mathrm{Tr}\hat{A}; \\ A'_{23} = A'_{31} = A'_{12} = 0. \end{aligned}\right\} \tag{7.67}$$

The spin Hamiltonian of Eq. 7.58 becomes isotropic; i.e.,

$$\mathcal{H}_{hf} = (\tfrac{1}{3}\mathrm{Tr}\hat{A})\hat{S} \cdot \hat{I}, \tag{7.68}$$

which is completely general, since $\mathrm{Tr}\hat{A}$ is an invariant.

## 7.10 Electron Nuclear Double Resonance (ENDOR)

ENDOR is an ingenious and elegant method that permits the determination of the hyperfine structure with a resolution approaching that of nuclear magnetic resonance. In explaining the principle of ENDOR, we are going to consider the simple case of a magnetically dilute paramagnetic substance with one unpaired electron and the orbital momentum completely quenched. For simplicity, we assume isotropic hyperfine interaction. The Hamiltonian, including the Zeeman nuclear term, is then

$$\mathcal{H} = g\mu_B \vec{B} \cdot \hat{S} + A\hat{S} \cdot \hat{I} - g_N \mu_N \vec{B} \cdot \hat{I}. \tag{7.69}$$

The eigenvalues of the Hamiltonian are

$$E_4 = \tfrac{1}{2} g\mu_B B + \tfrac{1}{2} \cdot \tfrac{1}{2} A - \tfrac{1}{2} g_N \mu_N B, \tag{7.70}$$

$$E_3 = \tfrac{1}{2} g\mu_B B - \tfrac{1}{2} \cdot \tfrac{1}{2} A + \tfrac{1}{2} g_N \mu_N B, \tag{7.71}$$

$$E_2 = -\tfrac{1}{2}g\mu_B B + \tfrac{1}{2}\cdot\tfrac{1}{2}A + \tfrac{1}{2}g_N\mu_N B, \qquad (7.72)$$

and

$$E_1 = -\tfrac{1}{2}g\mu_B B - \tfrac{1}{2}\cdot\tfrac{1}{2}A - \tfrac{1}{2}g_N\mu_N B. \qquad (7.73)$$

Allowed transitions are those occurring at $\Delta m_S = \pm 1$ and $\Delta m_I = 0$ (electronic transitions) and for $\Delta m_I = \pm 1$ and $\Delta m_S = 0$ (nuclear transitions). Allowed electronic transitions with absorption of energy are indicated in Fig. 28:

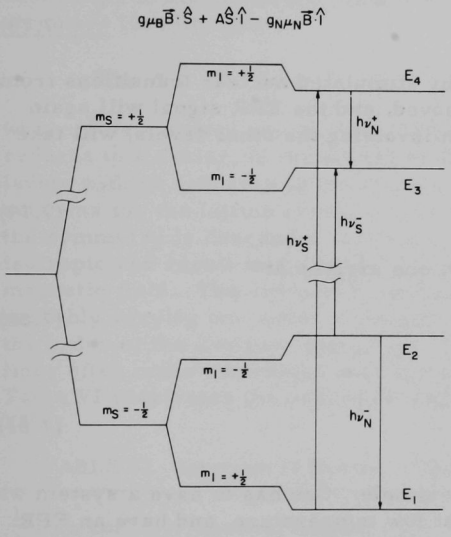


Fig. 28. Typical Scheme of ENDOR Transitions

(1) $E_1$ to $E_4$, by absorption of a photon of energy,

$$h\nu_S^+ = E_4 - E_1; \qquad (7.74)$$

and

(2) $E_2$ to $E_3$, by absorption of a photon of energy,

$$h\nu_S^- = E_3 - E_2. \qquad (7.75)$$

The energy difference between both transitions is the hyperfine constant A, which is then given by

$$A = h(\nu_S^+ - \nu_S^-). \qquad (7.76)$$

When the transitions occur at constant frequency and varying magnetic field, it is easily found that

$$A = g\mu_B \Delta B, \qquad (7.77)$$

where $\Delta B$ is the separation of the hyperfine doublet in units of magnetic field.

There is an important fact that limits the resolution in the determination of A by EPR: the width of the absorption lines that may not only distort but even hide any hyperfine structure due to overlapping. The resolution may be improved by performing an ENDOR experiment. Even more important, the nucleus responsible for the interaction may be unambiguously identified and its magnetic moment measured without knowledge of the electron wavefunction, with the sensitivity of EPR.

Electrons raised to the upper levels by absorption of microwave power return to the lower levels by spin-lattice interaction. If enough microwave power is fed into the sample at constant magnetic field for the

resonance of one of the transitions, the rate at which the electrons are raised becomes comparable to the rate at which they relax and saturation occurs. Both levels become equally populated, and power absorption stops. If a radio frequency, $\nu_N$, variable in the range of nuclear resonance, is now applied to the sample, it is possible to remove the saturation, provided the conditions for nuclear resonance are fulfilled. Consider, for example, saturation of the $E_1 \rightarrow E_4$ transition. Due to saturation, the population $N_4$ will become equal to $N_1$, and therefore larger than $N_3$ if the sample was in thermal equilibrium. Nuclear resonance will occur at

$$\nu_N^+ = (E_4 - E_3)/h, \tag{7.78}$$

and the population $N_4$ will decrease by stimulated nuclear transitions from $E_4$ to $E_3$; saturation will then be removed, and the EPR signal will again appear. The same process, although involving the other levels, will take place at the frequency

$$\nu_N^- = (E_2 - E_1)/h. \tag{7.79}$$

From Eqs. 7.70-7.73, 7.78, and 7.79, one arrives at

$$A = h(\nu_N^+ + \nu_N^-) \tag{7.80}$$

and

$$g_N \mu_N = \frac{h}{2B}(\nu_N^+ - \nu_N^-). \tag{7.81}$$

ENDOR experiments are not usually simple. One has to have a system with the correct relaxation times, work at low temperature, and have an EPR equipment permitting the experiment. In addition, the necessary radio-frequency unit, a separate coil around the sample to provide the radio-frequency field, and the need not to interfere with the basic EPR electronics do not simplify the situation. The dividends are high, however, and often justify the work.

# 8. CRYSTAL-FIELD TERMS

## 8.1 Crystal-field Splitting in Systems of $S \geq 1$

When there are two or more unpaired electrons in the paramagnetic center, it is necessary to include a term in the complete Hamiltonian in order to account for electron spin-electron spin interaction. Two or more unpaired electrons are coupled through crystal-field operators that reflect the local symmetry, giving rise to zero-field splittings and to a strong anisotropy in the spectrum. One may start by writing a so-called fine structure Hamiltonian

$$\mathcal{H}_{fs} = \hat{S} \cdot \hat{\Phi} \cdot \hat{S}, \tag{8.1}$$

where $\hat{\Phi}$ is a tensor representing the crystal field. In cubic symmetry, $\hat{\Phi}$ reduces to a scalar, to the second order in S, and produces a shift of the levels with no influence in the magnetic transitions. This term essentially accounts for the lattice energy and is important in other fields. As soon as the symmetry is descended, effects to the second order in S are no longer isotropic and result in splittings that change with the orientation of the magnetic field. The order of magnitude of this interaction is $10^0$ $cm^{-1}$, probably varying one order of magnitude above and below, and is clearly of the order of the Zeeman interaction. As a consequence, the absorption lines often make incursions over the entire region of the magnetic field. Table VI illustrates the orders of magnitude of various effects related to EPR.

TABLE VI. Spectrum of Energy of Various Atomic and Nuclear Interactions

| $\frac{1}{\lambda} = \frac{\nu}{c}$, $cm^{-1}$ | Spectral Region | Phenomenon |
|---|---|---|
| $10^5$ | UV | Crystal-field splitting of electronic levels. |
| $10^4$ | Visible | |
| $10^3$ | IR | Vibrations. |
| $10^2$ | | Rotations. |
| $10^1$ | Microwaves | Zeeman effects for magnetic fields ≈10 kG, crystal-field terms in $S^2$ (fine structure). |
| $10^0$ | | |
| $10^{-1}$ | | |
| $10^{-2}$ | Radiofrequencies | Hyperfine interactions. |
| $10^{-3}$ | | Nuclear Zeeman effects for fields ≈10 kG. |
| $10^{-4}$ | | Nuclear-quadrupole effects. |

Equation 8.1 may be put in operational form, easy for computation, after some minor algebraic handling. First, we write Eq. 8.1 in diagonal form, remembering what we know about second-rank tensors:

$$\hat{S} \cdot \hat{\Phi} \cdot \hat{S} = (\hat{S}_x \hat{S}_y \hat{S}_z) \cdot \begin{pmatrix} \Phi_1 & 0 & 0 \\ 0 & \Phi_2 & 0 \\ 0 & 0 & \Phi_3 \end{pmatrix} \cdot \begin{pmatrix} \hat{S}_x \\ \hat{S}_y \\ \hat{S}_z \end{pmatrix} = \Phi_1 \hat{S}_x^2 + \Phi_2 \hat{S}_y^2 + \Phi_3 \hat{S}_z^2. \qquad (8.2)$$

The conditions satisfied by the principal values are, as we already know:

Cubic symmetry: $\Phi_1 = \Phi_2 = \Phi_3 = \Phi$;

Axial symmetry: $\Phi_1 = \Phi_2 = \Phi_\perp$; $\Phi_3 = \Phi_\parallel$;

Lower symmetry: $\Phi_1 \neq \Phi_2 \neq \Phi_3$.

In cubic symmetry, Eq. 8.2 simplifies to

$$\hat{S} \cdot \hat{\Phi} \cdot \hat{S} = \Phi(\hat{S}_x^2 + \hat{S}_y^2 + \hat{S}_z^2) = \Phi \hat{S}^2 = \Phi S(S+1), \qquad (8.3)$$

and the term accounts for an even displacement of all levels. Therefore, a cubic field does not remove, to the second order in S, the spin degeneracy.

We proceed now to solve the totally asymmetric case of which the axial case will be a particular solution. First we write

$$\Phi_1 \hat{S}_x^2 + \Phi_2 \hat{S}_y^2 = \tfrac{1}{2}(\Phi_1 + \Phi_2)(\hat{S}_x^2 + \hat{S}_y^2) + \tfrac{1}{2}(\Phi_1 - \Phi_2)(\hat{S}_x^2 - \hat{S}_y^2) \qquad (8.4)$$

and define the parameters

$$E = \tfrac{1}{2}(\Phi_1 - \Phi_2) \qquad (8.5)$$

and

$$D = \Phi_3 - \tfrac{1}{2}(\Phi_1 + \Phi_2). \qquad (8.6)$$

The reason for this apparently arbitrary choice is the separation of the crystal-field effect into a cubic, an axial, and an orthorhombic component that facilitates the interpretation.

To simplify the Hamiltonian, we may subtract the average crystal-field energy which only displaces all levels alike. This term may be written

$$\tfrac{1}{3}(\Phi_1 + \Phi_2 + \Phi_3)\, S(S+1). \qquad (8.7)$$

In terms of Eq. 8.6, Eq. 8.7 may now be written

$$\left[\tfrac{1}{3}D + \tfrac{1}{2}(\Phi_1 + \Phi_2)\right] S(S+1) \qquad (8.8)$$

and subtracted from Eq. 8.2. After some algebraic handling, one arrives at a simplified expression of the anisotropic contribution to the fine-structure Hamiltonian

$$D\left[\hat{S}_z^2 - \tfrac{1}{3}S(S+1)\right] + E(\hat{S}_x^2 - \hat{S}_y^2), \tag{8.9}$$

which is the well-known expression of the crystal-field term widely used in the specialized literature.

For axial symmetry, the D term directly gives the zero-field splitting, since it does not contain the magnetic field. For example, for $S = 1$, the levels corresponding to $m_S = 0$ and $m_S = \pm 1$ are separated, in zero field, by $D(1^2 - 0^2) = D$. The orthorhombic parameter E is usually one order of magnitude below the axial D.

In cubic symmetries, especially when dealing with $^{2S+1}S$ ions, it is necessary to add a higher-order term,

$$\tfrac{1}{6}a(\hat{S}_x^4 + \hat{S}_y^4 + \hat{S}_z^4), \tag{8.10}$$

which results in minor corrections.

## 8.2 The Crystal-field Potential

The potential of the crystal field in the immediate neighborhood of a paramagnetic ion is calculated in the crystal-field approach in the region just inside the ligand charges or dipoles. In this region, the electric field satisfies the condition

$$\text{div } \vec{E} = 0, \tag{8.11}$$

which, remembering Eq. 1.7, may be written as

$$\text{div } \vec{E} = -\text{div grad } V = -\nabla^2 V, \tag{8.12}$$

from which it follows that

$$\nabla^2 V = 0. \tag{8.13}$$

This is known as Laplace's equation. Its solution in spherical polar coordinates of interest in crystal field is

$$V = \sum_n \sum_{m=n}^{-n} \sum_k A_n^m r^n Y_{n,m}(\theta_k, \phi_k), \tag{8.14}$$

where the summation k is over all electrons. The normalized spherical harmonics $Y_{n,m}$ are those of Eq. 3.12 with a phase factor $(-1)^n$ instead of $(-1)^{(m+|m|)/2}$. Because of orthogonality relations, terms with n larger than 4 vanish in d electrons, and terms with up to $n = 6$ have to be considered in f-electron configurations. Tables of the potential functions are available in the specialized literature.

Just as for electron wavefunctions, an alternative solution of Laplace's equation in orthogonal coordinates leads to polynomials of terms of the type given in Eq. 3.36. An analysis of the crystal field problem on the basis of polynomials in orthogonal coordinates is perhaps more intuitive and will be followed here. Calculations are easier in the spherical polar system, however, if one wishes to determine splitting energies as obtained from small distortions that can be considered perturbations to be added to the cubic splitting.

The existence of an inversion center or twofold axes that reverse the coordinates restricts the terms of the crystal field to even powers of the coordinates. The first, zeroth-order term has spherical symmetry and displaces all levels alike, corresponding to the term of Eq. 8.7. This term has no bearing in EPR and may therefore be subtracted from the Hamiltonian exactly the way we did in Eq. 8.8. The second-degree terms may be written

$$C_1x^2 + C_2y^2 + C_3z^2. \tag{8.15}$$

In cubic symmetry, $C_1 = C_2 = C_3$, and again we find an isotropic shift of all levels. The next term to consider is

$$A_1'x^4 + A_2'y^4 + A_3'z^4 + A_{12}'x^2y^2 + A_{23}'y^2z^2 + A_{31}'x^2z^2, \tag{8.16}$$

which reduces in cubic symmetry to

$$A'(x^4+y^4+z^4) + A_1(x^2y^2+y^2z^2+z^2x^2) = (A' - A_1/2)(x^4+y^4+z^4) + (A_1/2)r^4. \tag{8.17}$$

Anologous arguments in the other symmetries lead to the following second-degree terms:

Axial symmetry: $C_\perp(x^2+y^2) + C_\parallel z^2$; (8.18)

Lower symmetry: $C_1x^2 + C_2y^2 + C_3z^2$. (8.19)

When f orbitals and F states are studied, sixth-degree polynomials must be considered.

## 8.3 Nuclear-quadrupole Interaction

When the spin of the nucleus is equal or larger than one, the nucleus may have an electric quadrupole Q. It is in this case necessary to add a term

$$Q \cdot \Phi \cdot Q, \tag{8.20}$$

which may in turn be developed, following analogous lines of argument, as

$$P\left\{\hat{I}_z^2 - \tfrac{1}{3}I(I+1)\right\} + P'(\hat{I}_x^2 - \hat{I}_y^2). \tag{8.21}$$

The P term represents axial symmetry and is related to the nuclear electric quadrupole Q by

$$P = \frac{3e}{4I(2I-1)}\left(\frac{\partial^2 V}{\partial z^2}\right)Q, \tag{8.22}$$

where $\partial^2 V/\partial z^2$ is the electric field gradient at the nucleus, along the symmetry axis. The P' term accounts for orthorhombic distortion.

The greatest contribution to the field gradient at the nucleus is usually due to the unpaired electron; the contribution from the ligand molecules (crystal field) is negligible. Some orientations of the nucleus relative to the unpaired electron spin are then more favorable if the nucleus has a quadrupole moment so that there can be an electrostatic interaction that slightly modifies the electronic levels. The quadrupole effect is even in I, due to the existence of a mirror plane in the quadrupole, perpendicular to its axis. In this respect, a nuclear quadrupole may be represented by two negative point charges with a double positive charge midway between, no change in the configuration being therefore imposed by reflection through a plane perpendicular to the quadrupole and intersecting its axis in the middle point.

The order of magnitude of this effect varies between zero and $\approx 10^{-4}$ $cm^{-1}$, contributing mainly to broadening of the lines.

# APPENDIX A

Reprinted from AMERICAN JOURNAL OF PHYSICS, Vol. 37, No. 8, 793–799, August 1969
Printed in U. S. A.

## Symmetry and Properties of Crystals: Theorem of Group Intersection*

J. A. McMILLAN
*Argonne National Laboratory, Argonne, Illinois 60439*
(Received 23 January 1969)

Polarized crystals exhibit the symmetry of the intersection of the polarizing-field and the crystal-point groups, thus imposing conditions on spontaneous polarization. Introduction of time reversal and charge conjugation in magnetic and electric configurations leads, through the intersection theorem, to Shubnikov's groups. Intersection with the symmetry point groups of second-rank tensor fields imposes conditions on these latter. Tables of group intersections are given and some instructional examples are discussed.

### INTRODUCTION

The quality of a crystal of transforming a given independent variable into a certain dependent quantity is called a property. It is symbolically expressed by means of an $n$th-rank tensor. The independent variable and the dependent quantity are in turn expressed by tensors of appropriate rank. The ranks of the independent-variable and the dependent-quantity tensors determine the rank of the property tensor according to

(rank of property tensor) = (rank of independent-variable tensor) + (rank of dependent-quantity tensor).

In the case of property tensors of rank one or higher, the number of independent coefficients needed to define the property without ambiguity is determined by the crystal point symmetry. A general procedure for finding this number, based on the theorem of group intersection, is introduced and discussed in this publication as applied to first- and second-rank tensors. Although the conclusions arrived at are of course well known,[1] the method offers an alternate, group-theoretical approach to the usual procedure of finding invariant tensors under the symmetry operations of the crystallographic point group.

### THEOREM OF GROUP INTERSECTION

#### Theorem

*An experiment in which a crystal of symmetry point group* **G** *is in a uniform tensor field of symmetry point group* **G′** *has the symmetry of the intersection* **G″** *of* **G** *and* **G′**, i.e.,

$$\mathbf{G''} = \mathbf{G} \cap \mathbf{G'}. \tag{1}$$

The intersection **G″** satisfies the group postulates, being therefore a common subgroup of **G** and **G′**.

#### Corollary

Since property tensors cannot descend the symmetry of the crystal, the intersection of the property-tensor and the crystal point groups must be equal to the crystal point group. Therefore, the crystal point group must be a subgroup of the tensor point group. This condition imposes restrictions upon the form of the property tensor to be discussed in the following paragraphs.

A brief discussion of the notation used in this publication seems to be in order. Point groups are represented by their Schoenflies symbol. In this notation, $C_n$, $C_{nv}$, and $C_{nh}$ stand for groups with one $n$-fold rotation axis. Subscripts $v$ and $h$ indicate existence of planes of symmetry containing the rotation axis ($\sigma_v$) or one plane of symmetry perpendicular to the axis ($\sigma_h$). $D_n$, $D_{nd}$, and $D_{nh}$ are groups with two-fold rotation axes perpendicular to the principal axis, that is the axis of maximum $n$. Subscripts $d$ and $h$ are used to symbolize planes of symmetry that bisect two two-fold axes ($\sigma_d$) or a plane perpendicular to the principal axis ($\sigma_h$). $S_n$ ($n=2k$) are the groups of improper rotations. Among them $S_2$ and $S_6$ are usually symbolized $C_i$ and $C_{3i}$, respectively. Finally, $O$ and $T$ with and without subscripts symbolize groups of octahedral and tetrahedral symmetry, being characterized by the existence of four three-fold rotations axes. In crystals, due to requirements imposed by translational symmetry, the values of $n$ are restricted to 1, 2, 3, 4, and 6, which limits the number of crystallographic point groups to thirty-two. For uniform tensor fields in which any

* Based on work performed under the auspices of the U. S. Atomic Energy Commission.

[1] See, for example, S. Bhagavantam, *Crystal Symmetry and Physical Properties* (Academic Press Inc., New York, 1966).

rotation about an axis parallel to the direction of the field is an operation of symmetry one finds the groups $C_{\infty v}$, $C_{\infty h}$, and $D_{\infty h}$ with the meaning that follows from the preceding paragraphs. The operations of symmetry are symbolized in the following way: $\mathbf{C}_n$, $n$-fold rotation, $\sigma$, symmetry reflection, and $\mathbf{i}$, inversion.

## POLAR AND AXIAL PROPERTY VECTORS

Polar and axial vectors differ in their symmetry behavior in that polar vectors are reversed by spatial inversion, while axial vectors are not. The symmetry point groups of uniform fields of polar and axial vectors are readily determined after finding the complete set of symmetry operations in each case as follows.

All rotations about the direction of a uniform vector field send the field into itself; all the powers of $\mathbf{C}_\infty$ are therefore operations of symmetry. Reflection through $\sigma_v$ planes, containing the direction of the field, while reversing axial vectors,[2] does not affect the direction of polar vectors; the point group of a uniform polar-vector field is therefore $C_{\infty v}$. Reflection through planes perpendicular to the direction of the field $\sigma_h$ does not affect the direction of axial vectors,[3] but it reverses polar vectors; the point group of a uniform axial-vector field is therefore $C_{\infty h}$. Typical of each category are the polar, electric vectors $\mathbf{E}$ and $\mathbf{D}$ and the axial, magnetic vectors $\mathbf{H}$ and $\mathbf{B}$. Analogously, the electric and magnetic dipole vector operators are polar and axial, respectively.

Introduction of the time-reversal operator $\mathbf{R}_t$ in the magnetic field leads to the definition of a new symmetry operator

$$\tilde{\sigma}_v = \mathbf{R}_t \cdot \sigma_v, \tag{2}$$

although neither $\mathbf{R}_t$ nor $\sigma_v$ is a symmetry operator of the field; for both $\mathbf{R}_t$ and $\sigma_v$ reverse the magnetic vectors. The order of the point group is then doubled, and the new group is

$$D_{\infty h}(C_{\infty h}) = C_{\infty h} + \tilde{\sigma}_v \cdot C_{\infty h}, \tag{3}$$

where $C_{\infty h}$ is the subgroup of index two of spatial symmetry and $\tilde{\sigma}_v \cdot C_{\infty h}$ is the left coset of time-reversal operators.

Following the same line of argument, it is possible to define the charge-conjugation operator $\mathbf{R}_c$ in electric fields which, after multiplication by inversion $\mathbf{i}$, leads in turn to the charge-conjugation operator of symmetry

$$\tilde{\mathbf{i}} = \mathbf{R}_c \cdot \mathbf{i}. \tag{4}$$

The order of the electric group is then doubled, and the new group is

$$D_{\infty h}(C_{\infty v}) = C_{\infty v} + \tilde{\mathbf{i}} \cdot C_{\infty v}, \tag{5}$$

where $C_{\infty v}$ is the subgroup of index two of spatial symmetry and $\tilde{\mathbf{i}} \cdot C_{\infty v}$ is the left coset of charge-conjugation operators.

The point groups $D_{\infty h}(C_{\infty h})$ and $D_{\infty h}(C_{\infty v})$ are the generating bicolor field groups whose intersections with the colorless crystallographic point groups give rise to the Shubnikov color groups. It is to be understood, of course, that whenever time reversal $\mathbf{R}_t$ or charge conjugation $\mathbf{R}_c$ are used, they are included in the crystal point group. Since by assumption this latter lacks the double-valued attribute incorporated in the field group, it includes $\mathbf{R}_t$ (or $\mathbf{R}_c$) as a symmetry operator as well as its product by each and every spatial operator of the point group, its order being therefore doubled. This new group is referred to as the colorless group. It should not be mistaken for the monocolor group in which neither $\mathbf{R}_t$ (or $\mathbf{R}_c$) nor any of its products is a symmetry operator.

Table I displays the intersections of the 32 crystallographic point groups with axial ($C_{\infty h}$), polar ($C_{\infty v}$), and bicolor ($D_{\infty h}$) vector-field point groups at different orientations. They are readily derived from inspection of the stereographic projections of the crystallographic point groups[4] and of course from comparison of the list of symmetry operators of each crystallographic point group and the infinite point groups $C_{\infty v}$, $C_{\infty h}$, and $D_{\infty h}$.

[2] This is a consequence of the invariance of axial vectors under inversion. Consider that the axial vector is reversed by a rotation by $\pi$ about an axis perpendicular to $C_\infty$; let this operation be $\mathbf{C}_2'$. The product operation $\mathbf{C}_2' \cdot \sigma_v$ is equal to inversion which must leave the axial vector unchanged. Reflection through $\sigma_v$ should then undo what $\mathbf{C}_2'$ did, i.e., it must reverse the axial vector.

[3] Again, this is a consequence of invariance of axial vectors under inversion. Inversion $\mathbf{i}$ may be expressed as the product $\mathbf{i} = \sigma_h \cdot \mathbf{C}_\infty^r = \sigma_h \cdot \mathbf{C}_2$. Since neither $\mathbf{i}$ nor $\mathbf{C}_\infty^r = \mathbf{C}_2$ reverses an axial vector, this latter must remain invariant under $\sigma_h$.

[4] N. F. M. Henry and K. Lonsdale, Eds., *International Tables for X-Ray Crystallography* (Kynoch Press, Birmingham, England, 1952), Vol. 1.

Table A.I. Intersections of the crystallographic point groups with vector-field point groups.[a]

| | $C_\infty \parallel C_n$ | | |
|---|---|---|---|
| | $C_{\infty h}$ | $C_{\infty v}$ | $D_{\infty h}$ |
| $C_n$ | $C_n$ | $C_n$ | $C_n$ |
| $C_{nh}$ | $C_{nh}$ | $C_n$ | $C_{nh}$ |
| $C_{nv}$ | $C_n$ | $C_{nv}$ | $C_{nv}$ |
| $S_{2k}$ | $S_{2k}$ | $C_k$ | $S_{2k}$ |
| $D_n$ | $C_n$ | $C_n$ | $D_n$ |
| $D_{nd}$ | $S_{2n}$ | $C_{nv}$ | $D_{nd}$ |
| $D_{nh}$ | $C_{nh}$ | $C_{nv}$ | $D_{nh}$ |

| | $C_\infty \perp C_n$ | | |
|---|---|---|---|
| | $C_{\infty h}$ | $C_{\infty v}$ | $D_{\infty h}$ |
| $C_n$ $(n=2k)$ | $C_1$ | $C_1$ | $C_2$ [b] |
| $C_n$ $(n=2k+1)$ | $C_1$ | $C_1$ | $C_1$ |
| $C_{nh}$ $(n=2k)$ | $C_i$ | $C_s=C_{1v}$ | $C_{2h}$ [b] |
| $C_{nh}$ $(n=2k+1)$ | $C_1$ | $C_s=C_{1v}$ | $C_s=C_{1v}$ |

| | $\sigma_v \parallel C_\infty \perp C_n$ | | |
|---|---|---|---|
| | $C_{\infty h}$ | $C_{\infty v}$ | $D_{\infty h}$ |
| $C_{nv}$ $(n=2k)$ | $C_s=C_{1h}$ | $C_s=C_{1v}$ | $C_{2h}$ [b] |
| $C_{nv}$ $(n=2k+1)$ | $C_1$ | $C_s=C_{1v}$ | $C_s=C_{1v}$ |

| | $C_\infty \parallel C_2' \perp C_n$ | | |
|---|---|---|---|
| | $C_{\infty h}$ | $C_{\infty v}$ | $D_{\infty h}$ |
| $D_{1d}$ | $C_2$ | $C_2$ | $D_2$ |
| $D_{3d}$ | $C_{2h}$ | $C_2$ | $C_{2h}$ |
| $D_{2h}$ | $C_{2h}$ | $C_{2v}$ | $D_{2h}$ |
| $D_{3h}$ | $C_2$ | $C_{2v}$ | $C_{2v}$ |
| $D_{4h}$ | $C_{2h}$ | $C_{2v}$ | $D_{2h}$ |
| $D_{6h}$ | $C_{2h}$ | $C_{2v}$ | $D_{2h}$ |

| | $\sigma_d \parallel C_\infty \perp C_n$ | | |
|---|---|---|---|
| | $C_{\infty h}$ | $C_{\infty v}$ | $D_{\infty h}$ |
| $D_{2d}$ | $C_s=C_{1h}$ | $C_s=C_{1v}$ | $C_{2v}$ [b] |
| $D_{3d}$ | $C_i$ | $C_s=C_{1v}$ | $C_{2h}$ [b] |
| $D_{3h}$ | $C_2$ | $C_{2v}$ | $C_{2v}$ |

| | $C_\infty \parallel C_3$ | | |
|---|---|---|---|
| | $C_{\infty h}$ | $C_{\infty v}$ | $D_{\infty h}$ |
| $T$ | $C_3$ | $C_3$ | $C_3$ |
| $T_h$ | $S_6$ | $C_3$ | $S_6$ |
| $T_d$ | $C_3$ | $C_{3v}$ | $C_{3v}$ |
| $O$ | $C_3$ | $C_3$ | $C_3$ |
| $O_h$ | $S_6$ | $C_{3v}$ | $D_{3d}$ |

| | $C_\infty \parallel S_4$ | | |
|---|---|---|---|
| | $C_{\infty h}$ | $C_{\infty v}$ | $D_{\infty h}$ |
| $T_d$ | $S_4$ | $C_{2v}$ | $D_{2d}$ |
| $O$ | $C_4$ | $C_4$ | $D_4$ |
| $O_h$ | $C_{4h}$ | $C_{4v}$ | $D_{4h}$ |

| | $C_\infty \parallel C_2$ | | |
|---|---|---|---|
| | $C_{\infty h}$ | $C_{\infty v}$ | $D_{\infty h}$ |
| $T$ | $C_2$ | $C_2$ | $D_2$ |
| $T_h$ | $C_{2h}$ | $C_{2v}$ | $D_{2h}$ |

| | $C_\infty \parallel C_2' \perp C_4$ | | |
|---|---|---|---|
| | $C_{\infty h}$ | $C_{\infty v}$ | $D_{\infty h}$ |
| $O$ | $C_2$ | $C_2$ | $D_2$ |
| $O_h$ | $C_{2h}$ | $C_{2v}$ | $D_{2h}$ |

| | $\sigma_d \parallel C_\infty \perp S_4$ | | |
|---|---|---|---|
| | $C_{\infty h}$ | $C_{\infty v}$ | $D_{\infty h}$ |
| $T_d$ | $C_s=C_{1h}$ | $C_s=C_{1v}$ | $C_{2v}$ [b] |

[a] Groups with $\sigma_d$ containing $C_2'$ are listed under $C_\infty \parallel C_2'$ and excluded from $C_\infty \parallel \sigma_d$.
[b] $C_2 \perp C_\infty$.

The spatial-symmetry intersection groups are seventeen, classified into the following groups.

(1) Six axial- or polar-vector intersection groups: $C_1$, $C_2$, $C_3$, $C_4$, $C_6$, and $C_s$. If the direction of the field is taken as the $z$ axis, $C_s$ is interpreted in polar fields as the second-setting, monoclinic point group $C_{1v}$, while in axial fields it represents the first-setting monoclinic point group $C_{1h}$.

(2) Four polar-vector intersection groups: $C_{2v}$, $C_{3v}$, $C_{4v}$, and $C_{6v}$.

(3) Seven axial-vector intersection groups: $C_{2h}$, $C_{3h}$, $C_{4h}$, $C_{6h}$, $C_i$, $S_4$, and $C_{3i}$.

After introduction of the double-valued attribute, the following new intersections with $D_{\infty h}$ are obtained.

(4) Ten bicolor point groups, $D_2$, $D_3$, $D_4$, $D_6$, $D_{2d}$, $D_{3d}$, $D_{2h}$, $D_{3h}$, $D_{4h}$, and $D_{6h}$. Their subgroups of spatial symmetry are the intersections of the corresponding crystallographic point group, with $C_{\infty h}$ in the axial case and $C_{\infty v}$ in the polar case. Thus, the intersections of, say, the colorless point group $D_{2h}$ with $D_{\infty h}(C_{\infty h})$ and $D_{\infty h}(C_{\infty v})$ are $D_{2h}(C_{2h})$ and $D_{2h}(C_{2v})$, respectively, where the Schoenflies symbol in parentheses stands for the subgroup of index two of spatial symmetry. The intersections with $D_{\infty h}$ that are equal to the point group are the Shubnikov monocolor groups. Application of the intersection theorem to electric and magnetic polarization is discussed in the following paragraphs.

### Electric Polarization

Since molecular electric polarization is a structural phenomenon involving molecular rearrangement, it may spontaneously occur only in those point groups and at those orientations at which the intersections with $C_{\infty v}$ are equal to the crystal point groups themselves, because in such cases polarization will not descend the symmetry of the configuration. The orientations at which

$$\mathbf{G} = \mathbf{G} \cap \mathbf{G}', \tag{6}$$

are therefore the allowed directions of spontaneous electric polarization. From the tables one finds only ten point groups, the five $C_n$ ($n = 1, \cdots, 6$) and the five $C_{nv}$ ($n = 1, \cdots, 6$). It is easy to verify that the electric polarization $\mathbf{P}$ can only have the components indicated in Table II referred to the crystal reference frame.

Table A.II. Components of spontaneous electric polarization. The Schoenflies symbol is followed by the international notation.

| Point Group | $x$ | $y$ | $z$ |
|---|---|---|---|
| $C_1 = 1$ | $P_x$ | $P_y$ | $P_z$ |
| $C_s = m$ (first setting) | $P_x$ | $P_y$ | 0 |
| (second setting) | $P_x$ | 0 | $P_z$ |
| $C_2 = 2$ (first setting) | 0 | 0 | $P_z$ |
| (second setting) | 0 | $P_y$ | 0 |
| $C_3 = 3$, $C_4 = 4$, $C_6 = 6$, $C_{2v} =$ mm 2, $C_{3v} = 3$ m, $C_{4v} = 4$ mm, $C_{6v} = 6$ mm | 0 | 0 | $P_z$ |

### Magnetic Polarization

Since magnetic polarization does not involve molecular rearrangements, it may be found in all thirty-two point groups. However, in most cases it implies a descent in magnetic symmetry that leaves the structural symmetry unchanged. A typical case will serve as an example.

Ferromagnetic $\alpha$-Fe crystallizes in the point group $O_h$, space group $Im3m$. Its self-polarization is due to spin alignment parallel to one of the four-fold axes of symmetry. Application of the theorem of group intersection and the time-reversal operator $\mathbf{R}_t$ introduced in Eq. (2) leads to a complete description of the magnetic symmetry of the configuration. The full magnetic group is given by

$$D_{4h} = (O_h + \mathbf{R}_t \cdot O_h) \cap D_{\infty h}(C_\infty \,||\, C_4). \tag{7}$$

The subgroup of index two of spatial symmetry is in turn

$$C_{4h} = O_h \cap C_{\infty h}(C_\infty \,||\, C_4). \tag{8}$$

The bicolor group that accounts for the magnetic symmetry of $\alpha$-Fe is then $D_{4h}(C_{4h})$ which is one of the ninety Shubnikov crystallographic point groups discussed in an earlier publication.[5] The structural symmetry of $\alpha$-Fe, $O_h$, remains

[5] J. A. McMillan, Amer. J. Phys. **35**, 1049 (1967).

unchanged, as revealed by X-ray diffraction experiments.

## SECOND-RANK PROPERTY TENSORS

The point groups of second-rank tensor fields of different symmetries are readily derived from inspection of the dyadic form of a second-rank tensor.

A second-rank property tensor $\mathbf{T}$ transforms an independent vector variable

$$\mathbf{u} = u_i \mathbf{k}_i, \tag{9}$$

into a dependent vector quantity

$$\mathbf{v} = v_j \mathbf{k}_j, \tag{10}$$

where $\mathbf{k}_i$ are orthogonal unit vectors in the directions of $x$, $y$, and $z$.[6] Einstein summation is used; namely, that whenever a subscript appears more than once in a term, summation over such a subscript is to be understood, e.g.,

$$\mathbf{u} = u_i \mathbf{k}_i = u_1 \mathbf{k}_1 + u_2 \mathbf{k}_2 + u_3 \mathbf{k}_3. \tag{11}$$

The tensor $\mathbf{T}$ is then given by nine coefficients.

$$\mathbf{T} = \begin{pmatrix} T_{11} & T_{12} & T_{13} \\ T_{21} & T_{22} & T_{23} \\ T_{31} & T_{32} & T_{33} \end{pmatrix}, \tag{12}$$

with the meaning of

$$\mathbf{v} = v_j \mathbf{k}_j = T_{ji} \mathbf{k}_j \mathbf{k}_i \cdot u_i \mathbf{k}_i = \mathbf{T} \cdot \mathbf{u}. \tag{13}$$

The pair of unit vectors $\mathbf{k}_j \mathbf{k}_i$ without any sign between them is called a unit dyad.[7] The tensor $\mathbf{T}$ may then be rewritten in the dyadic form

$$\mathbf{T} = \begin{pmatrix} T_{11}\mathbf{k}_1\mathbf{k}_1 & T_{12}\mathbf{k}_1\mathbf{k}_2 & T_{13}\mathbf{k}_1\mathbf{k}_3 \\ T_{21}\mathbf{k}_2\mathbf{k}_1 & T_{22}\mathbf{k}_2\mathbf{k}_2 & T_{23}\mathbf{k}_2\mathbf{k}_3 \\ T_{31}\mathbf{k}_3\mathbf{k}_1 & T_{32}\mathbf{k}_3\mathbf{k}_2 & T_{33}\mathbf{k}_3\mathbf{k}_3 \end{pmatrix}. \tag{14}$$

An important property of second-rank tensors that immediately follows from inspection of the dyadic matrix of Eq. (14) is that since inversion reverses the three unit vectors, *a second-rank tensor is invariant under inversion*, for

$$\mathbf{k}_i \mathbf{k}_j = (-\mathbf{k}_i)(-\mathbf{k}_j) = \mathbf{i} \cdot (\mathbf{k}_i \mathbf{k}_j). \tag{15}$$

Property tensors are usually symmetric,[8] i.e., coefficients with permuted subscripts are equal, $T_{ij} = T_{ji}$. They are diagonalized by appropriate choice of an orthogonal reference frame,[9] taking the simpler, diagonal form

$$\mathbf{T} = \begin{pmatrix} T_{11}\mathbf{k}_1\mathbf{k}_1 & 0 & 0 \\ 0 & T_{22}\mathbf{k}_2\mathbf{k}_2 & 0 \\ 0 & 0 & T_{33}\mathbf{k}_3\mathbf{k}_3 \end{pmatrix}. \tag{16}$$

According to the values of $T_{11}$, $T_{22}$, and $T_{33}$, second-rank property tensors are classified as

Orthorhombic: $T_{11} \neq T_{22} \neq T_{33}$,

Axial: $T_{11} = T_{22} = T_{\perp}$; $T_{33} = T_{||}$, and

Cubic or Isotropic: $T_{11} = T_{22} = T_{33} = T$.

Isotropic tensors reduce to a scalar

$$\begin{pmatrix} T\mathbf{k}_1\mathbf{k}_1 & 0 & 0 \\ 0 & T\mathbf{k}_2\mathbf{k}_2 & 0 \\ 0 & 0 & T\mathbf{k}_3\mathbf{k}_3 \end{pmatrix} = T \begin{pmatrix} \mathbf{k}_1\mathbf{k}_1 & 0 & 0 \\ 0 & \mathbf{k}_2\mathbf{k}_2 & 0 \\ 0 & 0 & \mathbf{k}_3\mathbf{k}_3 \end{pmatrix} = T, \tag{17}$$

since

$$\begin{pmatrix} \mathbf{k}_1\mathbf{k}_1 & 0 & 0 \\ 0 & \mathbf{k}_2\mathbf{k}_2 & 0 \\ 0 & 0 & \mathbf{k}_3\mathbf{k}_3 \end{pmatrix},$$

---

[6] A second-rank property tensor may also transform an independent scalar quantity into a dependent second-rank tensor.

[7] In general, the dyad $\mathbf{rs}$ in the equation $\mathbf{v} = \mathbf{rs} \cdot \mathbf{u}$ operates on $\mathbf{u}$ in the following way. The scalar multiplication of $\mathbf{s}$ by $\mathbf{u}$ gives a number which is used to multiply $\mathbf{r}$. The resulting vector $\mathbf{v}$ has then the direction of $\mathbf{r}$, its length being given by the product of the length of $\mathbf{r}$ and the scalar product $\mathbf{s} \cdot \mathbf{u}$.

[8] Antisymmetric tensors have coefficients $T_{ij} = -T_{ji}$ and, of course, $T_{ii} = 0$. In three dimensions, second-rank antisymmetric tensors are axial vectors. It should be recalled that any second-rank tensor may be expressed as a sum of a symmetric and an antisymmetric second-rank tensor.

[9] As a matter of fact, the symmetric character may be thought of as deriving from the experimental fact that these tensors are always diagonal in a certain orthogonal reference frame.

is the identity tensor, i.e.,

$$u_i\mathbf{k}_i \equiv \mathbf{k}_i\mathbf{k}_i \cdot u_i\mathbf{k}_i. \tag{18}$$

Isotropic tensors remain invariant under the operations of the full rotation group[10] with inversion, for which the symbol O(3) is used. Therefore, this point group represents the symmetry properties of scalar fields. An axial tensor remains invariant under any rotation about the symmetry axis $\mathbf{k}_3$.[11] Since the elements of the tensor remain invariant under 180° rotations about all axes perpendicular to $\mathbf{k}_3$ and under inversion, its point group is $D_{\infty h}$. Orthorhombic tensors are sent into themselves by 180° rotations about each $\mathbf{k}_i$ axis. Being in addition invariant under inversion, their point group is $D_{2h}$.

In order to study the intersections it is convenient to classify crystals into

(1) *Cubic groups* $\mathfrak{K}$, including $O_h$, $O$, $T_d$, $T_h$, and $T$,

(2) *Axial groups* $\mathfrak{A}$, including $C_3$, $C_4$, $C_6$, $C_{3v}$, $C_{4v}$, $C_{6v}$, $C_{3h}$, $C_{4h}$, $C_{6h}$, $D_3$, $D_4$, $D_6$, $D_{3h}$, $D_{4h}$, $D_{6h}$, $D_{2d}$, $D_{3d}$, $C_{3i}$, and $S_4$,

(3) *Orthorhombic groups* $\mathfrak{R}$, including $C_{2v}$, $D_2$, and $D_{2h}$,

(4) *Monoclinic groups* $\mathfrak{M}$, including $C_2$, $C_s$, and $C_{2h}$, and

(5) *Triclinic groups* $\mathfrak{Z}$, including $C_1$ and $C_i$.

Table III gives the intersections at the orientations at which the descent of symmetry, if any at all, is minimum. In the cases labelled with a superscript, any other orientation descends the symmetry of the intersection.

Since physical properties represented by second-rank tensors must be restricted to those types and orientations at which the intersection is equal to the crystallographic point group, it is readily concluded that the property tensor has the following forms and number of independent coefficients.

[10] The full rotation group is the group of all proper rotations; it is symbolized by $O^+(3)$. The group $O(3)$ is the group of all the point-symmetry operations that can be performed on a sphere, namely, all proper and improper rotations.

[11] The $\mathbf{k}_3(z)$ axis is chosen, by convention, as the axis of rotation.

Table A.III. Intersections of the second-rank tensor field groups and the crystallographic point groups. Intersections without a superscript are independent of orientation.

| | $O(3)$ | $D_{\infty h}$ | $D_{2h}$ |
|---|---|---|---|
| $\mathfrak{K}$ | $\mathfrak{K}$ | $\mathfrak{A}^a$ | $\mathfrak{R}^b$ |
| $\mathfrak{A}$ | $\mathfrak{A}$ | $\mathfrak{A}^c$ | $\mathfrak{R}^b$ |
| $\mathfrak{R}$ | $\mathfrak{R}$ | $\mathfrak{R}^c$ | $\mathfrak{R}^b$ |
| $\mathfrak{M}$ | $\mathfrak{M}$ | $\mathfrak{M}^d$ | $\mathfrak{M}^e$ |
| $\mathfrak{Z}$ | $\mathfrak{Z}$ | $\mathfrak{Z}$ | $\mathfrak{Z}$ |

[a] $C_\infty$ parallel to $x$, $y$, or $z$.
[b] $C_2$, $C_{2'}$, $C_{2''}$ parallel to $x$, $y$, $z$.
[c] $C_\infty$ parallel to $z$.
[d] $C_\infty$ parallel to $z$ in first setting, to $y$ in second setting.
[e] $C_2$ parallel to $z$ in first setting, to $y$ in second setting.

*Cubic groups*:

$$\begin{pmatrix} T & 0 & 0 \\ 0 & T & 0 \\ 0 & 0 & T \end{pmatrix}, \quad \text{one independent coefficient,}$$

*Axial groups*:

$$\begin{pmatrix} T_\perp & 0 & 0 \\ 0 & T_\perp & 0 \\ 0 & 0 & T_{||} \end{pmatrix}, \quad \text{two independent coefficients,}$$

*Orthorhombic groups*:

$$\begin{pmatrix} T_{11} & 0 & 0 \\ 0 & T_{22} & 0 \\ 0 & 0 & T_{33} \end{pmatrix}, \quad \text{three independent coefficients,}$$

*Monoclinic groups*:

first setting:
$$\begin{pmatrix} T_{11} & T_{12} & 0 \\ T_{12} & T_{22} & 0 \\ 0 & 0 & T_{33} \end{pmatrix},$$

second setting:
$$\begin{pmatrix} T_{11} & 0 & T_{13} \\ 0 & T_{22} & 0 \\ T_{13} & 0 & T_{33} \end{pmatrix}.$$

Since the direction of only one axis is specified in the table (Table III), the number of independent coefficients is four.

*Triclinic groups*:

$$\begin{pmatrix} T_{11} & T_{12} & T_{13} \\ T_{12} & T_{22} & T_{23} \\ T_{13} & T_{23} & T_{33} \end{pmatrix}.$$

Since there are no restrictions in the orientation, the number of independent coefficients is six.

Symmetry requirements do not exclude the existence of property tensors of higher symmetry in less symmetric crystals such as axial tensors in orthorhombic crystals or scalar properties in all crystal groups. The conditions specified above actually state the *maximum* number of coefficients needed to determine completely a second-rank tensor property in a given crystal system.

**ACKNOWLEDGMENT**

The author is indebted to Dr. S. A. Marshall for his interest and useful suggestions during the preparation of the manuscript.

# APPENDIX B

## Tables of Hyperfine Interactions (prepared in collaboration with Dr. Teodoro Halpern)

TABLE B.I. Hyperfine Parameters

| | | | | Isotropic Splitting | | | | Anisotropic Splitting | | | |
|---|---|---|---|---|---|---|---|---|---|---|---|
| | | | | | $A^2 = 4\pi\psi^2_{ns}(0)$, | K | | | | $2\mu_B g_N \mu_N \langle r^{-3} \rangle$ | |
| Nucleus | % Abundance | Nuclear Spin I | $g_N\mu_N/h$, MHz/kG | Orbital | a.u. | MHz | Gauss | Orbital | $\langle r^{-3} \rangle$, a.u. | MHz | Gauss |
| I | II | III | IV | V | VI | VII | VIII | IX | X | XI | XII |
| $^{1}H$ | 99.9844 | 1/2 | 4.25759 | 1s | | 1,420 | 508 | | | | |
| $^{2}H$ | $1.56 \times 10^{-2}$ | 1 | 0.65357 | | | 218 | 78 | | | | |
| $^{3}H^{*a}$ | - | 1/2 | 4.5414 | | | 1,515 | 542 | | | | |
| $^{3}He$ | $10^{-7} - 10^{-5}$ | 1/2 | -3.2435 | | 22.6 | -6,125 | -2,192 | | | | |
| $^{6}Li$ | 7.43 | 1 | 0.6265 | 2s | 2.09 | 109 | 39 | | | | |
| $^{7}Li$ | 92.57 | 3/2 | 1.6547 | | | 288 | 103 | | | | |
| $^{9}Be$ | 100 | 3/2 | -0.5983 | | 7.15 | -358 | -128 | | | | |
| $^{10}B$ | 18.83 | 3 | 0.4575 | | 17.7 | 677 | 242 | 2p | 0.7756 | 44.5 | 15.9 |
| $^{11}B$ | 81.17 | 3/2 | 1.3660 | | | 2,022 | 723 | | | 133 | 47.6 |
| $^{13}C$ | 1.108 | 1/2 | 1.0705 | | 35.0 | 3,128 | 1,119 | | 1.6618 | 223 | 79.8 |
| $^{14}N$ | 99.635 | 1 | 0.3076 | | 60.5 | 1,557 | 557 | | 3.0205 | 117 | 41.9 |
| $^{15}N$ | 0.365 | 1/2 | -0.4315 | | | -2,184 | -781 | | | -163 | -58.3 |
| $^{17}O$ | $3.7 \times 10^{-2}$ | 5/2 | -0.5772 | | 96.1 | -4,637 | -1,659 | | 4.9490 | -358 | -128 |
| $^{19}F$ | 100 | 1/2 | 4.0055 | | 143 | 47,959 | 17,160 | | 7.5451 | 3,790 | 1,356 |
| $^{21}Ne$ | 0.257 | 3/2 | 0.3363 | | 204 | 27,630 | 9,886 | | 10.906 | 460 | 165 |
| $^{22}Na^{*}$ | - | 3 | 0.4434 | 3s | 6.66 | 247 | 88.4 | | 17.004 | 945 | 338 |
| $^{23}Na$ | 100 | 3/2 | 1.1262 | | | 627 | 224 | | | 2,401 | 859 |
| $^{24}Na^{*}$ | - | 4 | 0.322 | | | 174 | 62.3 | | 17.004 | 687 | 246 |
| $^{25}Mg$ | 10.05 | 5/2 | -0.2606 | | 15.3 | -333 | -119 | | 24.919 | -814 | -291 |
| $^{27}Al$ | 100 | 5/2 | 1.1094 | | 29.6 | 2,748 | 983 | 3p | 1.088 | 151 | 54.0 |
| $^{29}Si$ | 4.70 | 1/2 | -0.8458 | | 48.1 | -3,403 | -1,218 | | 2.027 | -215 | -76.9 |
| $^{31}P$ | 100 | 1/2 | 1.7236 | | 71.3 | 10,275 | 3,676 | | 3.266 | 706 | 253 |
| $^{33}S$ | 0.74 | 3/2 | 0.3266 | | 99.8 | 2,724 | 975 | | 4.8364 | 198 | 70.8 |
| $^{35}S^{*}$ | - | 3/2 | 0.508 | | | 4,236 | 1,516 | | | 308 | 110 |
| $^{35}Cl$ | 75.4 | 3/2 | 0.4172 | | 134 | 4,673 | 1,672 | | 6.7688 | 354 | 127 |
| $^{36}Cl$ | - | 2 | 0.4893 | | | 5,480 | 1,961 | | | 415 | 148 |
| $^{37}Cl$ | 24.6 | 3/2 | 0.3472 | | | 3,889 | 1,391 | | | 295 | 106 |
| $^{39}K$ | 93.08 | 3/2 | 0.1987 | 4s | 8.73 | 145 | 51.9 | | 8.9747 | 224 | 80.1 |
| $^{40}K^{*}$ | $1.19 \times 10^{-2}$ | 4 | -0.2470 | | | -180 | -64.4 | | | -278 | -99.5 |
| $^{41}K$ | 6.91 | 3/2 | 0.1092 | | | 80 | 28.6 | | | 123 | 44.0 |
| $^{42}K^{*}$ | - | 2 | -0.434 | | | -317 | -113 | | | -488 | -175 |
| $^{43}Ca$ | 0.13 | 7/2 | -0.2865 | | 17.4 | -418 | -150 | | 17.7403 | -637 | -228 |
| $^{45}Sc$ | 100 | 7/2 | 1.0344 | | 21.2 | 1,836 | 657 | 3d | 1.4294 | 185 | 66.2 |
| $^{47}Ti$ | 7.75 | 5/2 | -0.2400 | | 24.8 | -498 | -178 | | 1.9751 | -59 | -21.1 |
| $^{49}Ti$ | 2.401 | 7/2 | -0.2401 | | | -498 | -178 | | | -59 | -21.1 |
| $^{49}V^{*}$ | - | 7/2 | 1.02 | | 28.4 | 2,424 | 867 | | 2.5888 | 331 | 118 |
| $^{50}V$ | 0.24 | 6 | 0.4245 | | | 1,008 | 361 | | | 138 | 49.4 |
| $^{51}V$ | 99.76 | 7/2 | 1.1193 | | | 2,658 | 951 | | | 363 | 130 |
| $^{53}Cr$ | 9.54 | 3/2 | -0.2406 | | 32.1 | -645 | -231 | | 3.2812 | -49 | -17.5 |
| $^{53}Mn^{*}$ | - | 7/2 | 1.100 | | 35.9 | 3,297 | 1,180 | | 4.0597 | 560 | 200 |
| $^{55}Mn$ | 100 | 5/2 | 1.0553 | | | 3,163 | 1,132 | | | 537 | 192 |
| $^{57}Fe$ | 2.245 | 1/2 | 0.138 | | 39.8 | 459 | 164 | | 4.9306 | 85 | 30.4 |
| $^{56}Co^{*}$ | - | 4 | 0.7347 | | 43.8 | 2,692 | 963 | | 5.8997 | 544 | 195 |
| $^{57}Co^{*}$ | - | 7/2 | 1.01 | | | 3,701 | 1,324 | | | 747 | 267 |
| $^{58}Co^{*}$ | - | 2 | 1.544 | | | 5,661 | 2,026 | | | 1,142 | 409 |

[a]Radioactive element.

TABLE B.I (Contd.)

| | | | | Isotropic Splitting | | | | Anisotropic Splitting | | | |
|---|---|---|---|---|---|---|---|---|---|---|---|
| | | | | | $A^2 = 4\pi\|\psi_{ns}^2(0)$, | K | | | | $2\mu_B g_N \mu_N \langle r^{-3} \rangle$ | |
| Nucleus | % Abundance | Nuclear Spin I | $g_N\mu_N/h$, MHz/kG | Orbital | a.u. | MHz | Gauss | Orbital | $\langle r^{-3} \rangle$, a.u. | MHz | Gauss |
| I | II | III | IV | V | VI | VII | VIII | IX | X | XI | XII |
| $^{59}Co$ | 100 | 7/2 | 1.0103 | 4s | 43.8 | 3,702 | 1,325 | 3d | 5.8997 | 747 | 267 |
| $^{60}Co$* | - | 5 | 0.46 | | | 1,686 | 603 | | | 340 | 122 |
| $^{61}Ni$ | 1.25 | 3/2 | 0.379 | | 48.1 | 1,523 | 545 | | 6.9724 | 331 | 118 |
| $^{63}Cu$ | 69.09 | 3/2 | 1.1285 | | 52.4 | 4,947 | 1,770 | | 8.1540 | 1,154 | 413 |
| $^{64}Cu$* | - | 1 | 0.30 | | | 1,315 | 471 | | | 307 | 110 |
| $^{65}Cu$ | 30.91 | 3/2 | 1.2090 | | | 5,300 | 1,896 | | | 1,236 | 442 |
| $^{67}Zn$ | 4.12 | 5/2 | 0.2664 | | 57.0 | 1,269 | 454 | | 9.450 | 316 | 113 |
| $^{69}Ga$ | 60.2 | 3/2 | 1.0219 | | 87.3 | 7,454 | 2,667 | 4p | 2.8908 | 370 | 132 |
| $^{71}Ga$ | 39.8 | 3/2 | 1.2984 | | | 9,471 | 3,389 | | | 471 | 169 |
| $^{73}Ge$ | 7.61 | 9/2 | -0.1485 | | 120 | -1,494 | -535 | | 4.7334 | -88 | -31.5 |
| $^{75}As$ | 100 | 3/2 | 0.7292 | | 157 | 9,590 | 3,431 | | 6.8542 | 627 | 224 |
| $^{77}Se$ | 7.50 | 1/2 | 0.8131 | | 198 | 13,461 | 4,816 | | 9.2715 | 945 | 338 |
| $^{79}Se$* | - | 7/2 | -0.2211 | | | -3,660 | -1,310 | | | -257 | -92.0 |
| $^{79}Br$ | 50.57 | 3/2 | 1.0667 | | 243 | 21,700 | 7,764 | | 11.9994 | 1,605 | 574 |
| $^{81}Br$ | 49.43 | 3/2 | 1.1499 | | | 23,394 | 8,370 | | | 1,730 | 619 |
| $^{83}Kr$ | 11.55 | 9/2 | -0.164 | | 293 | -4,022 | -1,439 | | 14.8867 | -306 | -109 |
| $^{85}Kr$* | - | 9/2 | 0.170 | | | 4,169 | 1,492 | | | 317 | 113 |
| $^{81}Rb$* | - | 3/2 | 1.02 | 5s | 16.3 | 1,388 | 497 | | 20.097 | 2,571 | 920 |
| $^{85}Rb$ | 72.8 | 5/2 | 0.4111 | | | 559 | 200 | | | 1,036 | 371 |
| $^{86}Rb$* | - | 2 | (-)0.65 | | | (-)884 | (-)316 | | | (-)1,638 | (-)586 |
| $^{87}Rb$ | 27.2 | 3/2 | 1.3932 | | | 1,896 | 678 | | | 3,511 | 1,256 |
| $^{87}Sr$ | 7.02 | 9/2 | -0.1845 | | 30.0 | -4,628 | -1,656 | | 25.8947 | -5,991 | -2,144 |
| $^{89}Y$ | 100 | 1/2 | -0.2086 | | 37.6 | -656 | -235 | 4d | 1.7117 | -44.8 | -16.0 |
| $^{91}Zr$ | 11.23 | 5/2 | -0.3958 | | 44.1 | -1,458 | -522 | | 2.3974 | -119 | -42.6 |
| $^{93}Nb$ | 100 | 9/2 | 1.0407 | | 50.0 | 4,349 | 1,556 | | 3.1220 | 407 | 146 |
| $^{95}Mo$ | 15.78 | 5/2 | -0.2774 | | 55.6 | -1,290 | -462 | | 3.9001 | -136 | -48.7 |
| $^{97}Mo$ | 9.60 | 5/2 | -0.2833 | | | -1,317 | -471 | | | -139 | -49.7 |
| $^{99}Tc$* | - | 9/2 | 0.9583 | | 61.0 | 4,887 | 1,749 | | 4.7390 | 569 | 204 |
| $^{99}Ru$ | 12.81 | 5/2 | -0.19 | | 66.2 | -1,052 | -376 | | 5.6438 | -134 | -47.9 |
| $^{101}Ru$ | 16.98 | 5/2 | -0.21 | | | -1,163 | -416 | | | -149 | -53.3 |
| $^{103}Rh$ | 100 | 1/2 | -0.1340 | | 71.3 | -799 | -286 | | 6.6185 | -111 | -39.7 |
| $^{105}Pd$ | 22.23 | 5/2 | -0.174 | | 76.3 | -1,110 | -397 | | 7.6666 | -167 | -59.8 |
| $^{107}Ag$ | 51.35 | 1/2 | -0.1723 | | 81.3 | -1,170 | -419 | | 8.7911 | -190 | -68.0 |
| $^{109}Ag$ | 48.65 | 1/2 | -0.1981 | | | -1,346 | -482 | | | -218 | -78.0 |
| $^{111}Ag$* | - | 1/2 | -0.221 | | | -1,501 | -537 | | | -244 | -87.3 |
| $^{111}Cd$ | 12.86 | 1/2 | -0.9028 | | 86.1 | -6,500 | -2,326 | | 9.9041 | -1,121 | -401 |
| $^{113}Cd$ | 12.34 | 1/2 | -0.9444 | | | -6,800 | -2,433 | | | -1,173 | -420 |
| $^{113}In$ | 4.16 | 9/2 | 0.9310 | | 123 | 9,551 | 3,417 | 5p | 4.4572 | 520 | 186 |
| $^{115}In$* | 95.84 | 9/2 | 0.9329 | | | 9,571 | 3,425 | | | 521 | 186 |
| $^{115}Sn$ | 0.35 | 1/2 | -1.392 | | 160 | -18,640 | -6,669 | | 6.7468 | -1,178 | -421 |
| $^{117}Sn$ | 7.67 | 1/2 | -1.517 | | | -20,313 | -7,268 | | | -1,283 | -459 |
| $^{119}Sn$ | 8.68 | 1/2 | -1.587 | | | -21,250 | -7,603 | | | -1,343 | -481 |
| $^{121}Sb$ | 57.25 | 5/2 | 1.019 | | 200 | 17,019 | 6,089 | | 9.2313 | 1,180 | 422 |
| $^{123}Sb$ | 42.75 | 7/2 | 0.5518 | | | 9,216 | 3,297 | | | 639 | 229 |
| $^{123}Te$ | 0.89 | 1/2 | -1.116 | | 242 | -22,584 | -8,081 | | 11.9366 | -1,671 | -598 |
| $^{125}Te$ | 7.03 | 1/2 | -1.345 | | | -27,217 | -9,738 | | | -2,013 | -720 |
| $^{127}I$ | 100 | 5/2 | 0.8519 | | 287 | 20,459 | 7,320 | | 14.8724 | 1,589 | 569 |
| $^{129}I$* | - | 7/2 | 0.5669 | | | 13,614 | 4,871 | | | 1,057 | 378 |
| $^{129}Xe$ | 26.24 | 1/2 | -1.178 | | 336 | -33,055 | -11,827 | | 17.8266 | -2,633 | -942 |
| $^{131}Xe$ | 21.24 | 3/2 | 0.3490 | | | 9,793 | 3,504 | | | 780 | 279 |
| $^{127}Cs$* | - | 1/2 | 2.15 | 6s | 21.0 | 3,771 | 1,349 | | 23.2545 | 6,270 | 2,243 |
| $^{129}Cs$* | - | 1/2 | 2.24 | | | 3,929 | 1,406 | | | 6,532 | 2,337 |

TABLE B.I (Contd.)

| | | | | Isotropic Splitting | | | | Anisotropic Splitting | | | |
|---|---|---|---|---|---|---|---|---|---|---|---|
| | | | | | | K | | | | $2\mu_B g_N \mu_N \langle r^{-3} \rangle$ | |
| Nucleus | % Abundance | Nuclear Spin I | $g_N \mu_N / h$, MHz/kG | Orbital | $A^2 = 4\pi \psi^2_{ns}(0)$, a.u. | MHz | Gauss | Orbital | $\langle r^{-3} \rangle$, a.u. | MHz | Gauss |
| I | II | III | IV | V | VI | VII | VIII | IX | X | XI | XII |
| $^{131}Cs$* | - | 5/2 | 1.06 | 6s | 21.0 | 1,859 | 665 | 5p | 23.2545 | 3,091 | 1,106 |
| $^{133}Cs$ | 100 | 7/2 | 0.5585 | | | 980 | 351 | | | 1,629 | 583 |
| $^{134}Cs$* | - | 4 | 0.564 | | | 989 | 354 | | | 1,645 | 589 |
| $^{135}Cs$* | - | 7/2 | 0.594 | | | 1,042 | 373 | | | 1,732 | 620 |
| $^{137}Cs$* | - | 7/2 | 0.618 | | | 1,084 | 388 | | | 1,802 | 645 |
| $^{135}Ba$ | 6.59 | 3/2 | 0.4230 | | 37.3 | 1,318 | 472 | | 29.0659 | 1,542 | 552 |
| $^{137}Ba$ | 11.32 | 3/2 | 0.4732 | | | 1,474 | 527 | | | 1,725 | 617 |
| $^{138}La$ | 0.089 | 5 | 0.5617 | | 38.9 | 1,824 | 653 | 4f | 3.694 | 260 | 93.0 |
| $^{139}La$ | 99.911 | 7/2 | 0.6014 | | | 1,953 | 699 | | | 279 | 99.8 |
| $^{141}Ce$* | - | 7/2 | 0.035 | | 40.3 | 118 | 42.2 | | 4.3005 | 18.9 | 6.76 |
| $^{141}Pr$ | 100 | 5/2 | 1.195 | | 41.8 | 4,177 | 1,495 | | 4.9127 | 736 | 263 |
| $^{143}Nd$ | 12.20 | 7/2 | -0.272 | | 43.3 | -984 | -352 | | 5.5410 | -189 | -67.6 |
| $^{145}Nd$ | 8.30 | 7/2 | 0.17 | | | 615 | 220 | | | 118 | 42.2 |
| $^{147}Nd$* | - | 9/2 | 0.037 | | | 134 | 47.9 | | | 25.7 | 9.20 |
| $^{147}Sm$ | 15.07 | 7/2 | -0.15 | | 46.2 | -579 | -207 | | 6.8637 | -129 | -46.2 |
| $^{149}Sm$ | 13.84 | 7/2 | -0.12 | | | -463 | -166 | | | -103 | -36.9 |
| $^{151}Eu$ | 47.77 | 5/2 | 1.049 | | 47.7 | 4,179 | 1,495 | | 7.5645 | 995 | 356 |
| $^{153}Eu$ | 52.23 | 5/2 | 0.4638 | | | 1,848 | 661 | | | 440 | 157 |
| $^{154}Eu$ | - | 3 | 0.51 | | | 2,032 | 727 | | | 484 | 173 |
| $^{155}Gd$ | 14.68 | 3/2 | -0.12 | | 49.1 | -493 | -176 | | 8.2938 | -125 | -44.7 |
| $^{157}Gd$ | 15.64 | 3/2 | -0.17 | | | -698 | -250 | | | -177 | -63.3 |
| $^{159}Tb$ | 100 | 3/2 | 0.772 | | 50.6 | 3,268 | 1,169 | | 9.0537 | 876 | 313 |
| $^{161}Dy$ | 18.73 | 5/2 | 0.12 | | 52.1 | 523 | 187 | | 9.8451 | 148 | 53.0 |
| $^{163}Dy$ | 24.97 | 5/2 | 0.16 | | | 698 | 250 | | | 198 | 70.8 |
| $^{165}Ho$ | 100 | 7/2 | 0.722 | | 53.7 | 3,240 | 1,159 | | 10.6693 | 966 | 346 |
| $^{167}Er$ | 22.82 | 7/2 | 0.104 | | 55.2 | 480 | 172 | | 11.5275 | 150 | 53.7 |
| $^{169}Tm$ | 100 | 1/2 | 0.349 | | 56.8 | 1,657 | 5,929 | | 12.4204 | 544 | 195 |
| $^{171}Yb$ | 14.27 | 1/2 | 0.751 | | 58.4 | 3,664 | 1,311 | | 13.3495 | 1,257 | 450 |
| $^{173}Yb$ | 16.08 | 5/2 | -0.21 | | | -1,024 | -366 | | | -352 | -126 |
| $^{175}Lu$ | 97.40 | 7/2 | 0.486 | | 71.8 | 2,918 | 1,044 | 5d | 3.3816 | 206 | 73.7 |
| $^{176}Lu$* | 2.60 | 6 | 0.53 | | | 3,182 | 1,139 | | | 225 | 80.5 |
| $^{177}Hf$ | 18.39 | 7/2 | 0.13 | | 82.9 | 901 | 322 | | 4.4934 | 73 | 26.1 |
| $^{179}Hf$ | 13.78 | 9/2 | -0.080 | | | -555 | -199 | | | -45 | -16.1 |
| $^{181}Ta$ | 100 | 7/2 | 0.509 | | 93.0 | 3,957 | 1,416 | | 5.6057 | 358 | 128 |
| $^{183}W$ | 14.28 | 1/2 | 0.175 | | 102.4 | 1,498 | 536 | | 6.7504 | 148 | 53.0 |
| $^{185}Re$ | 37.07 | 5/2 | 0.9586 | | 111 | 8,911 | 3,188 | | 7.9414 | 955 | 342 |
| $^{187}Re$ | 62.93 | 5/2 | 0.9684 | | | 9,002 | 3,221 | | | 964 | 345 |
| $^{187}Os$ | - | 1/2 | 0.18 | | 120 | 1,800 | 644 | | 9.1859 | 207 | 74.1 |
| $^{189}Os$ | 16.1 | 3/2 | 0.3307 | | | 3,307 | 1,183 | | | 381 | 136 |
| $^{191}Ir$ | 38.5 | 3/2 | 0.0813 | | 128 | 1,107 | 396 | | 10.4886 | 107 | 38.3 |
| $^{193}Ir$ | 61.5 | 3/2 | 0.086 | | | 1,171 | 419 | | | 113 | 40.4 |
| $^{195}Pt$ | 33.7 | 1/2 | 0.9153 | | 135 | 10,366 | 3,709 | | 11.8527 | 1,360 | 487 |
| $^{197}Au$ | 100 | 3/2 | 0.0731 | | 143 | 874 | 313 | | 13.2809 | 122 | 43.7 |
| $^{198}Au$* | - | 2 | 0.19 | | | 2,271 | 813 | | | 316 | 113 |
| $^{199}Au$* | - | 3/2 | 0.12 | | | 1,434 | 513 | | | 200 | 71.6 |
| $^{197}Hg$* | - | 1/2 | 0.79 | | 150 | 9,923 | 3,550 | | 14.6560 | 1,452 | 520 |
| $^{199}Hg$ | 16.86 | 1/2 | 0.760 | | | 9,547 | 3,416 | | | 1,397 | 500 |
| $^{201}Hg$ | 13.24 | 3/2 | -0.280 | | | -3,517 | -1,258 | | | -515 | -184 |
| $^{203}Tl$ | 29.52 | 1/2 | 2.433 | | 205 | 41,625 | 14,893 | 6p | 7.5553 | 2,305 | 825 |
| $^{205}Tl$ | 70.48 | 1/2 | 2.457 | | | 42,035 | 15,040 | | | 2,328 | 833 |
| $^{207}Pb$ | 21.11 | 1/2 | 0.8899 | | 258 | 19,195 | 6,868 | | 10.9883 | 1,226 | 439 |
| $^{209}Bi$ | 100 | 9/2 | 0.6842 | | 312 | 17,869 | 6,394 | | 14.5706 | 1,250 | 447 |

TABLE B.II. Angular Parameters

| | $p_x$ | $p_y$ | $p_z$ | $d_{z^2}$ | $d_{x^2-y^2}$ | $d_{xy}$ | $d_{xz}$ | $d_{yz}$ |
|---|---|---|---|---|---|---|---|---|
| $t_{xx}$ | $\frac{4}{5}$ | $-\frac{2}{5}$ | $-\frac{2}{5}$ | $-\frac{2}{7}$ | $\frac{2}{7}$ | $\frac{2}{7}$ | $\frac{2}{7}$ | $-\frac{4}{7}$ |
| $t_{yy}$ | $-\frac{2}{5}$ | $\frac{4}{5}$ | $-\frac{2}{5}$ | $-\frac{2}{7}$ | $\frac{2}{7}$ | $\frac{2}{7}$ | $-\frac{4}{7}$ | $\frac{2}{7}$ |
| $t_{zz}$ | $-\frac{2}{5}$ | $-\frac{2}{5}$ | $\frac{4}{5}$ | $\frac{4}{7}$ | $-\frac{4}{7}$ | $-\frac{4}{7}$ | $\frac{2}{7}$ | $\frac{2}{7}$ |

## SUGGESTED REFERENCES

The list of books that follows is by no means complete. The reader will, however, find much of the information available in the literature according to the number in parentheses following each reference with the meaning:

1 Theory

2 Applications

3 Techniques

4 General

5 Tables

A. Abragam, The Principles of Nuclear Magnetism, Oxford, 1961. (1)

A. Abragam and B. Bleaney, Electron Paramagnetic Resonance of Transition Ions, Oxford, 1970. (1), (2)

R. S. Alger, Electron Paramagnetic Resonance: Techniques and Applications, Interscience, John Wiley & Sons, New York, 1968. (2), (3)

P. B. Ayscough, Electron Spin Resonance in Chemistry, Methuen, London, 1967. (1), (2)

C. J. Ballhausen, Introduction to Ligand Field Theory, McGraw-Hill, 1962. (1), (4)

M. Bersohn and J. C. Baird, An Introduction to Electron Paramagnetic Resonance, Benjamin, 1966. (1), (2)

A. Carrington and A. D. McLachlan, Introduction to Magnetic Resonance, Harper & Row, 1967. (1)

E. U. Condon and G. H. Shortley, Theory of Atomic Spectra, Cambridge University Press, Cambridge and New York, 1935. (1), (4)

J. S. Griffith, The Theory of Transition Metal Ions, Cambridge, 1964. (1)

H. F. Hameka, Advanced Quantum Chemistry: Theory of Interaction between Molecules and Electromagnetic Fields, Addison-Wesley, Reading, Massachusetts, 1965. (1)

D. J. E. Ingram, Free Radicals as Studied by Electron Spin Resonance, Butterworth, London, 1958. (2)

Landolt-Börnstein, New Series, Group II: Atomic and Molecular Physics, Volume 1: Magnetic Properties of Free Radicals; Volume 2: Magnetic Properties of Coordination and Organo-Metallic Transition Metal Compounds, Springer-Verlag, Berlin, Heidelberg, New York, 1966. (5)

W. Low, Paramagnetic Resonance in Solids, Academic Press, 1960. (1), (2)

J. D. Memory, Quantum Theory of Magnetic Resonance Parameters, McGraw-Hill, 1968. (1)

J. A. McMillan, Electron Paramagnetism, Reinhold, 1968. (1), (4)

G. E. Pake, Paramagnetic Resonance, Benjamin, 1962. (1), (2)

C. P. Poole, Electron Spin Resonance: A Comprehensive Treatise on Experimental Techniques, Interscience, John Wiley & Sons, 1967. (3)

C. Schlichter, Principles of Magnetic Resonance, Harper & Row, 1963. (1)

I. Ursu, LaRésonance Paramagnétique Electronique, Dunod, Paris, 1968. (1), (2), (3)

In addition, a vast number of review articles have already appeared in well-known journals. A key to the specialized literature may be found in most books cited in this list.

B